

384
49-20-75

CONF-770402-8

D. 506

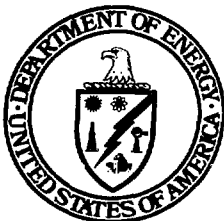
MASTER

MHD

A STUDY OF THE PROCESSES RESULTING
FROM THE USE OF ALKALINE SEED
IN NATURAL GAS FIRED MHD FACILITIES

**U.S.-U.S.S.R. COOPERATIVE PROGRAM
IN MHD POWER GENERATION**

April 13-21, 1977
Washington, D.C.



U.S. Department of Energy
Assistant Secretary for Energy Technology
Division of Magnetohydrodynamics

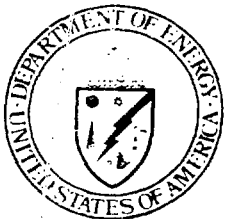
MHD

A STUDY OF THE PROCESSES RESULTING
FROM THE USE OF ALKALINE SEED
IN NATURAL GAS FIRED MHD FACILITIES

**U.S.-U.S.S.R. COOPERATIVE PROGRAM
IN MHD POWER GENERATION**

April 13-21, 1977
Washington, D.C.

NOTICE
This report was prepared as an account of work sponsored by the United States Government. Neither the United States nor the United States Department of Energy, nor any of their employees, contractors, subcontractors, or their employees, makes any warranty, express or implied, or assumes any legal liability or responsibility for the accuracy, completeness or usefulness of any information appearing in this report. It is the policy of the United States Government to disseminate as widely as possible the results of its research and development.



U.S. Department of Energy
Assistant Secretary for Energy Technology
Division of Magnetohydrodynamics

A STUDY OF THE PROCESSES RESULTING
FROM THE USE OF ALKALINE SEED
IN NATURAL GAS-FIRED MHD FACILITIES

M. A. Styrikovich and I. L. Mostinskii

CONTENTS

INTRODUCTION

Chapter I. Ionizing Seed Injection

Chapter II. The Ionizing Seed in the Combustion Chamber of the MHD Facility

Chapter III. The Ionizing Seed in the Gas Train of the MHD Facility

Chapter IV. Seed Recovery and Regeneration from the Combustion Products Exhaust

A Study of the Processes Resulting
from the Use of Alkaline Seed in
Natural Gas-Fired MHD Facilities

M. A. Styrikovich, I. L. Mostinskii

Various ways of ionizing seed injection and recovery, applicable to open-cycle magnetohydrodynamic (MHD) power generation facilities, operating on sulfur-free gaseous fossil fuel, are discussed and experimentally verified.

The physical and chemical changes of the seed and the heat and mass transfer processes resulting from seed application are investigated using the U-02 experimental MHD facility and laboratory test facilities.

Engineering methods for calculating the processes of seed droplet vaporization, condensation and the precipitation of submicron particles of K_2CO_3 on the heat exchange surface are also included.

The following persons participated in the experimental research and calculations at various stages of the work: Candidates of Science A. Yu. Val'berg, E. A. Vikhrov, Ya. M. Vizel', M. P. Kurkin, E. G. Smirnova, V. M. Tkachenko, engineers E. G. Apukhtina, V. V. Bordacheva, A. I. Valuev, I. M. Gaponov, A. S. Golubkova, A. V. Zagorodnikh, V. E. Kartun, D. I. Lamden, M. A. Laricheva, R. S. Nekhoroshev, V. R. Pesochin, G. S. Sorokin, V. I. Stepanov, V. I. Sukhov, Zh. S. Fainberg, and others.

Introduction

The rapid development of industry throughout the world, including the Soviet Union, requires an even more rapid development of power generation. Consequently, the world electric power output has more than doubled in the last ten years [1]. Today we are using the energy of the rivers and the atom, of the sun and the wind, of tidal waves and geothermal waters ; however, the main source of energy (more than 70%) is fossil fuel: coal, oil, gas. In spite of the vigorous development of nuclear power, fossil fuels will remain predominant at least until the end of the 20th century.

In the meantime, the efficiency of fuel utilization leaves much to be desired: the efficiency of small electric power stations is at times no more than 20%, and even in modern large co-generation power plants with millions of kilowatts output, the enthalpy extraction is, at best, some 40%.

If one considers that many industrially developed regions lack own fuel sources or have limited fuel recovery, and that fuel must be transported from afar, the problem of raising power plant efficiency becomes quite urgent. This is precisely the situation in the European part of the Soviet Union.

There, fuel for power generation, such as coal, oil and natural gas has to be transported by railway or by pipeline over distances of thousands of kilometers.

Under these conditions a large economic benefit for electric power generation can be expected from the use of magnetohydrodynamic generators. Technico-economic calculations [2, 3] have shown that power plants with MHD generators (MHDPS's) will, in the near future, have efficiencies on the 50% level versus the maximum 40-42% for steam power plants. The significant advantage of the MHD

power plant is its load-following capability - the MHD start-up generator requires only a few minutes.

Economical operation of an MHD generator requires low temperature plasma, i.e., products of fuel combustion having an electrical conductivity of $10 - 100 \text{ ohm}^{-1} \cdot \text{m}^{-1}$. However, their inherent thermal ionization, even at temperatures as high as 3500-4000 K, is very low, and for the practical application of the MHD method one must raise the conductivity by 2-3 orders of magnitude. At the present time this is achieved by the addition of easily ionized substances -- heavy alkaline metals. Table I gives values for the ionization potentials of alkaline and alkaline earth metals [4], as well as of other elements contained in the fossil fuel combustion products. As can be seen from the table, the ionization potentials of the alkaline metals are significantly lower than those of the combustion product components. Cesium appears to be the best substance for the production of an electrically conductive plasma; however, when selecting the seed material for the MHD power generators, it is necessary to consider the distribution of the element in nature, the cost of its production, and the production scale at present and in the future. Cesium does not meet these requirements; it is rare, the deposits of it are small, its production is very limited, and the cost is high. Therefore, the loss of even 0.2% of the injected* cesium will obliterate all the advantage gained by the use of MHD generators.

Rubidium is completely unpromising for power generation: it is expensive, scarce, and its ionization potential differs little from that of potassium.

Therefore, the use of potassium as the ionizing seed in the open-cycle MHD generators is the most realistic solution. The natural reserves of this

* For a 3 million kW MHD power plant this is about one thousand tons per year.

element are quite large, and the common use of potassium and its salts in industry has led to the development of its production. The cheapest and most common potassium salts are its chloride KCl and sulfate K_2SO_4 , which occur in the natural state, and its carbonate K_2CO_3 , which is produced either from the two natural salts or sodium - potassium solutions in the production of aluminum from nephelines [5]. There are also other methods of producing K_2CO_3 .

It would seem that the large natural deposits of KCl would make this substance the most promising for direct use in MHD power plants, since no processing is required after its recovery except for mechanical cleaning or beneficiation. However, the chlorine content of KCl makes its use impracticable. The reaction of chlorine ions with the stainless steel, the main construction material of the MHD channel and the downstream components of the power plant, leads to an increased brittleness and cracking in the metal [6], while deposits of potassium chloride increase high-temperature corrosion [7].

The main substance used as an ionizing seed in MHD units operating with the combustion products of a sulfur-free fuel is potassium carbonate. As will be shown below, the potassium will circulate in the loops of these units in just this form, regardless of the composition initially introduced.

When an MHD generator is operated with the combustion products of a sulfur-containing fuel, K_2SO_4 with a small amount of K_2CO_3 will circulate in the circuit, and the seed selection will be made depending on the need to neutralize the sulfur. In that case K_2CO_3 or KOH would be used, otherwise the seed would be K_2SO_4 .

The ionizing seed is injected upstream of the MHD generator and by the time it enters the MHD channel it must be well mixed with the working gas,

dissociated and ionized. It is difficult to ensure these conditions. On the one hand, in order to reduce heat losses in the combustion chamber, the process of combustion must be accelerated by increasing the furnace volume utilization. On the other hand, in order to achieve maximum seed ionization, it is necessary either to increase the ionization time or to create conditions that would help to accelerate the ionization. A reduction in the size of the injected particles to the order of tens of microns will contribute to the latter; this is in itself a difficult task. All this is made even more difficult by the need to inject this finely pulverized seed in amounts of several dozen tons per hour.

The amount of the injected seed material will be about 2 wt % of the combustion products flow rate. To mix such a small quantity of seed with the gas flow in several milliseconds is a task requiring special attention on the part of the MHD combustor designers. The complex thermal and aerodynamic circumstances reduce the accuracy of vaporization, ionization and mixing processes and calculations and require special experiments.

When the state of thermodynamic equilibrium is achieved, the seed in the combustion products circulating through the MHD channel is primarily in the state of potassium vapors and potassium hydroxide [8, 9]. The presence of relatively cool surfaces in the channel (cooled insulating walls and "cold" electrodes) leads to condensation of KOH vapor, and to the formation on these surfaces of seed deposits, which has a significant effect on the operation of the MHD generator and of the heat exchange equipment located downstream. Deposits on pipes not only impair heat transfer, but also block the gas passages, increasing the hydraulic resistance in the gas loop. The effectiveness of the methods used to remove seed deposits off the pipes without component shut-down depends on the physical-chemical properties of the deposits.

The reaction of the seed with the metal of the pipes is of great practical interest. Based on thermodynamic considerations one should assume that KOH vapors will condense on the pipe surfaces. It is known [10] that in an alkaline environment, thermally stressed austenite steel is subject to transcrystalline corrosion leading to the propagation of cracks penetrating through the steel. How will a KOH melt affect the strength of the metal? Will it be necessary to abandon the use of austenite steel? Only research can give an answer to these questions.

An important task is the adequate (both from the standpoint of economics and of health standards) recovery of ionizing seed from the exhaust. This is difficult because of the highly dispersed state of the dust: the seed in an MHD power plant is a condensation product with particle sizes on the order of 0.1μ . Equipment operating on the inertial principle (cyclones, multi-cyclones, etc.) is totally unsuited for trapping such fine particles, and the effectiveness of electro-static precipitators requires experimental verification.

The recovered seed must be returned to the cycle. However, its state in the recovery system differs from its initial state at the time of injection into the combustion chamber. The presence of ceramic surfaces in the gas loop of the MHDG, for example in the Cowpers, causes the gases to become contaminated with ceramic dust, which is trapped together with the seed. The seed is also contaminated with products of metal corrosion. Moreover, there are differences in the chemical compositions of the injected and recovered seed. All these deviations are magnified as the seed circulates in the loop, and the recovered seed may prove unsuitable for further use. In order to avoid this, a special system for seed regeneration must be designed into the MHD

power plants, and in order to design it, the chemical composition and basic impurities of the recovered seed must be known.

At the present time, the most advanced MHD research deals with generators operating with the combustion products of natural gas. In 1964 the U-02 facility with an open-cycle MHD generator, which included all the basic elements of future MHD power plants began operation in Moscow [11]. Ten years of research carried out at this facility have helped to identify and study specific physical-chemical processes and to remove many of the technological obstacles to the creation of the MHD facilities. In parallel with the tests at the U-02, experiments and theoretical research were being performed at the Mass Transfer Section of the Institute for High Temperatures, U.S.S.R. Academy of Sciences. This approach provided a fairly clear picture of the ionizing seed behavior in an open-cycle MHD generator operating with the combustion products of sulfur-free gaseous fuel, and made it possible to make some recommendations concerning injection recovery and regeneration methods.*

Chapter I

Injection of Ionizing Seed

1. The seed material, its properties and basic methods for injecting it into the cycle.

The natural gas used as fuel for MHD power plants contains more than 90% saturated hydrocarbons and small amounts of CO_2 and nitrogen, but, in contrast to coal and fuel oil, it does not contain sulfur. When it is combusted in atmospheric or oxygen-enriched air, the gases produced contain CO_2 , H_2O , N_2 and CO or O_2 . With the high temperatures typical of MHD generators (on the

* A list of articles presenting this material during the succeeding stages of research from 1967 to 1975 is contained in the Appendix.

order of 3000 K) certain of these substances dissociate, forming H_2 , O_2 , O and NO , as well as the OH^- , H^+ and O ions, which exist only in this temperature range. Thermodynamic calculations of composition of the combustion products obtained during the combustion of such gaseous fuel have been made both in the U.S.S.R. [8] and abroad [9], and the results are quite similar. Figure 1 is an example of the composition of the products of methane combustion in atmospheric air at high temperatures [8]. Any compound of potassium injected into the combustion chamber melts, evaporates, dissociates and the resultant atomic potassium is partially ionized. At the same time new potassium compounds, more stable under these conditions, are formed.

In an environment containing H_2O , and especially OH^- ions, potassium hydroxide is such a compound. However, at lower temperatures the hydroxide cannot exist in contact with carbon dioxide: a reaction occurs between them and potassium carbonate is formed.

Thus, the seed recovered from the MHD cycle is primarily potassium carbonate (K_2CO_3) and, partially, as will be shown below, as potassium bicarbonate ($KHCO_3$). Ionizing seed should be injected as K_2CO_3 .

Potassium carbonate in pure form is a white crystalline powder that does not flow freely, is very hygroscopic and is readily soluble in water: at $t = 20^\circ C$ its solubility is 110 g K_2CO_3 per 100 g H_2O and at $t = 100^\circ C$ it is 155 g [12].

The density of solid K_2CO_3 at $20^\circ C$ is about 2400 kg/m^3 , while the bulk density of its powder varies over wide limits: from 1500 kg/m^3 for caked moist K_2CO_3 to $200\text{-}300 \text{ kg/m}^3$ for dry, loose powder.

The melting point of K_2CO_3 according to [13] is $901^\circ C$. At temperatures above $700^\circ C$ potassium carbonate begins to break down into K_2O and CO_2 . Reference [13] gives data on a change in the pressures of CO_2 (formed because

of dissociation of K_2CO_3) and of K_2CO_3 vapor above the melt. The heat of vaporization of K_2CO_3 from melt was calculated on the basis of these data: $\Delta H_{K_2CO_3} = 1760 \pm 16$ kJ/kg. The heat of fusion is 200 ± 3 kJ/kg. Values for the heat capacity and change of enthalpy at temperatures to 1250 K are given in the JANAF tables [14].

To step up seed ionization, dry potassium carbonate must be injected into the combustion chamber as a finely dispersed powder with particle size on the order of tens of microns. However, it is difficult to do this because of the high hygroscopicity of K_2CO_3 , its poorly flowing texture and its tendency to cake and form rat holes even in dry form. Specifically, attempts made at the U-02 facility to inject dry potassium carbonate did not have favorable results. The attempt made by Gadda [15] was practically speaking also unsuccessful: the system proposed by him provided for a more or less reliable feed of technical-grade potassium carbonate powder having particles from 150 to 400 μ , i.e., rather large.

The task of injecting the seed becomes substantially simpler when a K_2CO_3 solution is used, since the technology of transporting the liquid through pipes, metering and spraying it is well developed. At the same time the use of a K_2CO_3 solution relaxes the specifications for the conditions for preparation and, especially, for the storage of ready-to-use seed.

Potassium carbonate is not soluble in organic liquids, including petroleum and its products, but water, as has already been mentioned, is an excellent solvent for K_2CO_3 : even at room temperature a solution of 50% concentration can be produced. The use of an aqueous solution significantly simplifies the task of designing a closed cycle for the ionizing seed at the MHD power plant, and facilitates its recovery from the loop and its transportation and regeneration.

The injection of potassium carbonate as a 50% aqueous solution has been tested in experiments on MHD generators operating on gaseous fuel, for example [16, 17]. In operations with liquid fuel, alcohol solutions of KOH as well as organic compounds of potassium are often used, but for an MHD power plant this method is not promising.

2. The optimum concentration for the ionizing seed

The operating efficiency of a power-producing MHD generator is directly dependent on the electrical conductivity of the working gas. The ionizing seed increases this conductivity, basically by increasing the number of free electrons. Low mobility ions play a small role in the transfer of charges. However, the seed injection is accompanied by an increase in the effective electron capture cross section and a reduction of the gas temperature, and, when an aqueous solution of K_2CO_3 is used, by an increase in the concentration, which actively absorb electrons. The existence of these contradictory factors leads to the existence of a maximum of electrical conductivity for any given seed concentration. This concentration will be optimal, if the electrical conductivity of the gases of the MHD channel entrance is taken as the optimization criterion. A calculation has been made of the optimum ionizing seed concentration injected into the combustion products of natural gas in the form of dry powdered K_2CO_3 and as 50% or 67% aqueous K_2CO_3 solutions. The problem was set up as follows: the ionizing seed is added to the combustion products of natural gas (for the sake of precision pure methane in air with a given oxygen level was assumed) with the initial temperature and pressure of the combustion products being T_0 and P_0 . The pressure does not change with the seed injection, while the temperature drops significantly and then stabilizes at a certain temperature level. The calculation also takes into account

certain changes in the chemical composition of the combustion products caused by seed injection. The electrical conductivity was computed for these new conditions. Such calculations were made for the following range of main parameters:

Combustion temperature T_0 (before seed injection), K	2400-3200
Pressure P_0 , bar	1-10
Mass fraction x :	
Oxygen in oxidizer, x_{O_2}	0.21-0.5
Potassium in combustion products, x_K	0.002-0.5
Amount of water in solution, C_{H_2O} , kg	
H ₂ O/kg K ₂ CO ₃	0-1
Air excess coefficient, α	1

The data produced are presented in Figures 2, 3, 4 and 5 as dependences of $\sigma = f(x_K)$ for assigned value of P_0 , x_{O_2} and C_{H_2O} . All the curves have a clear maximum. For low seed levels ($x_K < 0.002$) such effects of injection as the reduction of temperature and the increase in the electron capture cross section, are not great, and the electrical conductivity is practically speaking independent of the initial seed form. Therefore, the curves corresponding to K₂CO₃ injected in dry form and as aqueous solutions are similar.

An increase in the seed concentration begins to affect the temperature, and curves 2 and 3, which correspond to 67% and 50% K₂CO₃ solutions, decline. The lower the seed concentration in the solution the more pronounced is this effect and the earlier is the σ maximum reached. When the 50% solution ($C_{H_2O} = 1$) is used with $x_{O_2} = 0.21$ and $P = 1$ bar (Figure 2), the maximum conductivity in the region of low temperatures ($T_0 = 2400$ K) is reached for a molar concentration $x_K = 0.006$. The use of a more concentrated solution

shifts the maximum toward greater x_K and when $C_{H_2O} = 0.5$, the maximum conductivity corresponds to $x_K^{opt} = 0.009$.

When dry K_2CO_3 is injected, the temperature reduction is relatively small, and the $\epsilon = f(x_K)$ curve is conspicuously affected by the increase in electron capture cross section. The maximum is less pronounced and at the same temperatures is approximately 0.015.

With an increase in the initial temperature the optimum potassium concentration increases: when $C_{H_2O} = 0.05$ and $P = 1$ bar an increase of T_0 from 2400 to 3200 K leads to a two-fold increase x_K^{opt} from 0.006 to 0.013. These changes are represented in Figures 2-5 by the almost equidistant dot-dash lines "a-a," "b-b" and "c-c," connecting the maximum values of ϵ for different T_0 , but for identical seed injection methods.

Figures 2-5 each show graphs of $\epsilon = f(x_K)$ for 1, 3 and 10 bar. It is clear that the value of x_K^{opt} has a weak dependence on the pressure, though ϵ_{max} changes greatly. For a tenfold change in pressure the value of ϵ_{max} changes threefold for $T_0 = 3200$ K and almost sevenfold for $T_0 = 2600$ K, while the corresponding x_K^{opt} changes only 15-25%.

When oxygen-enriched air is used, the amount of "passive" nitrogen decreases and the proportion of dissociating H_2O and CO_2 increases. On the one hand, this leads to increased effective heat capacity of the combustion products and, consequently, to a decreased reduction of their temperature when the seed is injected; on the other hand, it leads to an increase in the effective collision cross section and to an intensified capture of electrons by the OH^- ions. This last effect is strongly felt for small x_{H_2O} (the combustion products of coal, coke and to lesser degree, fuel oil). When natural gas is combusted, even in atmospheric air ($x_{O_2} = 0.21$) the H_2O level in the combustion products is sufficiently high, causing a noticeable reduc-

tion of this effect. Therefore, for low seed concentrations there is practically no difference between the use of atmospheric air (cf. Figure 2) and oxygen-enriched air (Figures 3-5). With an increase in x_K the temperature reduction begins to play an increasing role, but this, as was mentioned above, decreases with air oxygen enrichment. Therefore, the $\zeta = f(x_K)$ curves in Figures 3-5 are flatter than in Figure 2, with the ζ maximums shifted to the right. Thus, for a 67% K_2CO_3 solution and an oxygen enrichment to 50% at $P = 1$ bar and $T_0 = 2600$ K (Figure 5), the optimum x_K value is 0.014, while without enrichment (cf. Figure 2) it is significantly lower, 0.010. The dependence of x_K^{opt} on temperature remains as before even when oxygen-enriched air is used: increasing T_0 from 2400 to 3200 K when $x_{O_2} = 0.5$, also leads to a doubling of x_K^{opt} .

If dry K_2CO_3 is added, the curves of $\zeta = f(x_K)$ are even more flattened with an increase in x_{O_2} , and their maximums shift to $x_K = 0.025-0.030$. Therefore, depending on the conditions in the combustion chamber and the seed injection method the optimum seed concentration changes almost fivefold. It should be noted, however, that the maximum becomes flattened with a reduction in C_{H_2O} , thus making it possible to reduce the x_K^{opt} value in practical application, without a significant ζ reduction. Thus, for $x_{O_2} = 0.21$ and $T_0 = 3200$ K (Figure 2), if the amount of seed injected as dry K_2CO_3 is reduced to one half of x_K^{opt} , ζ is then reduced by only 7%. An increase in the degree of oxygen enrichment also fails to alter the picture.

These calculations give a general idea of the optimum seed requirements. A more rigorous optimization of the seed consumption should involve technico-economic criteria, that take into account the capital and operating costs for all the components of an integrated facility with MHD generators.

3. High-concentration aqueous solutions of potassium carbonate

The great technological advantages of injecting a K_2CO_3 solution compared to injecting this same substance as a fine powder make it imperative to search for ways of reducing the thermodynamic imperfections of the first method. The main direction of research is obvious -- to raise the concentration of the solution (Figure 6) and, if possible, the enthalpy. The solubility of potassium carbonate at temperatures below $100^\circ C$ has been studied by many investigators. An analysis of the available experimental data was made and the "most probable values" were given in [12] (broken curves in Figure 6). Studies of the solubility of K_2CO_3 at higher temperatures have shown that it is possible to produce very concentrated solutions (75-80 wt %).

A study made jointly with IONKh [Institute of General and Inorganic Chemistry], U.S.S.R. Academy of Sciences, was devoted to investigation of phase equilibria in the system $K_2CO_3-H_2O$ at high parameters [18]. The experiments were performed in a thick-walled 43 cm^3 autoclave made of corrosion resistant Kh18N25S type steel. Since under these conditions there was no possibility of visually observing the moment of solid phase precipitation, the investigators used the vapor pressure above the solution at constant temperature as an indicator: for nonsaturated solutions the vapor pressure fell with an increase in the amount of salt, while for saturated solutions it remained constant. The vapor pressure above nonsaturated and saturated solutions was measured the temperatures range from 250 to $450^\circ C$, with solution concentrations up to 80% by weight. The main experimental results of the study are given in Table II. Representation of these data in a "pressure-composition" diagram (Figure 7) allows the parameters of the saturated solution to be found by the discontinuity of the isotherms (Table III).

It is known that for pure substances the dependence of the saturated vapor pressure on temperature can be properly described by an expression of the type

$$\lg P_s = A - \frac{B}{T_s}, \quad (1)$$

where P_s and T_s are the pressure (bar) and absolute temperature (K) of the boiling liquid and A and B are constants.

In a semilogarithmic coordinate system ($\log P$ vs $1/T$) equation (1) is represented by a straight line. A similar representation of the data obtained (Figure 8) showed that solutions of constant concentration can also be viewed as definite substances, an approach that will have to be used.

The linearity of the dependence $\lg P = f(1/T)$ for isoconcentration conditions allowed it to be extrapolated to a temperature of 500°C and to find the vapor pressure above unsaturated boiling solutions corresponding to this temperature (broken lines on Figure 7).

An analysis of the data obtained shows that the pressure above the boiling K_2CO_3 solutions, especially for high concentrations, is substantially lower than the pressure of the saturated steam of pure water at the same temperature. The high temperature depression of solutions, accompanying the good solubility of K_2CO_3 , made it impossible to achieve a critical state even at 450°C. Clear separation of the liquid and vapor phases for high-concentration K_2CO_3 solutions extends to a temperature region exceeding the critical temperature of the solvent by hundreds of degrees. This phenomenon is characteristic of salts with a positive solubility coefficient.

The results of a study of the degree of K_2CO_3 hydrolysis at high temperatures presents much practical interest. Even though these data are quite tentative, they should be considered. Measurements of amount of carbon dioxide

released during vaporization showed that at temperatures below 450°C no discernable hydrolysis of K_2CO_3 occurs; at temperatures of 500 and 550°C the concentration of hydrolysis product, KOH, is a fraction of a percent, while at 600°C it reaches 1%. The indicated amounts of potassium hydroxide formed are not maximum: with separation of the vapor (and with it CO_2) hydrolysis continues and KOH accumulates in the solution. The highly corrosive action of this component upon construction materials, including stainless steels of the austenite type, requires attention to the rate of hydrolysis. Of course, this problem exists only at temperatures above 400°C.

The data cited gives a fairly complete picture of the parameters and phase equilibria in the system $K_2CO_3-H_2O$. In processing the study results, the density of the vapor phase was assumed to be equal to the density of pure superheated water vapor inasmuch as the solubility of K_2CO_3 in the vapor, if it exists, would not significantly change its thermal and physical properties.

The specific volume of the liquid phase can differ from the specific volume of the solvent. Unfortunately, experimental measurements of this value were not made in [18]. However, a quantitative estimate of the specific volumes of high-concentration K_2CO_3 solutions at high temperatures and pressures can be made from the data of [19] and [20].

Measurements were made in [19] of the specific volumes of boiling aqueous K_2CO_3 solutions having moderate concentrations (up to 30 wt %) at temperatures from 25 to 340°C; in [20] the density of more concentrated solutions (up to about 65 wt %) was measured, but at relatively low temperatures (20-135°C). A relationship mentioned by many investigators makes it possible to extrapolate with fair accuracy these measurements of the specific volumes into the region of high concentrations and high temperatures and pressures: the temperature dependent curves of the solution density for various substances are almost

equidistant from the corresponding curve for the solvent, i.e.,

$$\rho = \rho_0 + B, \quad (2)$$

where ρ and ρ_0 are the density of the solution and the solvent, respectively, and B is a value which depends on the properties of the solvent and the dissolved substance, the concentration and, to a much lesser degree, on the temperature.

The dependence of the B value on the solution concentration is almost linear and generally is well described by the expression

$$B = (a + bc)c \quad (bc \ll a), \quad (2a)$$

where a and b are constant values for a given substance, and c is the weight concentration of the solution.

All this is clearly confirmed by the data of [21], which was produced in experiments with aqueous solutions of KCl (Figure 9). In the moderate temperature range (to 250°C) the saturation curve for water and the isoconcentration curves for KCl solutions are practically equidistant. With an increase in temperature the density of boiling water declines sharply, while the decrease in density of the KCl solutions (particularly at 10-20% concentrations) progresses significantly slower. This is understandable, if one considers that the critical states for these solutions lie far to the right, by 100 degrees and more.

The dependence of the density on temperature and concentration for aqueous K_2CO_3 solutions (Figure 10) was constructed on the basis of the diagram (cf. Figure 9). Isoconcentration curves for 10, 20 and 30% were constructed by interpolation of the data of [19] and the beginning of isoconcentration curves for 40, 50 and 60% were based on the data of [20]. In extrapolating

the isoconcentration curves into the high temperature region (broken lines) dependences (2) and (2a) were used, with the constants being based on available data. The 70% isoconcentration curve was constructed in the same way. From above, the diagram is limited by the line of saturated solutions, constructed according to the t - C diagram (cf. Figure 7). Despite this relatively rough method for estimating the density of a boiling solution of K_2CO_3 in the high-temperature region, the accuracy of the ρ value is estimated to be, in the worst case, $\pm 10\%$.

The existence of the P - t - C diagram for K_2CO_3 solutions (cf. Figure 8) as well as the density data made it possible to calculate the differential heat of water evaporation from solution, using the Clapeyron equation:

$$\frac{dP_s}{dT_s} = \frac{100r}{T_s(V'' - V')}, \quad (3)$$

where r is the heat of liquid vaporization, kJ/kg; T_s is the temperature, K; P_s is the pressure of vapor in equilibrium with the liquid at this temperature bar; V' and V'' are the specific volumes of boiling liquid and vapor in equilibrium with it, m^3/kg .

A solution of given concentration was viewed as a substance for which the temperature dependence of the vapor pressure, when the vapor is in equilibrium with the liquid phase, is expressed by an equation of the type

$$\lg P_s = A - \frac{B}{T_s},$$

where A and B are empirical constants.

Hence

$$\frac{dP_s}{dT_s} = 2.303 \cdot \frac{P_s B}{T_s^2} \quad (4)$$

Substituting expression (4) into expression (3) and making the proper transpositions, we obtain

$$z = 4,303 \cdot 10^{-4} \cdot \frac{P_s B}{T_s} (v'' - v'), \quad (5)$$

The differential heat of water vaporization from K_2CO_3 solutions was calculated by equation (5) over a wide range of basic parameters: temperature 100-450°C, pressure 1-200 bar, concentration 30-80 wt %. The values of B, V' and V'' needed for the calculations were found in the following manner: from the data of Figures 1-20 [sic] values of B were found. The data of Figure 10 was used to determine the specific volume of liquid phase V' , and the value of V'' was determined as the specific volume of superheated water vapor at given values of P and T. The results of the calculations are given in Table III. The error in the determination of r ranges from $\pm 1\%$ for low-concentration solutions to $\pm 2\%$ for high-concentration solutions.

As can be seen from the table, the water evaporation heat rises with an increase in the solution concentration. Similar data were obtained for aqueous solutions of sodium and potassium hydroxides. This is due to a reduction in the thermal vibration of the water molecules in the strong electrostatic ion field when the electrolyte solution concentration is increased [22, 23].

Thus, in principle the possibility of producing high-concentration aqueous solutions of potassium carbonate has been demonstrated and the parameters of these solutions at boiling have been determined; the specific volumes of these solutions have been estimated and the differential heat of water evaporation from K_2CO_3 solutions has been calculated.

4. The technology for producing high-concentration aqueous solutions of potassium carbonate at an MHD power plant.

Analysis of operation and design principles of ordinary evaporation equipment demonstrates its lack of potential for the production of high-concentration K_2CO_3 solutions in power plants with MHD generators.

First of all, almost all standard evaporation facilities are designed to use steam as the heating agent. Meanwhile, the boiling point of a 75% K_2CO_3 solution at a pressure of 100 bar is 400°C, i.e., it will be necessary to either use steam at supercritical parameters or to use greatly superheated steam at a low coefficient of utilization. Both are economically unsound.

For high seed flow rates (tens and hundreds of tons per hour), the evaporation facilities must provide evaporation of approximately the same amount of water, and, furthermore, at high pressure. Under these conditions evaporation units of the ordinary type will be very cumbersome and will require great quantities of metal.

For power plants with MHD generators the only economically and technologically justifiable evaporation equipment will be that which has been designed to fit into the thermal system of the power plant. Clearly, in developing design concepts for the production of high-concentration K_2CO_3 solutions, the extensive experience accumulated in the U.S.S.R. and abroad in the design and operation of steam generators for combined heat and power plants should be taken into account. Thus, it seems feasible to evaporate the aqueous K_2CO_3 solutions in a once-through steam generation loop with a separator. The steam generating tubes can be located in the gas duct downstream of the MHD channel, in the zone where the temperature of the combustion products is 1100-1200 K. A purified 40% K_2CO_3 solution is pumped into these tubes by a high pressure pump from the seed regeneration system and evaporated

till it reaches the desired concentration. In the separator, it is separated from the steam and injected into the combustion chamber of the MHD generator through nozzles. The high-temperature, high-pressure steam produced should be utilized in the steam cycle.

The advantage of this once-through evaporation unit is that it is compact and can produce high-concentration solutions of K_2CO_3 . However, a number of problems must be solved before the proposed system can be built. First of all, data are needed on the temperature conditions of the steam-generating tubes, where the highly concentrated K_2CO_3 solution circulates and boils. It is necessary to know whether it is possible to ensure operation without deposit buildup and under what conditions; the boundaries of this operating mode and the intensity of appropriate heat transfer must be determined; the corrosion resistance of the steam-generating tubes must be determined. The use of secondary steam in the steam cycle requires data on its purity, i.e., on the amount of mechanical entrainment of liquid in the process of separating the steam from the K_2CO_3 solution and the solubility of K_2CO_3 (and of its hydrolysis product KOH) in the generated steam. No direct answer to these questions was found in the literature, but indirect data give hope for a favorable solution to the problem. A special study of these matters was made at IVTAN [Institute for High Temperatures, U.S.S.R. Academy of Sciences]. The experiments were performed on an experimental test facility, shown in the diagram in Figure 11.

An aqueous solution of potassium carbonate from 10 to 50% in concentration was pumped (ND-25 piston pump [3]) from supply tank (1) through a Nitron [polyacrylonitrile] filter (2) into buffer tank (4), which served to smooth out the pulsations in the liquid flow arising because of the piston pump action. From the buffer tank via a second nitron filter (5) the solution entered the experimental section (6), which consisted of two sequentially connected hori-

zontal tubes 10 x 2 mm made from steel 1Kh18N10T. Each tube was 1200 mm long (between the current busses). The tubes were directly heated by inherent ohmic resistance to a low-voltage alternating current supplied from two OSU-20/05 transformers. The current was regulated by voltage regulators RNO-250-10. Each tube has a separated transformer and regulator. The electrical circuit was decoupled using an insulating insert (7) made of fluoroplastic* mounted on the cold solution entrance side. The circuit was grounded on the hot solution side.

The vapor-liquid mixture formed in the experimental section entered the separator (8) via a tangentially mounted tube. Here the vapor and liquid phases were separated. An MEI-system level gauge was installed on the separator in order to monitor the solution level. The solution was transferred to the spray nozzle through an opening near the bottom of the separator, and the vapor from the upper part of the separator, via an opening in the cover, entered first a steam superheater (9) and then the steam jacket (10), heating the line containing the highly concentrated solution and, finally, it entered condenser (11). The single-tube condenser was cooled with tap water flow.

The solution was sprayed into the atmospheric tank (12) through conical nozzles.

The separator, steam heater and steam jacket were equipped with nichrome electrical heaters and were heat-insulated.

All parts of the unit were made from Kh18N10T steel.

Aqueous solutions of potassium carbonate prepared from "analytically pure" salt and distilled water were used in the experiments. The solutions produced were analyzed for total alkalinity (titration with 0.1 N HCl solution with methyl orange as an indicator) and total bound carbon dioxide (after Fresenius). The results of the analyses converted for K_2CO_3 content coincided

* Probably PTFE--Translator

excellently, indicating the virtual absence of either KHCO_3 or KOH in the solution.

Preliminary experiments with boiling distilled water allowed the accuracy of the thermocouple readings to be verified and data to be obtained on the heat transfer during the boiling of water, which correspond well (with accuracy of $\pm 12\%$) both to the experimental data [24] and to the results of calculations using the formula for a boiling liquid in thick-walled tubes [25].

Experiments with aqueous K_2CO_3 solutions were made at pressures of 10, 49, 98 and 147 bar, mass velocity of $150\text{-}200 \text{ kg/m}^2\text{s}$, heat flows of $70\text{-}150 \text{ kW/m}^2$ for concentrations ranging from 20 to 75 wt %.

The coefficient of heat transfer was computed in the usual way:

$$\alpha = \frac{q}{t_{cm}^{bn} - t_{sp}}, \quad (6)$$

where q_{bn} is the heat flux from the internal surface of the tube, kW/m^2 , t_{cm}^{in} is the temperature of this surface, $^{\circ}\text{C}$; t_{sp} is the boiling point of the solution, $^{\circ}\text{C}$.

The specific heat flux was determined from the electrical power input, taking into account the heat losses, which were 2-3% of the N_E , and the temperature of the heat transfer surface t_{cm}^{bn} was determined by the measured temperature of the experimental tube external surface and the temperature drop in the wall with internal heat sources.

In calculating the local heat transfer coefficient to the aqueous solution of K_2CO_3 boiling in the tube, it must be kept in mind that as the water along the tube evaporates, the concentration of the solution, and, consequently, its boiling point, rise. A determination of t_{sp} is possible from the

data of [18] if the pressure and solution concentration in the same cross section where the wall temperature is measured, are known.

The calculation method developed for this case made it possible to find the cross sectional average concentration of the flow with an error not greater than ± 2 wt %. The inaccuracy in t_{sp} caused by this error should be estimated as $\pm 2^\circ\text{C}$ at $P = 10$ bar and as $\pm 5^\circ\text{C}$ at $P = 150$ bar. The accuracy of measuring the wall temperature was $\pm 0.5^\circ\text{C}$ in the experiments. Taking into account both these errors, and also the errors connected with inaccuracies in determining the pressure, heat flux and the temperature difference in the tube wall, the total error in the determination of the heat transfer coefficient is estimated as $\pm 30\%$. This figure corresponds well to the scattering of the experimental points about the averaged curves.

Treatment of the experimental data as the dependence $\alpha = f(q)$ for various pressures and K_2CO_3 solution concentrations, showed that in this range of heat fluxes this dependence corresponds to the conventional one for boiling pure liquids:

$$\alpha \propto q^{0.7} \quad (7)$$

The relationship established between α and q permitted the reduction of all the data obtained to a single value for the heat flux, equal to 100 kW/m^2 , in order to identify the dependence of the heat transfer coefficient on the solution concentration:

$$\alpha_t = \alpha \left(\frac{100}{q} \right)^{0.7}. \quad (8)$$

The values of α_t plotted in Figure 12 show that over the whole range of concentrations investigated ($C_{\text{K}_2\text{CO}_3} = 20\text{-}70$ wt %) the heat transfer coefficient

cient for the boiling process decreases monotonically with an increase in concentration. These data, with a point scattering of $\pm 30\%$, can be described by the following empirical formula:

$$\lg \alpha_t = 1,66 - 0,018 C_{K_2CO_3}, \quad (9)$$

where α_t is the coefficient of heat transfer, $\text{kW/m}^2 \cdot \text{degree}$, and $C_{K_2CO_3}$ is the solution concentration wt %.

It is interesting to note that for K_2CO_3 solutions greater than 20% in concentration the value of α turned out to be practically independent of pressure. This may be explained, to some extent, by the following: the dependence of the heat transfer coefficient on pressure is fairly weak in the region far from the critical state of a boiling liquid and sharply increases as the pressure approaches P_{cr} . However, for solutions containing even 20% K_2CO_3 the critical pressure can (by analogy with the $KCl-H_2O$ system [21]--cf. Figure 9) significantly exceed the critical pressure of water. Thus, the pressures covered by the experiments, 49, 98, and 147 bar, appear to be removed from the critical region, and the difference in the values of the heat transfer coefficient when the solutions boil at these pressures ought to be lower than in the experiments with pure water. The critical pressure will evidently increase with an increase in solution concentration, while coefficient values of heat transfer to the boiling solution will converge even more.

An investigation of the conditions of salt (K_2CO_3) deposition on the surface of the steam-generating tube was made at a pressure of 50 bar. At this pressure an aqueous K_2CO_3 solution becomes saturated at a concentration of 77% [18]. However, in the flow of solution boiling in the steam-generating tube, there exists a concentration field with the highest $C_{K_2CO_3}$ value in

the boundary layer. Solution saturation will be reached here first of all, accompanied by precipitation of the salt on the wall and an elevation of the temperature of the heating surface.

The difference between the average solution concentration in the flow and its concentration in the boundary layer during vigorous boiling is determined primarily by the heat flux value. Obviously, the lower the heat flux, the lower this difference will be, and consequently, the higher the concentration of solution that can be produced in the tube without salt precipitation on the tube wall, i.e., without disturbing its temperature of operation. An increase in the heat flux limits the possibility of increasing the solution concentration, since salt begins to deposit on the wall at a lower average concentration.

To determine the limits of impaired operation, special experiments were conducted; the heat flux was increased to a level of solution saturation in the near-wall region at the end of the steam-generating tube, resulting in salt precipitation and temperature increase. These were recorded with a PSI-10 automatic potentiometer. In the experiments under these conditions, the wall temperature at the end of the tube rapidly increased to 500°C, and in some experiments to 650-700°C (red hot). Then the load was removed and the experiment was stopped. The results obtained (Figure 13) established these operation limits for K_2CO_3 solution boiling at $p = 50$ bar and $p_w = 200$ kg/m²s.

The experiment showed that under the test conditions a 75% solution can be produced only at heat fluxes below 70 kW/m². With an increase in the intensity of heating the deposition of salt on the heating surface began at lower solution concentrations in the core of the flow: at $q = 120$ kW/m² this maximum permissible concentration was $C_{K_2CO_3} = 73.5\%$ and at $q = 150$ kW/m² was

$C_{K_2CO_3} = 72\%$. This circumstance should be taken into account in the selection of working parameters for the solution evaporation system; one should strive to reduce the gradient of solution concentration across the tube section by restricting the heat flux value. It is also possible to approach the problem by raising the operating pressure, i.e., increasing the concentration of the saturated solution: in experiments where $P = 98$ and 147 bar, salt deposition did not occur even up to a 75% solution concentration with $q = 130 \text{ kW/m}^2$.

The economy of the seed injection system using this type of K_2CO_3 solution depends on the possibility of using the steam (formed during solution production) in the steam cycle of the plant, and this in turn depends on the purity of the steam. An experimental estimate of the K_2CO_3 entrainment with the steam was made simultaneously with the experiments on solution evaporation. For this purpose the steam leaving the separator was condensed in the condenser and the condensate was analyzed. The analysis results are given in Table V.

It follows from the data of the table that the amount of K_2CO_3 in the condensate changes little with a change in pressure, remaining at the $10\text{-}30 \text{ mg/litre}$ level for solution concentrations of $30\text{-}60\%$ over the entire investigated range of P .

Apparently, one of the causes (but only at low pressures) of potassium carbonate contamination of steam was mechanical entrainment. The velocity of the steam in the separator, 2 cm/s at 10 bar and 0.4 cm/s at 49 bar contributed to this, and the vapor space varied from 0.3 to 0.6 m (without including the effect of swelling). With an increase in pressure to 98 and 147 bar the steam velocity fell to 2 and 1 mm/s , respectively, which contributed to a reduction in mechanical entrainment, but at these pressures the solubility of K_2CO_3 in water vapor should have increased and remained significant. This salt level significantly exceeds the limits imposed on the purity of steam in thermal

power plants, thus the steam cannot be used in the turbine without a preliminary wash with condensate. Other ways of economical steam utilization are also possible.

On the whole, the results of the experimental study of the K_2CO_3 solution evaporation process in a steam-generating tube appear to be quite promising, encouraging further search for a favorable resolution of the problems connected with the technology of producing large amounts of high-concentration K_2CO_3 solutions and the rational recovery of the generated steam. The system for the production and injection of a 75% K_2CO_3 solution built at the U-02 facility supported this conclusion.

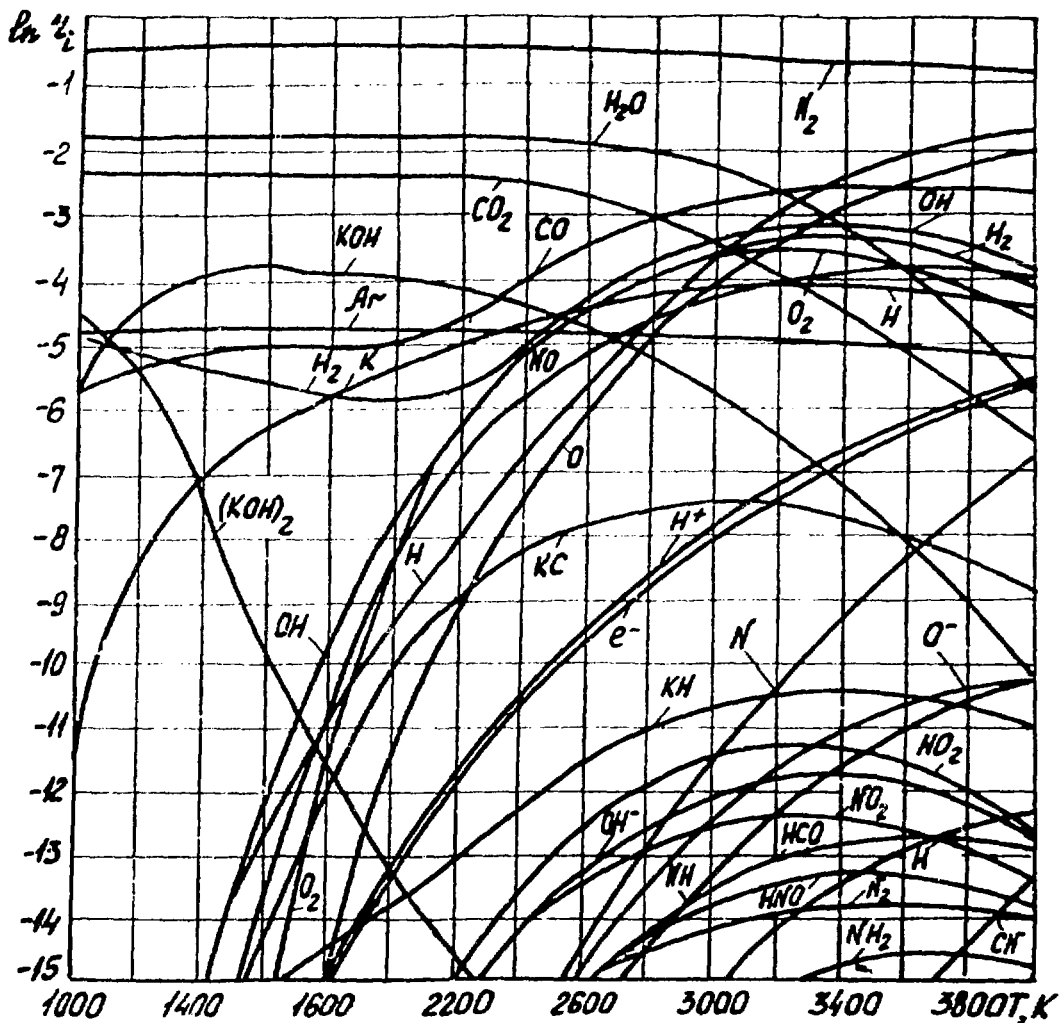


Figure 1. The composition of the products from the combustion of methane in atmospheric air with 1 atom % potassium.

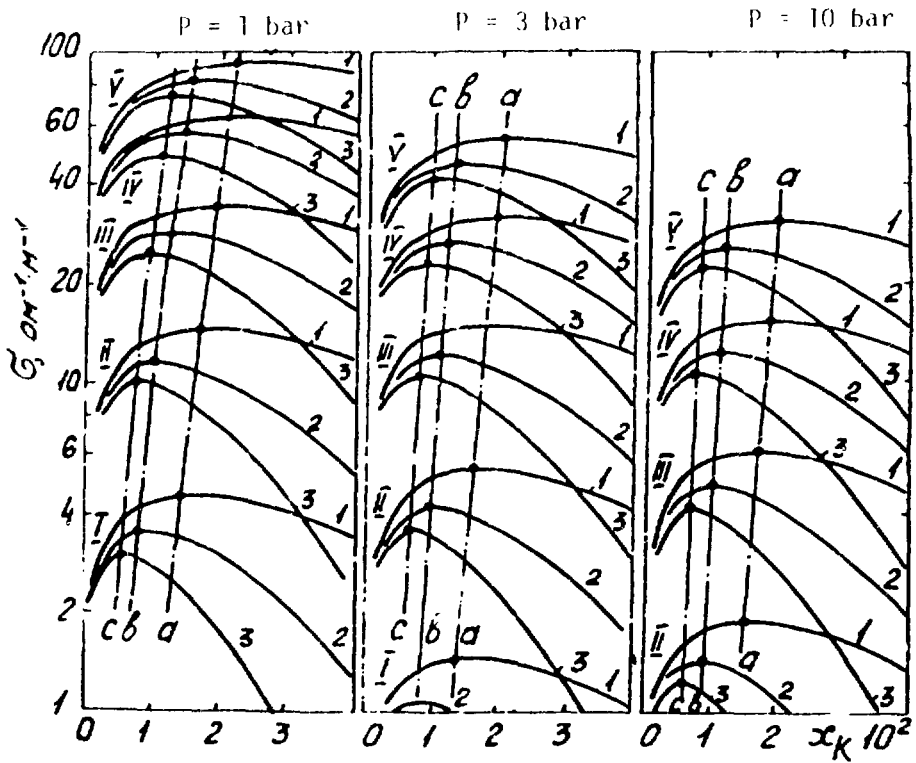


Figure 2. The dependence of the electrical conductivity of the combustion products σ_0 on the concentration of injected seed x_K ; $x_{O_2} = 0.21$

$\text{I} - T_0 = 2400 \text{ K}; \text{II} - T_0 = 2600 \text{ K}; \text{III} - T_0 = 2800 \text{ K};$
 $\text{IV} - T_0 = 3000 \text{ K}; \text{V} - T_0 = 3200 \text{ K},$
 $1 - C_{H_2O} = 0; 2 - C_{H_2O} = 0.5; 3 - C_{H_2O} = 1$

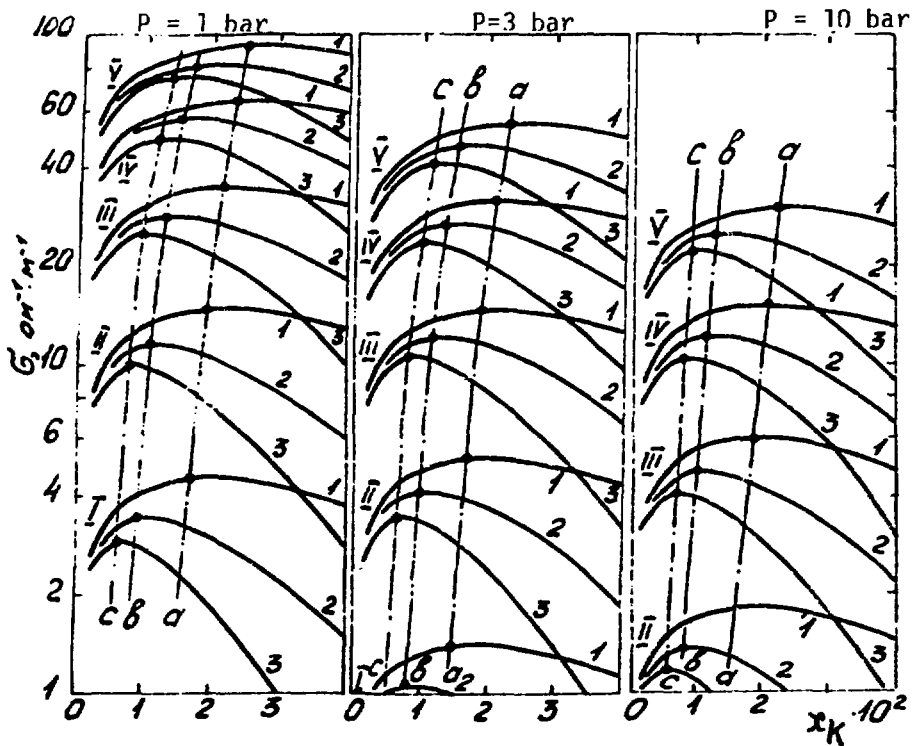


Figure 3. The dependence of the electrical conductivity of the combustion products σ on the concentration of injected seed x_K ; $x_{O_2} = 0.30$.

I - $T_0 = 2400$ K; **II** - $T_0 = 2600$ K; **III** - $T_0 = 2800$ K;
IV - $T_0 = 3000$ K; **V** - $T_0 = 3200$ K
 1 - $C_{H_2O} = 0$, 2 - $C_{H_2O} = 0,5$, 3 - $C_{H_2O} = 1,0$

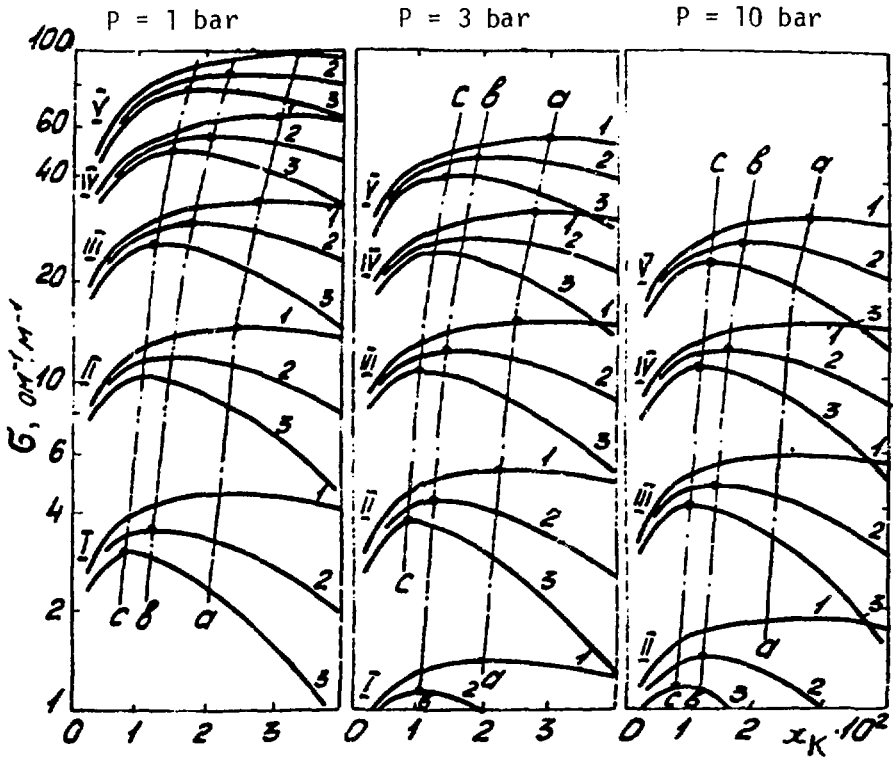


Figure 4. The dependence of the electrical conductivity of the combustion products σ on the concentration of injected seed x_K ; $x_{O_2} = 0.40$.

$\text{I} - T_0 = 2400 \text{ K}, \text{II} - T_0 = 2600 \text{ K}, \text{III} - T_0 = 2800 \text{ K},$
 $\text{IV} - T_0 = 3000 \text{ K}, \text{V} - T_0 = 3200 \text{ K}.$
 $1 - \text{CH}_2\text{O} = 0, 2 - \text{CH}_2\text{O} = 0.5, 3 - \text{CH}_2\text{O} = 1.0$

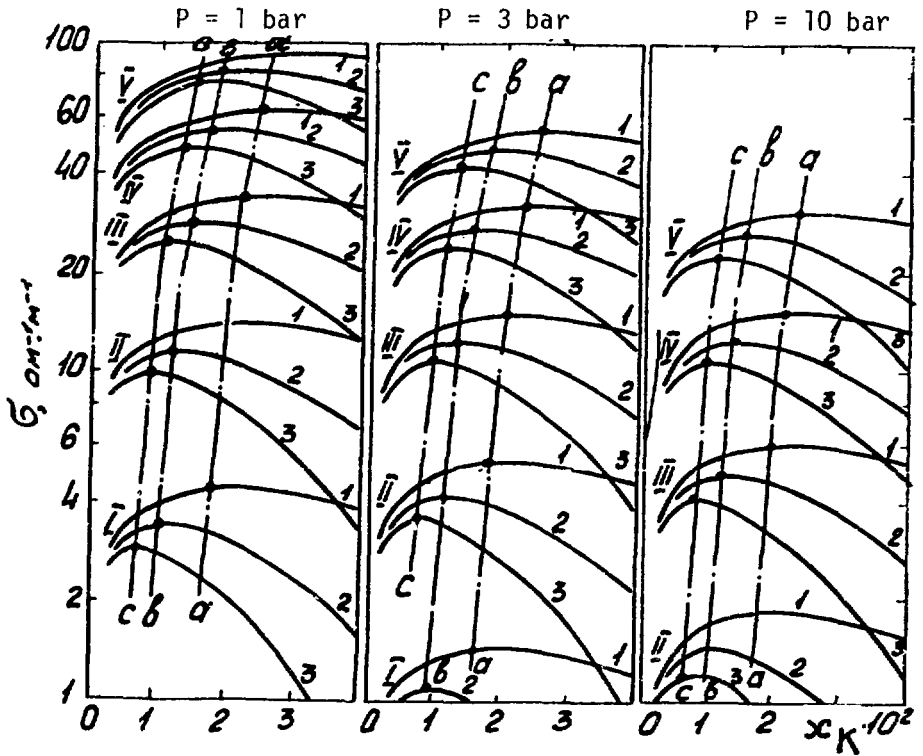


Figure 5. The dependence of the electrical conductivity of the combustion products σ on the concentration of injected seed x_K ; $x_{O_2} = 0.050$.

I - $T_0 = 2400$ K, II - $T_0 = 2600$ K, III - $T_0 = 2800$ K,
 IV - $T_0 = 3000$ K, V - $T_0 = 3200$ K
 1 - $C_{H_2O} = 0$, 2 - $C_{H_2O} = 0.5$, 3 - $C_{H_2O} = 1.0$

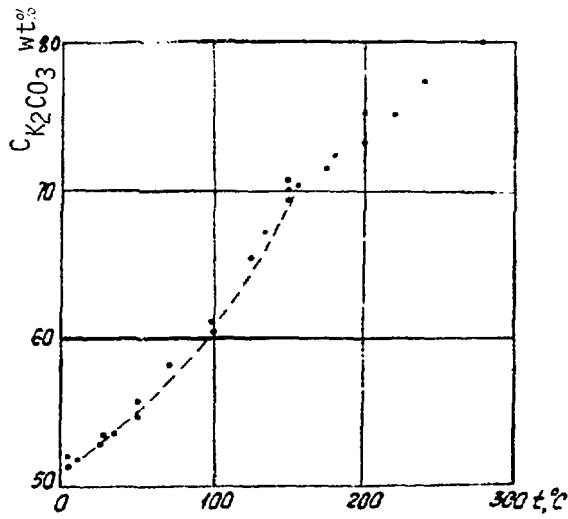


Figure 6. The solubility of K_2CO_3 in water.

- - Experimental data of various authors
- - Most probably values

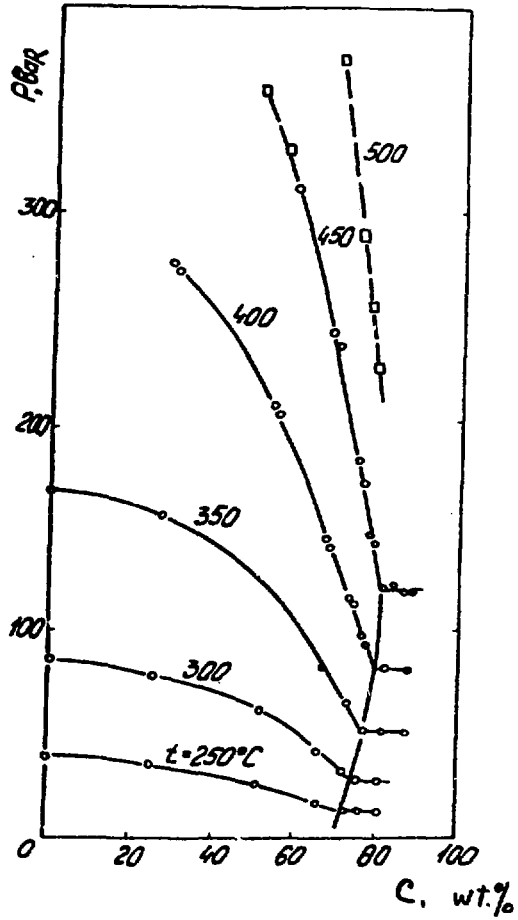


Figure 7. Pressure-composition-temperature diagram for boiling aqueous K_2CO_3 solutions.

- - Experimental data
- - Extrapolation of isobars

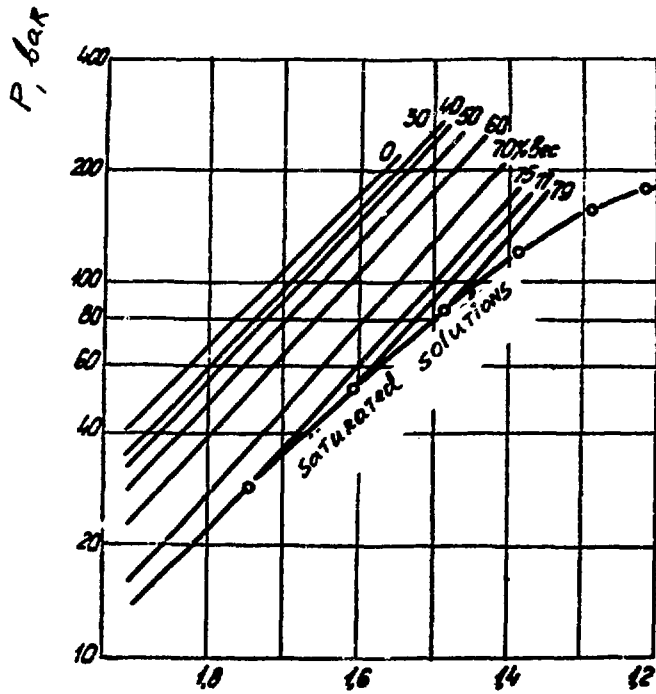


Figure 8. The dependence of pressure on reciprocal temperature for boiling aqueous K_2CO_3 solutions.

Numbers on isoconcentrational curves = amount of K_2CO_3 , wt %.

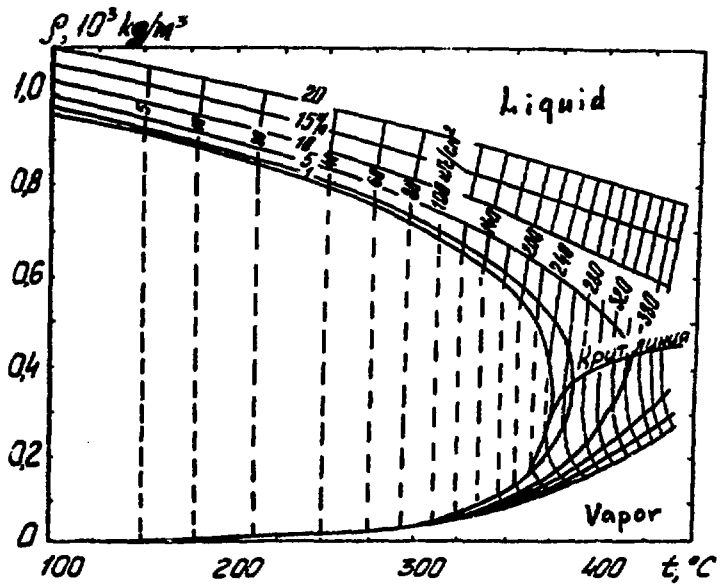


Figure 9. Phase equilibrium diagram for the KCl-H₂O system.

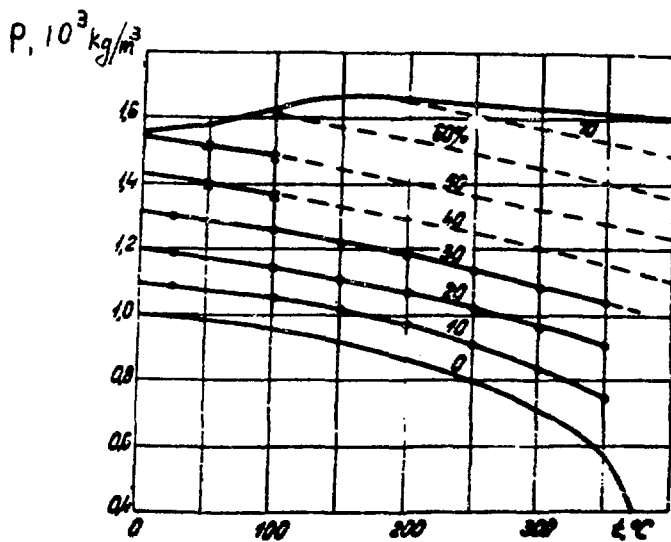


Figure 10. The dependence of the density of boiling solutions of K_2CO_3 on temperature and concentration.

● - data of [19]; x - data of [20]; --- - extrapolation

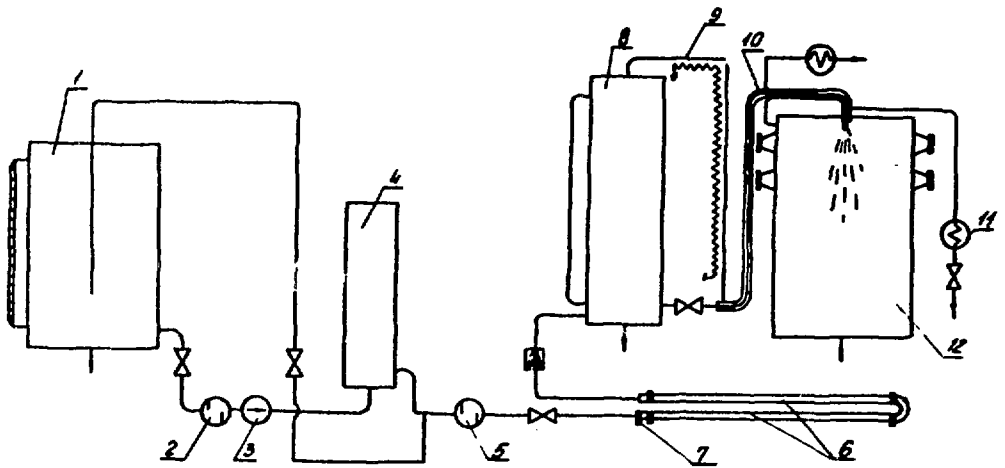


Figure 11. Diagram of experimental facility for study of the K_2CO_3 solution.

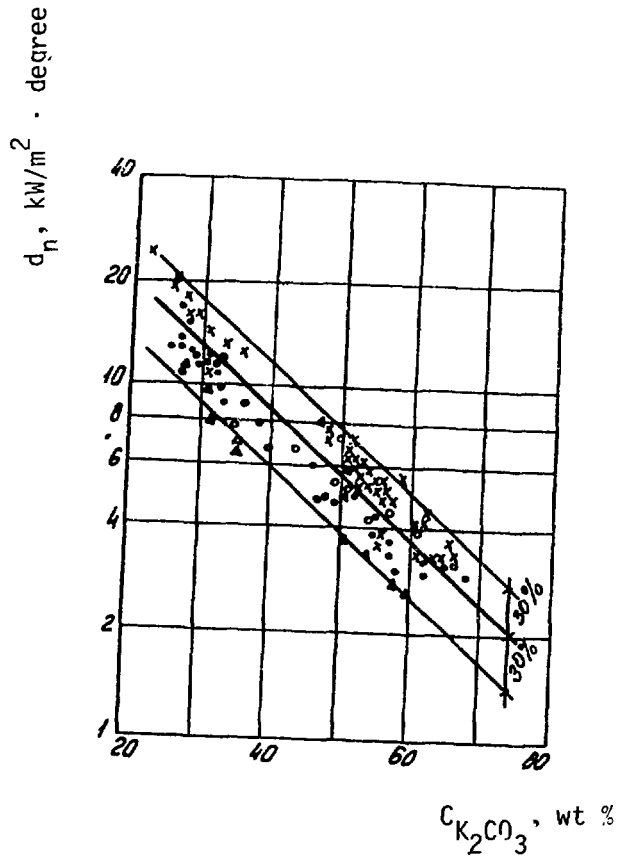


Figure 12. The dependence of the heat transfer coefficient on concentration in the boiling K_2CO_3 solution.

- \circ - $P = 10 \text{ bar}$; \times - $P = 49 \text{ bar}$;
- \circ - $P = 98 \text{ bar}$; \triangle - $P = 147 \text{ bar}$

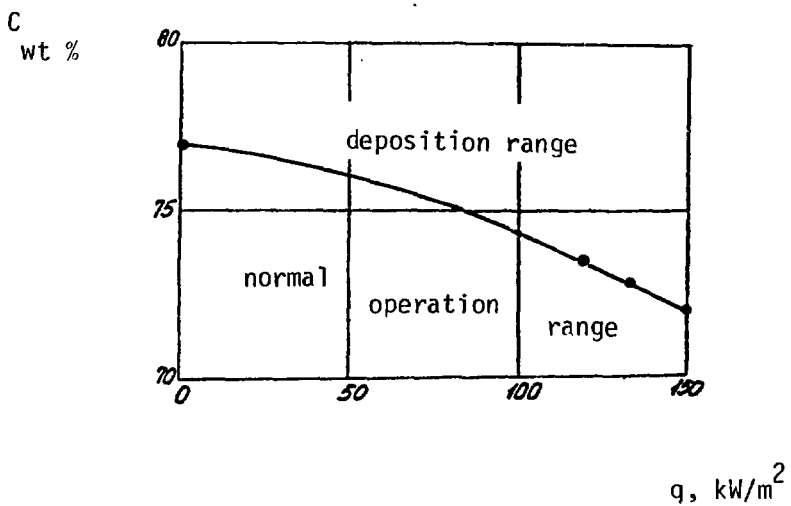


Figure 13. The limit of the beginning of salt deposition in the boiling aqueous solution of K_2CO_3 .

Table 1. Ionization potentials of elements (eV).

Chemical element	Li	Na	K	Rb	Cs
Ionization potential	5.390	5.138	4.339	4.176	3.893
Chemical element	Be	Mg	Ca	Sr	Ba
Ionization potential	9.320	7.644	6.111	5.692	5.210
Chemical element	C	S	Al	Fe	Si
Ionization potential	11.264	10.357	5.984	7.90	8.149
Chemical element	H	N	O	Ar	He
Ionization potential	13.54	14.51	13.57	15.755	24.58

Table II. Vapor pressure of aqueous solutions of potassium carbonate.

K_2CO_3 liquid phase, wt %	P, bar	K_2CO_3 liquid phase, wt %	P, bar	K_2CO_3 liquid phase, wt %	P, bar	K_2CO_3 liquid phase, wt %	P, bar	K_2CO_3 liquid phase, wt %	P, bar
250°C		300°C		350°C		400°C		450°C	
25,2	35,2	25,6	78,0	26,9	134,0	30,0	278,0	58,8	310
51,1	26,9	51,7	61,0	53,1	120,0	55,0	202,5	69,7	236
65,6	17,4	66,0	41,5	66,5	83,0	67,9	139,8	76,1	170
71,7	13,5	72,0	32,5	72,7	64,2	74,0	110,3	78,7	142
72,6	12,8	76,0	27,5	76,5	52,5	77,1	93,2	83,6	120
80,6	12,3	81,0	27,5	81,2	51,4	82,2	82,0	88,5	118
80,8	12,3	85,9	27,2	86,5	50,2	87,2	80,7		

-42-

$$\frac{K_2CO_3 \cdot 100}{K_2CO_3 + H_2O}, \%$$

Note: The data shown below the line correspond to a saturated solution containing solid phase, and the numerical values refer to the weight percent based on the carbonate and water introduced.

Table III. Solubility and vapor pressure of saturated aqueous solutions of potassium carbonate.

Temperature, °C	Solution concentration $C_{K_2CO_3}$, wt %	Pressure P, bar
250	73	12,5
300	75	27,6
350	77	50
400	79	81
450	81	120
500		147
550		176
600		191

Approximate
Values

Table IV. Boiling point of aqueous K_2CO_3 solutions and the heat of water evaporation from these solutions.

Solution concentration, wt %	Temperature, °C	Heat of vaporization of water r, kJ/kg	Solution concentration, wt %	Temperature, °C	Heat of vaporization of water r, kJ/kg
	P = 4,9 bar		70	320	2102
30	160	2158	75	342	2156
40	165	2197		P = 98 bar	
50	171	2242	30	315	1482
60	182	2292	40	322	1573
70	198	2343	50	331	1669
	P = 9,8 bar		60	350	1806
30	188	2093	70	372	1932
40	193	2140	75	394	2007
50	200	2190		P = 147 bar	
60	211	2245	30	346	1212
70	230	2303	40	352	1322
	P = 19,6 bar		50	362	1454
30	221	2000	60	379	1612
40	226	2053	70	407	1797
50	233	2108	75	429	1886
60	245	2169		P = 196 bar	
70	265	2238	30	370	960
	P = 49 bar		40	376	1100
30	270	1779	50	387	1276
40	276	1849	60	400	1435
50	284	1919	70	434	1679
60	298	2004	75	457	1787

Table V. Amount of K_2CO_3 in the condensate of steam produced in the evaporation of a solution.

Pressure, bar	10	49	98	147		
Solution concentration, wt % K_2CO_3	36-40	55-58	29-34	33-40	35-43	55-57
Amount of K_2CO_3 in condensate, mg/l	13.7	12.4	18.6	25.1	20.1	32.4

Chapter 2

The Ionizing Seed in the Combustion Chamber of an MHD Facility

1. Seed vaporization in the combustion chamber

Ionizing seed must be vaporized, dissociated and should maximally approach the thermodynamically balanced degree of ionization by the time it enters an MHD channel. At the same time it must be well mixed with the combustion products and be evenly distributed over the cross section of the channel. The most convenient point for injecting the seed is the combustion chamber, where reverse and vortex flows ensure vigorous mixing with the combustion products, and the high combustion temperatures accelerate the physical and chemical processes and ionization. The completeness of the seed dissociation and ionization processes depends on its particle size and residence time in the combustion chamber, which is determined primarily by the rate of the combustion process. An increase of this rate is undesirable, because it would require the lengthening of the combustion chamber and would lead to increased thermal losses. Thus, the only active way to promote acceleration of the seed ionization process, is to decrease the seed particle size.

Ionizing seed injected into the combustion chamber as fine particles of K_2CO_3 or droplets of its aqueous solution, heats, melts, vaporizes, dissociates, and is ionized by the hot gases (2800-3200 K). The sequence of these steps up to vaporization can be represented in the following manner (Figure 14): particles of dry K_2CO_3 powder (curve 1, Figure 14) are at first heated during time τ_1' to the melting point of this substance, i.e., to 901°C, then during time τ_2' the particles melt and become liquid droplets, which during time τ_3' are heated to the equilibrium temperature of vaporization and vaporize during time τ_4' . As the K_2CO_3 vaporizes it diffuses into

the combustion products, mixes with them and dissociates, forming atomic potassium, which is then ionized.*

There are no data on the coefficient of linear expansion for K_2CO_3 . However, by analogy with other crystalline substances, one can expect that it is not large. This makes it possible to neglect the change in the diameter of the particles during their heat-up. The process of melting monolithic particle also does not make a significant change in d_0 . According to [26] the density of a K_2CO_3 melt at $901^\circ C$ is 1900 kg/m^3 , i.e., only about 20% less than the density of the solid at $t = 20^\circ C$. Such a change in the density causes a 6% increase in the diameter of the particle, which does not have a significant effect on the vaporization process. Therefore, one can assume that the first three steps of the process occur at constant particle size, and only in the fourth step (vaporization) does its size change from d_0 to 0.

When the seed is injected as an aqueous potassium carbonate solution (curve 2, Figure 14), the droplets are heated during time τ_1 to the equilibrium temperature of vaporization of water from solution. With the large thermal flows typical for the combustion chambers of MHD facilities, this temperature is near the boiling point of the solutions. As the water vaporizes during τ_2 , the droplet temperature rises somewhat because of the increase in concentration, until the solution becomes saturated and release of solid phase begins. However, this change in the temperature is small compared to the temperature of the combustion products: if a 50% K_2CO_3 solution is intro-

* Although, in conformity with [13], K_2CO_3 dissociation can begin at substantially lower temperatures than the equilibrium temperature of vaporization, in order to simplify the design concept and the seed vaporization calculations this process will be ignored for the time being in the liquid phase and will be wholly transferred to the vapor phase of K_2CO_3 , sufficiently far removed from the surface of the droplet.

duced, this temperature change is about 20°C, or still less if more highly concentrated solutions are injected. Therefore, in calculations this temperature can be assumed to be constant.

The process of conversion from a droplet to a solid particle is very complex and has been little investigated. For the present we will assume that vaporization of the water results in a solid spherical particle with a density corresponding to that of the solid substance, i.e., $\rho = 2400 \text{ kg/m}^3$. Next, the sphere is heated to the melting point during τ_3'' with subsequent melting in τ_4'' . After this, during the τ_5'' time the liquid droplet is heated to the equilibrium temperature of vaporization and, finally, it vaporizes during the τ_6'' . The last four steps are analogous to the steps of heat-up, melting and vaporization of a solid K_2CO_3 particle introduced into the combustion chamber (curve 1, Figure 14), but if the particle and the droplet are assumed to have the same size, in the second case there is a step of preliminary change in the size of the particle (water vaporization) from d_0 to d_1 , and therefore the time segments τ'' are smaller than the corresponding segments τ' . This stepwise character of the vaporization process fits the case of very high thermal conductivity in the droplet (particle) material, i.e., $\lambda_{dr} = \infty$.

Accordingly, calculations were made of the ionizing seed particle (droplet) vaporization time in the combustion chamber based on the following proposition:

Heat is transferred to the particle by convection and radiation:

$Q = Q_c + Q_r$. In order to simplify the calculations the relative gas velocity is ignored during the first stage, i.e., we consider the droplet to be carried by the gas flow. In this case the value of the Nusselt number can be assumed to be constant, equal to 2.* Then, assuming that the droplet (particle) is

* In [27] the authors assume $Nu = 3$, thereby taking into account the high gas flow turbulence in the combustion chamber.

spherical in form, we have

$$Q_c = 2\pi\lambda_{cp} d_{dr} (T_{cp} - T_{dr}), \quad (10)$$

where λ_{cp} is the thermal conductivity of the combustion products at the average temperature of the boundary layer W/m · degree;

d_{dr} is the droplet (particle) diameter, m;

T_{cp} and T_{dr} are the temperatures of the combustion products and the droplet (particle), respectively, K

The radiation flow to such droplet (particle) is equal to

$$Q_r = \pi C_a \epsilon a_{cc} d_{dr}^2 (T_{cp}^4 - T_{dr}^4), \quad (11)$$

where

C_a is Boltzmann's constant;

ϵ is the spectral emissivity of the droplet;

a_{cc} is a coefficient, encompassing the radiation conditions in this particular combustion chamber (field of temperatures and concentrations, thickness of radiating layer, its composition and dust content, the influence of the walls, etc.)

Formulas (10) and (11) can be used to determine the time of droplet (particle) heat-up in segments of constant size with the condition $\lambda_{dr} = \infty$ ($Bi = 0$), i.e., without including in the calculation the variability of the droplet heat-up:

$$\Delta T_i = \frac{\pi C_{dr} \rho_{dr} d_{dr}^3 (T_{i+1} - T_i)}{6 (Q_r + Q_c)}, \quad (12)$$

where

C_{dr} is the specific heat capacity of the droplet (particle), J/kg · degree;

T_i and T_{i+1} are the temperatures of the droplet (particle) before and after heat-up, K;

ρ_{dr} is the density of K_2CO_3 or its aqueous solution, kg/m^3 ,

During the evaporation of water from a droplet of solution or the vaporization of K_2CO_3 from the surface of a molten droplet in the combustion chambers of MHD units, the liquid passes into a gaseous state, producing a flow of vapor from the surface, and cooling the boundary layer around the droplet. At the high evaporation rate characteristic in these conditions, the cooling factor can have a significant effect on the value of Q_c and consequently on the rate of evaporation.

The equation for the thermal balance of an evaporating droplet with constant thermal-physical properties of the gas in the boundary layer, without consideration of the radiation flow, has the following form:

$$\frac{d^2T}{d\bar{r}^2} + \left[\frac{\lambda}{\bar{r}} - \frac{WC_{v1}}{4\pi\lambda\bar{r}^2} \right] \frac{dT}{d\bar{r}} = 0, \quad (13)$$

where

w is the rate of droplet evaporation, kg/s ;

d_{dr} is the droplet diameter, m ;

\bar{r} is a dummy radial coordinate, m ;

C_{v1} is the specific heat capacity of the vapor for $P = \text{const}$, $J/kg \cdot \text{degree}$;

λ is the thermal conductivity of the gas in the boundary layer, $W/m \cdot \text{degree}$;

ρ_{dr} is the density of the droplet, kg/m^3 .

Equation (13) is solved for the boundary conditions:

- At the droplet surface $\bar{r} = d_{dr}/2 = \bar{r}_{dr}$, $T = T_{dr}$

- Beyond the limits of the boundary layer $\bar{r} > \bar{r}_0$, $T = T_g$

It is valid for $\lambda = \text{const}$. In fact, the thermal conductivity of the gas is a function of its temperature and of the vapor concentration of the substance

being vaporized. Therefore, in order to avoid complications certain average effective thermal conductivity for the boundary layer λ^* is used. Then the solution of equation (13) will be

$$\frac{T - T_{dr}}{T_g - T_{dr}} = \frac{\exp(-a\bar{r}_{dr}/\bar{r}) - \exp(-a)}{\exp(-a\bar{r}_{dr}/\bar{r}_0) - \exp(-a)}, \quad (16)$$

where

$$a = \frac{Wc_v}{4\pi\lambda^*\bar{r}_{dr}} = \frac{Nu_0 c_{pm} (T_g - T_{dr})}{z}, \quad (17)$$

r is the heat of vaporization, J/kg

Equation (16) can be differentiated to find the temperature gradient at the droplet surface:

$$\left. \frac{dT}{d\bar{r}} \right|_{\bar{r}_k} = \frac{a(T_p - T_k)}{\bar{r}_k} \left\{ \exp\left[a\left(1 - \frac{\bar{r}_k}{\bar{r}_0}\right)\right] - 1 \right\}. \quad (18)$$

The thermal balance at the droplet surface is expressed by the equality

$$4\pi\lambda^*\bar{r}_k^2 \left. \frac{dT}{d\bar{r}} \right|_{\bar{r}_{dr}} = Wz. \quad (19)$$

From equations (16) and (19), taking into account $1 - \bar{r}_{dr}/\bar{r}_0 = 1/Nu_0$, after algebraic transposition we obtain the correction factor recommended by Spalding [28] for the vapor flow from the droplet surface:

$$\frac{Nu}{Nu_0} = \frac{Co(1+B)}{B}, \quad (20)$$

where Nu and Nu_0 are Nusselt numbers for the droplet with and without vapor flow;

B is the mass driving force
$$\frac{c_{vl} (\pi_g - \pi_{dr})}{z}$$
.

And although, strictly speaking, correction factor (20) does not consider the change in the thermal-physical properties in the boundary layer and requires the use of some "effective" values for them, we will use it in the subsequent calculations of the seed droplet vaporization.

The equation of thermal balance for a vaporizing droplet, including the radiation flow, can be represented in the following form:

(21)

$$(Q_r + Q_c) d\tau = \frac{\pi}{z} \rho_{dr} r d_{dr}^2 \frac{dd_{dr}}{d\tau}$$

where

ρ_{dr} is the density of the vaporizing substance (the K_2CO_3 melt or water from the solution), kg/m^3 ;

r is the heat of vaporization of this substance, J/kg ;

d_{dr} is the droplet diameter, m ;

τ is the time of vaporization, s .

The value of Q_r is computed from formula (11) and that of Q_c by formula (10) with consideration of the correction factor for the outflow of vapor:

(22)

$$Q_c = 2\pi r_{cp} d_{dr} (\pi_p - \pi_{dr}) \frac{ca(1+B)}{B}$$

Substituting the values for Q_r and Q_c into equation (21) and solving it relative to $d\tau$, we obtain

$$d\tau = \frac{\rho_{dr}^2}{2C_0 \epsilon \alpha_{cc} (T_{cp}^4 - T_{dr}^4)} \cdot \frac{d_{dr} dd_{dr}}{2\lambda_{cp} (T_{cp} - T_{dr}) \ln(1+B) + d_{dr}} \quad (23)$$

If one assumes that droplet vaporization progresses at a constant temperature T_{dr} , then integration of this equation makes it possible to determine the droplet evaporation time $\Delta\tau$; during this time its size changes from d_0 to d_{dr} :

$$\Delta\tau = \frac{\rho_{dr}^2}{2C_0 \epsilon \alpha_{cc} (T_{cp}^4 - T_{dr}^4)} \cdot \left[d_0 - d_{dr} - K \ln \left| \frac{1 + \frac{d_0}{K}}{1 + \frac{d_{dr}}{K}} \right| \right], \quad (24)$$

where

$$K = \frac{2\lambda_{cp} (T_{cp} - T_{dr}) \ln(1+B)}{C_0 \epsilon \alpha_{cc} (T_{cp}^4 - T_{dr}^4) \cdot B}$$

The only unknown value in expression (24) is the equilibrium temperature of droplet evaporation T_{dr} , which is determined from the equation of the droplet thermal balance:

$$\alpha_0 (T_{cp} - T_{dr}) \frac{\ln(1+B)}{B} + C_0 \epsilon \alpha_{cc} (T_{cp}^4 - T_{dr}^4) = \beta (C_M - C_{\infty}) \cdot z, \quad (25)^*$$

or

$$\alpha_0 = \frac{2\lambda_{cp}}{d_{dr}}, \quad \beta = \frac{2D}{d_{dr}}$$

λ_{cp} , D are the thermal conductivity of the combustion products and the diffusion coefficient of K_2CO_3 vapor in them, related to the average temperature of the boundary layer, in $W/m \cdot \text{degree}$ and m^2/s , respectively. As the

* Two formulae (25) in Russian text. Tr.

calculations showed the value of T_{dr} is determined basically by the temperature of the combustion products and by the dependence of $C_{пк}$ on T_{dr} , remaining practically constant in the process of droplet vaporization.

Equations (12) and (24) were used to calculate the duration of the sequential stages of heating, melting and vaporization of seed particles (droplets). The results are given in Figure 14.

It follows from the data of Figure 14 that the heating of K_2CO_3 particles or of aqueous solution droplets with an initial diameter of 100 μ , takes place in a relatively short period of time. The greater portion of the time is consumed by water evaporation from the droplet and, primarily, by the vaporization of the K_2CO_3 itself. Thus, if a particle K_2CO_3 of this diameter is vaporized in 32 ms, then only 12 ms are required for the melting and heat-up, i.e., less than 40%. In the case where an aqueous K_2CO_3 solution is injected, 6 ms are required to evaporate the water contained in a droplet 100 μ in diameter, and 10 ms are required to vaporize the K_2CO_3 with a total time of 22 ms. The time required for complete vaporization decreases with a reduction in the initial droplet size, but the time ratio of separate stages is preserved rather well.

A reduction of the combustion products temperature has almost no effect on the stages of water evaporation and of the heating and melting of the K_2CO_3 particles, but significantly increases the vaporization period of the actual K_2CO_3 .

Let us recall that all these calculations were based on the following assumptions:

- 1) The droplet is stationary with respect to the combustion products;
- 2) When the water is evaporated from the droplet of K_2CO_3 solution, a solid particle with a density of 2400 kg/m^3 is produced;

3) The process occurs with a clear separation of the steps:

heating - water evaporation - heating - melting - K_2CO_3 vaporization,
i.e., for $Bi_{dr} = \infty$ ($Bi = 0$);

4) Decomposition of the K_2CO_3 occurs in the vapor phase beyond the limits of the boundary layer.

Since reality may fail to support these assumptions, an attempt will be made to estimate the resultant error.

The effect of the initial velocity of the droplet can be manifested in the area of deceleration. In the case of a droplet of d_{dr} diameter sprayed from the jet nozzle at a relative velocity W_0 , the deceleration process with the conditions of constant mass (heating of the droplet or particle and its melting) and the absence of a newly-formed vapor flow is described by the following equation

$$m \cdot \frac{dW}{dz} = mg \frac{\rho_{dr} \rho_g}{\rho_{dr}} - \frac{\pi}{8} C_{dr} W^2 \rho_g d_{dr}^2 \quad (25)^*$$

where

m is the mass of the droplet, kg;

ρ_{dr}, ρ_g are the densities of the droplet and gas, kg/m^3 .

C_{dr} is the coefficient of resistance of the droplet, calculated for $Re = 1-100$ using the formula

$$C_{dr} = \frac{24}{Re} + \frac{4,4}{Re^{0,5}} + 0,32.$$

If gravitational forces are neglected, then

$$m \frac{dW}{dz} = - \frac{\pi C_{dr} W^2 \rho_g d_{dr}^2}{8} \quad (26)$$

* See note in page 53. Tr.

Numerically integrating this equation from W_0 to W , we obtain the time of droplet deceleration. Thus, for droplet deceleration with $\alpha_{dr} = 100$ in MHD facility combustion chamber ($P = 1 \text{ kg/cm}^2$, $T_{cp} = 3000 \text{ K}$) the relative velocity falls from 100 to 10 m/s in approximately 13 s. Meanwhile the dimensionless heat transfer coefficient Nu_0 decreases from 4 to 2.6, i.e., during a rather lengthy period (13 out of 22 ms, Figure 14) and the heat exchange rate remains substantially higher than that assumed above. Approximately the same ratio of the vaporization and deceleration times is preserved for droplets of other sizes.

The influence of the relative droplet velocity can be taken into account, in a first approximation, by calculating the degree of deceleration in each of the heating and vaporization stages and by subsequent determination of the average value of Nu_0 for the period in question. This influence will be felt most strongly in the early stages, i.e., the periods of heating the droplets of solution, evaporating the water, and also the heating and melting of the resultant particle and the subsequent heating of the K_2CO_3 droplet. The relative velocity of the droplet has much less effect on the process of K_2CO_3 vaporization when the seed is injected in solution.

If the seed is injected as solid K_2CO_3 particles with a density of 2400 kg/m^3 , the deceleration will progress more slowly and the influence of the relative particle (droplet) velocity will be felt over a longer period of time.

This method of accounting for the relative velocity was used in calculations of the total seed droplet (particle) vaporization time in the MHD facility combustor and subsequently for comparison of calculation with experiment.

A more rigorous solution of the problem involving the deceleration of a vaporizing droplet in a hot gas flow was also obtained. In this instance the problem is reduced to the solution of an equation system of heat-mass exchange

$$\frac{dd_{dr}}{dt} = - \frac{2Nu\lambda_{cp}(T_{cp} - T_{dr})}{\rho_{dr} d_{dr}}, \quad (27)$$

and of hydrodynamics

$$\frac{dw}{dt} = - \frac{3}{4} C_{dr} \frac{\rho_{cp}}{\rho_{dr}} \cdot \frac{W^2}{d_{dr}}, \quad (28)$$

where λ_{cp} - heat conductivity of combustion products in the boundary layer, W/m · degree

ρ_{cp} , ρ_{dr} - density of combustion products and seed droplet, respectively, in kg/m³

d_3 and C_{dr} - diameter and resistance coefficient of the droplet with the initial conditions

$$t = 0, d_{dr} = d_0, W = W_0. \quad (29)$$

Considering the process of pure liquid evaporation, the following empirical dependences are assumed as dimensionless coefficients of mass exchange and resistance:

$$Nu = (2 + 0,6 Re^{0,5} Pr^{1/3}) \frac{Pr^{(1+B)}}{B} \quad (30)$$

(31)

$$C_{dr} = \frac{24}{Re} + \frac{4,4}{Re^{0,5}} + 0,32 .$$

in accordance with reference [29] there is no great effect of the transverse flow on the full resistance of sphere in these conditions. The system of equations (27) - (29) was solved using a specially developed method, based on the selection of the slowly changing functions.

The solution has the following form:

$$\Delta \tau = A d_0^2 \Phi(\kappa, \mu) \left[1 - \frac{\Phi(\kappa \tilde{d}_{dr}, \mu)}{\Phi(\kappa, \mu)} \cdot \tilde{d}_{dr}^2 \right], \quad (32)$$

$$\tilde{W} = \tilde{d}_{dr} \frac{dw}{dr}, \quad (33)$$

where:

\tilde{d}_{dr} , w are the dimensionless diameter and velocity of the droplet (relative to the initial values);

A, C_1, μ are certain clusters of parameters, which depend on the properties of the gas and substance of the droplet.

$$A = \frac{\rho_{dr} \nu B}{8 \lambda_{cp} (T_{cp} - T_{dr}) \ln(1+B)},$$

$$C = \frac{8 \lambda_{cp} (T_{cp} - T_{dr}) \ln(1+B)}{3 \gamma_{cp} \rho_{cp} \nu B},$$

$$\mu = \frac{4 C_1 \mathcal{X}_0}{12 + C_1 \mathcal{X}_0},$$

$$K = 0.3 Re_0^{0.5} Pr^{1/3},$$

$$\mathcal{X}_0 = \frac{1 + 0.3 Re_0^{1/2} Pr^{1/3}}{1 + 0.183 Re_0^{1/2} + 0.013 Re_0}.$$

Φ is a universal function, amenable to tabulation

$$\Phi(\mathcal{X}, \mu) = \begin{cases} \sum_{n=0}^{\infty} (-1)^n \frac{\mu}{n+\mu} \mathcal{X}^n; & \mathcal{X} \leq 1 \\ \frac{\pi \mu}{\sin \pi \mu} \mathcal{X}^{-\mu} + \sum_{n=1}^{\infty} (-1)^n \frac{\mu}{n-\mu} \mathcal{X}^{-n}; & \mathcal{X} > 1 \end{cases}$$

For a quiescent droplet $\Phi(\mathcal{X}, \mu) \rightarrow 1$ and expression (32) is simplified to the ordinary dependence

$$\Delta \mathcal{X} = A d_0^2 (1 - \tilde{a}_{dr}^2). \quad (34)$$

Figure 15 shows the results of the calculation of the vaporization of a potassium carbonate molten particle having a $d_0 = 100$ in a stream of combustion products when $w_0 = 100$ m/s, $T_{cp} = 3000$ K and $P = 10$ bar. Neglect

of the relative velocity and its change in the vaporization process can introduce a large error in the determination of complete vaporization time. Of course, this stage completes the vaporization and before it begins the relative particle velocity is, as a rule, small (substantially less than 100 m/s).

The influence of the porosity of the K_2CO_3 particle produced when the water is evaporated from the droplet of solution is felt in the process of droplet vaporization through an increase in the starting diameter and the reduction of thermal conductivity of the solid remainder. The dried particles usually have a spherical shape, but their density can vary over broad limits depending on the molecular structure of the solution and the mode of drying. The rate of moisture vaporization from droplets is dependent both on the external conditions of heat and mass transfer and on the movement of the solvent within the particle (especially after separation of solid phase). With high thermal flows the external surface of solution droplet rapidly becomes solid, and the passage of moisture through it becomes more difficult. Excess pressure is created inside the particle and because of vapor formation, the particle inflates and becomes hollow.

Unfortunately, there are no data on the process of the vaporization of a droplet of K_2CO_3 solution in the combustion chamber of MHD units, on the formation of the solid phase and the density of the particle produced. In order to simplify the simulation of this process, experiments were conducted involving boiling droplets of an aqueous K_2CO_3 solution in spheroidal state over a high-temperature surface. An experimental facility was built, having a working section consisting of a vertical solid cylinder 55 mm in diameter made of stainless steel, whose upper face had a spherical depression 47 mm in diameter and 5.8 mm deep. A droplet of the investigated solution was placed

on the lowest point of the depression with a medical syringe. A regulated electrical heater allowed the temperature of the cylinder to be raised to a level ensuring the formation of a spheroidal state of the droplet, where the liquid was separated from the heated surface by a layer of vapor. The behavior of the droplet during vaporization was recorded cinematographically on movie film.

Experiments were conducted with aqueous 20 and 50% K_2CO_3 solutions. The surface temperature varied from 200 to 600°C. The droplets were applied to the heated surface with medical syringes through needles with outside diameters of 1.53 and 0.34 mm. This produced droplets with 3.7 and 2.7 mm diameters.

Recording the droplet size on film made it possible to determine the dependence of liquid vaporization rate on the temperature of the heated surface and the size of the particles remaining after vaporization of the solvent. It was noted that a process of smooth reduction in the droplet size occurs only in the initial stage of vaporization, and only in droplets with a low K_2CO_3 concentration. Then the droplet begins to pulsate, alternating between a spherical shape and an oblate spheroid shape, at the same time producing "explosions" accompanied by the ejection of tiny droplets. Finally the solid residue remains, which is most often of a deformed spherical shape, porous and sometimes hollow. Its dimensions depend on the temperature of the hot surface and the initial solution concentration, but in any case they significantly exceed the dimensions of the dense nucleus with $\rho = 2400 \text{ kg/m}^3$ used by us in the calculations. Usually the diameter of the dry particles equals the starting diameter of the droplet and sometimes even exceeds it. If in the first approximation d_1 is assumed to be equal to d_0 , the average density of a particle will be 750 kg/m^3 and the relative porosity will be 70%.

It is known that the thermal conductivity of porous materials is significantly less than that of solid materials. In this case it may lead to a situation where the stages of particle heating, melting, heating to vaporization temperature and the actual vaporization will be accomplished practically simultaneously, i.e., because of the low thermal conductivity of the particle material ($\lambda_{dr} \approx 0$) the heating and melting zones will be located on the inner surface of a thin layer vaporizing from the external surface. In calculating the time of droplet vaporization under these conditions the term r in formula (24) should be replaced by the sum $[C'_{dr} (T_{fu} - T_1) + r_{fu} + C''_{dr} (T_{dr} - T_{fu}) + r]$, where T_1 , T_{fu} , T_K are the temperatures of moisture evaporation from the droplet, the melting point and the equilibrium temperature of droplet vaporization, K; C'_{dr} and C''_{dr} are the specific heat capacities of solid potassium carbonate and its melt, J/kg · degree; r_{fu} and r are the heats of melting and vaporization of K_2CO_3 , J/kg · $\rho_{dr} = 750 \text{ kg/m}^3$ should be used instead of $\rho = 2400 \text{ kg/m}^3$.

Calculations of the droplet vaporization process made by this method with consideration of the porosity of the particles obtained (with $d_1 = d_0$) showed that the total time virtually does not change: for a droplet of 50% solution with $d_0 = 100 \mu$ it proved to be 20 ms, versus 22 ms in the step-by-step calculation.

Since the first value corresponds to $\lambda_{dr} = 0$ and the second to $\lambda_{dr} = \infty$, while in fact the thermal conductivity of the particle has a finite, nonzero value, the time for complete droplet vaporization must fall between the calculated values. However, these values are similar, since the error resulting from both the neglect of the porosity and the size of the produced droplets as well as from the calculation method chosen for the process (for individual or combined stages) is evidently small. Thus, it is possible to conclude that

the proposed method (cf. Figure 14) can be used to calculate the total droplet vaporization time.

The results of calculations of the seed droplet (particle) vaporization in the combustion chamber of an MHD unit are shown in Figure 16 as dependences of the total vaporization time from the initial droplet (particle) diameter. A correction term for the relative velocity of the droplets in the hot gases was added in the calculation, i.e., for each stage of heating, melting, and vaporization an average dimensionless heat transfer number Nu was determined. The inclusion of the relative velocity led to a reduction of the calculated vaporization time value of K_2CO_3 droplet (particle) by, approximately, 30% (cf. Figure 14).

The time of total vaporization, including the heating and melting, decreases sharply with a reduction in the initial diameter of the particles (droplets): for particles with $d_0 = 50 \mu$, $\tau = 6$ ms; for droplets of the same size, $\tau = 4$ ms.

A reduction of T_{cp} to 2500 K causes a noticeable increase in the total droplet vaporization time (broken line, 3, Figure 16). Moreover, this increase is greater, the greater the initial diameter of the droplet, i.e., the lower the proportion of the convection component of the heat flow.

The seed introduced into the combustion chamber as an aqueous solution of K_2CO_3 is dispersed through a spray nozzle. This produces a size distribution of droplets with diameters differing by an order of magnitude and more. Since the time of droplet vaporization depends strongly on their size (in conformity with Figure 16 $\tau \sim d_0^{1.8 - 2.0}$), the fine droplets will evaporate rapidly, while the larger ones may not have had time to heat up. As a result, the process of seed vaporization becomes protracted. We will attempt to calculate the rate of this process, making the following assumptions:

1. The range of seed droplet size in the combustor is described by equations constructed for the case of a liquid dispersed in air under normal conditions.

2. The droplets are sufficiently far from each other, i.e., in calculating the vaporization of one droplet the influence of the neighboring droplets can be ignored.

3. The volumetric concentration of droplets in the gas stream is small, and other droplets do not affect the radiation heat flow to the surface of the droplet in question.

4. The change in temperature of the combustion products and the seed concentration in them during the vaporization process are ignored, i.e., just as in the calculation of a single droplet, we consider that $T_{cp} = \text{const}$ and $P_{K_2CO_3, \infty} = 0$.

5. In the calculations of the vaporization process the process scheme represented in Figure 14 will be used.

The droplet size distribution for any spray nozzle can be described by the Rozin-Ramler formula

(35)

$$G_{Si} = 1 - e^{-\left(\frac{d_{ki}}{\bar{d}_k}\right)^n},$$

where

G_{Si} is the total relative weight, i.e., the sum of the relative weights of all droplets with diameter less than or equal to d_{ki} ;

\bar{d}_k is a size constant;

n is a distribution constant.

The correlation between \bar{d}_k and n is given by the equation

(36)

$$\bar{d}_n = \frac{d_m}{(\ln 2)^{1/n}},$$

where d_m is the median droplet diameter.

The greater the value of d_k , the larger the droplets, the greater the value of n , the narrower is their size distribution. Constants d_k and n depend both on the design of the spray nozzle and on all parameters which determine the process of liquid dispersal. For a wide range of parameters the value of n varies over quite narrow limits: from 1.5 to 2.0. Specifically, the value $n = 1.5$ characterizes the size distribution of droplets in dispersal of a 50%-aqueous K_2CO_3 solution with a centrifugal nozzle, providing a flow rate of 100 g/s for a pressure differential of 100 bar. If the total weight of droplets of one or another diameter is known, a_{ki} , the above method can be used to calculate the time needed for their vaporization. In addition, it is possible to determine the amount of potassium carbonate vaporized during a time period which is somewhat less than the time of total vaporization, but greater than the time required for all the preparatory steps (vaporization of water, heating and melting of particles, heating of droplets to equilibrium vaporization temperature).

The results of such calculations for the droplet size distribution of a 50% K_2CO_3 solution with $d_m = 100\mu$ are given in Figure 17 (curve 2) as the dependence of the weight quantity of vaporized seed, related to the total weight of the injected seed $g_n = G_{vap} / \Sigma G_{dr}$, on the residence time in the combustion chamber. It follows from an analysis of the curve that the greatest rate of vaporization is reached several milliseconds after the moment of seed injection. During this time fine droplets are vaporized and vaporization of

the larger ones begins. As a result, more than 60% of the injected K_2CO_3 is vaporized in 20 ms. Then the vaporization rate gradually decreases and the vaporization of large droplets extends to 100 ms and more.

A reduction of the median diameter of the droplets to 50μ (cf. Figure 17), i.e., a twofold reduction, greatly increases the vaporization rate. In this case, $g_n = 0.65$ after only 10 ms and 32 ms are required for practically complete ($g_n = 0.95$) vaporization rather than the 100 ms required for the droplet size distribution with $d_m = 100\mu$.

Increasing d_m to 150μ leads to a significant reduction in the vaporization rate (curve 3, Figure 17).

The calculations, including those illustrated in Figure 17, show that, since the time for the vaporization of large droplets or particles is several times greater than the actual residence time of the gases in the combustion chamber, it is not feasible to seek complete seed ionization and in designing combustion chambers optimum solutions should be sought, which would take into account, along with other factors, the degree of seed vaporization.

In the calculation of the ionizing seed vaporization in the MHD combustion chamber, the assumption was made that K_2CO_3 dissociation occurs neither in the liquid phase nor in the immediate vicinity of the droplet surface. It was assumed that this process takes place in the vapor phase of the K_2CO_3 at a significant (greater than the thickness of the boundary layer) distance from the droplet. In this case, since the vapor is continuously leaving the droplet, K_2CO_3 dissociation begins soon after it begins to vaporize. Let us designate this lag by $\Delta\tau^*$ and attempt to estimate it. Evidently, it depends on outflow time for the first portion of vapor formed beyond the limits of the boundary layer and can be estimated on the basis of the following considerations:

$$Sh = \frac{\beta d_{dr}}{D} = \frac{d_{dr}}{\delta_{ad}}, \quad (37)$$

where: d_{dr} is the diameter of the droplet, m;

D is the coefficient of K_2CO_3 vapor diffusion in the combustion products; m^2/s ;

β is the mass transfer coefficient characterizing the velocity of K_2CO_3 vapor outflow from the droplet, m/s;

δ_{ad} is the reduced thickness of the boundary layer, m

Since in these symbols

$$\Delta \tau^* = \frac{\delta_{ad}^2}{\beta}, \quad (38)$$

by transposing equality (37), we obtain

$$\Delta \tau^* = \frac{d_{dr}^2}{Sh^2 D}. \quad (39)$$

The value of Sh for a droplet can be computed using conventional formulas [30]. This estimate of the lag time in the beginning of the dissociation process compared to the beginning of the process of vaporization of a $100 \mu K_2CO_3$ droplet, gave $\Delta \tau^* \approx 10^{-5}$, i.e., a value much less than the vaporization time. This circumstance allows us to consider that the processes of vaporization and dissociation begin at practically the same time, even though they occur in spatially separate zones.

The lack of data on the rates of K_2CO_3 dissociation and potassium ionization prevents an accurate calculation of the time required by these processes. However, a rough estimate can be made. For this we will use the recommendations contained in [31], where it is shown that for the usual expression of

the reaction rate constant

$$k = A e^{-\frac{E}{RT}} \quad (40)$$

the preexponential multiplier A is most probably in the range between 12 and 14. Since the total energy of the formation of K_2CO_3 from K_2O and CO_2 is 395 kJ/mol, the expected activation energy E should not exceed 160 kJ/mol. In this case for $T_{cp} = 3000$ K the dissociation time of K_2CO_3 will be on the order of 10^{-7} through 10^{-9} s, i.e., not commensurate with the time of seed droplet (particle) vaporization. Equally incommensurate figures are produced in estimating the K_2O (or KOH) dissociation time, up to the formation of potassium atoms, and of the potassium ionization time. Therefore, the actual dissociation and ionization reaction time in the combustion chamber can be ignored and the total ionization time can be equated to the total K_2CO_3 droplet (particle) vaporization time, i.e., all vaporized seed is considered to have achieved a state of thermodynamic equilibrium with the combustion products.

The precision of these calculations of the seed vaporization time is, of course, rather limited because of the very complex thermal situation in the combustion chamber and the results obtained require experimental verification. This verification was performed in the experimental MHD facility U-02.

2. Experimental study of seed ionization in the combustion chamber of an MHD facility.

In the U-02 MHD facility the seed is injected in the form of aqueous K_2CO_3 solution. For this purpose four seed injection systems were designed and tested in operation. Their basic working parameters are given in Table VI.

Three seed injection systems are shown schematically in Figure 18:

I -- Cold 50% K_2CO_3 solution;

II -- Superheated 50% K_2CO_3 solution;

III -- Hot K_2CO_3 solution of high concentration.

Systems I and II have a common tank for storage of the prepared solution (1), a grid filter for coarse filtration (2), a water tank (3), a service tank (4) and filters for stage II purification (5). System III is completely independent.

The main operating system is system I, which supplies a 50% cold solution of K_2CO_3 ($t = 20^\circ C$). In addition to the units mentioned above, it includes two parallel rotor valve pumps (6), an electrical decoupling unit (7) and spray nozzles (8).

System I allows operation both with centrifugal and pneumatic spray nozzles. In the latter case the dispersal is ensured using air from the existing compressed air line. All nozzles have a water-cooled housing and are incorporated into the combustion chamber or, in individual cases, upstream of it into the hot air duct.

The centrifugal injectors have replaceable nozzles with exit orifices of 0.5, 0.7 and 1.0 mm, while the pneumatic nozzles have openings of 0.7 and 1.0 mm. Operating experience has shown that the nozzles do not clog up with the existing stage II filters, which are made from glass fiber or Nitron. It was found that the cause of clogging in the initial period of operation was crystallization of the K_2CO_3 at the moment when the first portions of solution entered the superheated nozzle or when it was shut off. Supplying water from tank (3) before starting solution feed and a careful wash of the jets with solution immediately after shutdown eliminated the possibility of potassium carbonate crystallization, and consequently the clogging of the jets.

This seed injection system operated for a total time of more than ten thousand hours and the operating experience showed that a cold 50% K_2CO_3 solution does not cause noticeable corrosion of the equipment, even that made from carbon steel (storage tanks, pumps). Stainless steel 1Kh18N10T showed no corrosion whatsoever.

In order to improve seed dispersal in the combustion chamber it was decided to raise the pressure and temperature of the injected K_2CO_3 solution. System II, with a piston pump ND-60 capable of pressures up to 110 bar, was designed for this purpose. Buffer chamber (10) is used to reduce pulsations in the flow. Steam (12) and electric (13) heaters raise the temperature of the solution upstream of the nozzle to 250°C. The viscosity and surface tension of the solution decrease with an increase in temperature; this, together with the increase in pressure and reduction in the dimensions of the nozzle exit orifice should contribute to the production of smaller droplets. If, in addition, a superheated solution, hotter than the solution boiling point and commensurate in pressure with that in the combustion chamber issues from the nozzle, then there may be boiling of the solution and a secondary break-up of the droplets.

The solution enters this system from delivery tank via the filters for stage II purification. However, the use of small diameter nozzles ($d_n = 0.45$ mm) necessitated the installation of another Nitron filter. This system operated without failure and makes it possible to study the effect of increased pressure and heat of the K_2CO_3 solution on the seed ionization in the U-02 combustion chamber.

When using a 50% solution, one kilogram of ballast water is used per kilogram of K_2CO_3 which leads to further temperature reduction of the combustion products and, consequently, of conductivity. The adverse effect of the

water can be reduced by raising the solution concentration. As was mentioned in Chapter 1, the solubility of K_2CO_3 increases with an increase in temperature and even at atmospheric pressure a 67% solution can be produced. The boiling point of this solution is $135^\circ C$. When a 67% solution is used, only 0.5 kg water is required per kg K_2CO_3 and the injection of this solution allows the temperature drop to be reduced by several dozen degrees, which ought to have a significant effect on the electrical conductivity and, subsequently, on the economy of the MHD power plant. System III at the U-02 was designed for the practical realization of this concept and for the development of the production, transportation and spraying techniques for the aqueous K_2CO_3 solutions of increased concentration.

The creation of this system also had another purpose -- to support research into the seed regeneration, specifically, concentration of the solutions produced in systems for wet seed recovery.

System III consists of two 1 m^3 evaporator tanks (14) equipped with steam heating (a submerged coil) and a propeller-type electric agitator, two grid filters for coarse purification (15), two ND-160 pumps (16), two fiberglass filters for fine purification (17), an electrical decoupling unit (18) and nozzles (19). The danger of solid phase precipitation should the solution temperature fall, made it imperative to maintain the temperature at the $135\text{-}140^\circ C$ level along the entire flow train. To do this the main components of the system (filters, pumps, valves) are located in a batching unit, with an insulated housing containing steam heating pipes. The pipelines carrying the solution are equipped with steam satellite pipelines and are carefully heat-insulated right up to the spray nozzles.

Tests conducted on the production and dispersal of highly concentrated K_2CO_3 solutions at high temperature and pressure (cf. Chapter 1) made it

possible to design at the U-02 a system for injecting the seed in the form of a 73-75% potassium carbonate solution (system IV). Its basic layout is shown in Figure 19. An aqueous K_2CO_3 solution, 50 wt % in concentration, from delivery tank (1) via filters (2) is pumped by piston pump (3) to buffer tank (4), used to eliminate pulsations in the liquid flow due to the pump operation. From the buffer tank the solution passes through steam (5) and electrical (6) heaters and is fed to the steam-generating section (8), a vertical coil made of a 1Kh18N10T steel pipe $\varnothing 25 \times 2.5$ mm. The pipe is 14 m long between the current busses. The steam-generating section is directly heated by low-voltage alternating current. The electrical circuit is decoupled by a fluoroplastic insulating insert (7) on the cold solution side. The circuit is grounded on the hot solution side.

From the steam-generating coil the vapor-liquid mixture enters separator (9), made from 210 x 10 mm pipe. The separator is 2 m in height. The separated solution is transferred to nozzle (10) via a 12 x 2 mm pipe, while the steam acts to heat this pipe. Measurements of the temperature and pressure of the solution at the coil exit and in the separator make it possible to estimate the concentration of the solution being supplied to the combustion chamber.

The availability of the four systems for injecting the ionizing seed made it possible to conduct at the U-02 a series of studies dealing with the rate of seed ionization in the combustion chamber. The tests were made in a special once-through combustion chamber with a thermal capacity of 3 MW at a combustion product flow rate of 1 kg/s. Natural gas served as the fuel and hot air as the oxidant ($t = 800-1200^\circ\text{C}$; either atmospheric or oxygen-enriched to 30-40 wt %). The layout of this chamber is shown in Figure 20. The chamber consists of four separate sections: section (1) with ignition device (2),

section containing the burners (3) and natural gas manifold (4), experimental sections (5) and (6) with openings for the ionizing seed injection nozzles (8) and ports with 100 mm pitch (10) for experimental probes. The combustion chamber ends in a nozzle (7), whose flange is connected with the flange of the MHD channel.

The housing of the combustion chamber and the nozzle is water cooled metal. The ignition section and the front part of the combustion section are lined with high alumina concrete. The remaining surface of the combustion chamber in contact with gases containing ionizing seed is lined with a zirconia-base rammed mass. The lining thickness is 195 mm. The internal diameter of the combustion chamber is 300 mm. The total length of the chamber is 1670 mm, and its experimental section is 1200 long. The direct flow combustion device consists of eight gas-air slots shaped as equilateral trapezoids 75 mm high with sides of 20 and 35 mm located around the periphery of the back wall of the combustor between circumferences having a diameter of 150 mm and 300 mm. Air is mixed vigorously with natural gas in the slots.

When the combustor is started the combustion mixture is ignited by the pilot burner of the ignition device. Subsequently stable combustion is maintained because of the input of thermal energy to the gas-air streams from the recirculation zone of hot combustion products (9) (cf. Figure 20), which is just beyond the burner on the longitudinal axis of the combustion chamber.

The ionizing seed is injected into the combustor in the form of aqueous K_2CO_3 solutions of given parameters and is dispersed by centrifugal or pneumatic jets.

In the tests we determined the electrical conductivity of the gases and its change along the axis and in the cross section of the combustion chamber when the seed is injected into the recirculation zone at a distance

of 100 mm from the burner. σ was determined with a special probe inserted through port holes into the combustion chamber. The probe for the electrical conductivity of the plasma was an induction coil of a variable L-C circuit, located in a protective cover. The total error in the measurements of the electrical conductivity of the gases, caused by the error of the measuring instrumentation and by the presence of a thermal boundary layer around the probes, was not over $\pm 25\%$.

Tests were conducted for a range of starting combustion products temperatures* $T_0 = 2600-2800$ K, flow rates $G_{cp} = 0.5-0.8$ kg/s at an absolute pressure of 0.8-0.9 bar. The majority of the experiments involved atmospheric air as the oxidant and only in some instances was the air enriched with oxygen up to 35-40 wt %. The seed flow rate was calculated to provide 0.7 mol % of potassium in the combustion products.

The conductivity was measured along the flow train in three cross sections of the combustion chamber in a horizontal diametric plane. An oscillograph recorded the value of σ along the radius of the chamber. In this way the electrical conductivity field was determined.

Figure 21a shows the electrical conductivity field of the combustion products in a horizontal plane of the combustion chamber during injection of a room-temperature 50% K_2CO_3 solution by means of the centrifugal nozzle with the exit orifice diameter $d_n = 0.45$ mm. In this case the surface-volume average diameter of the droplets was estimated to be 90μ . The conductivity was measured in cross sections 0.3, 0.5 and 0.8 m distant from the face of the spray nozzle. First of all, there is a conspicuous progressive increase in σ from one cross section to the next, indicative of incompleteness of

* Not taking into account the decrease in temperature caused by seed injection.

the ionization process. At the same time there is a change in the profile of σ . At $L = 0.3$ m there is a reduction of σ value in the central part of the combustion chamber close to the recirculation zone in the radial coordinate, and then there is an increase of σ and another decline near the wall. The dip of σ at the axis is evidently due to the imperfect seed distribution over the cross section. At the 0.8 m cross section this dip does not occur, but a zone of low conductivity is clearly visible at the combustor wall, due to the increased thickness of the boundary layer. A similar pattern is observed when injecting seed solution heated to 211°C (Figure 21b); however, the leveling of the conductivity field progresses somewhat faster and the σ values are higher.

The increase of σ along the length of the combustion chamber is shown more graphically in Figures 22 and 23, where the maximum value of σ is plotted on the ordinate and the distance between the point of seed injection and a given cross section is plotted along the abscissa.

Figure 22 shows the picture of the change in σ_{max} along the axis of the combustion chamber for injection of a cold aqueous K_2CO_3 solution through centrifugal and pneumatic nozzles 0.7 and 1.0 mm in diameter. Neither type showed a distinct advantage over the other in the experiments (a significant difference in the electrical conductivity was produced only in the 0.3 m cross section when using the centrifugal nozzle with $d_n = 1$ mm); a change in the diameter of the nozzle orifice also had little effect. However, in all cases there was a steep rise in the curve of $\sigma = f[L]$ indicating that the seed ionization was obviously incomplete. The largest σ value was near $7 \text{ ohm}^{-1} \cdot \text{m}^{-1}$, while the thermodynamic equilibrium value under these conditions is about $15 \text{ ohm}^{-1} \cdot \text{m}^{-1}$.

Thus, only 20% of the injected seed had time to be vaporized and ionized during the residence time in the chamber (~ 8 ms). Calculated seed vaporization value results in approximately the same figure if $d_m = 150$.

A slight increase in the rate of seed ionization was noted when the injected solution was superheated (the solution was dispensed with a centrifugal nozzle having an orifice $d_n = 0.45$ mm) (data shown in Figure 23). In spite of a certain reduction in the temperature of the combustion products ($T_0 = 2670$ K, $\sigma_{equi} = 12 \text{ ohm}^{-1} \cdot \text{m}^{-1}$), approximately the same levels of σ were achieved, and the superheating contributed to an increase in the rate of σ growth in the initial section. This evidently should be explained by an increase in the mass of the fine fractions. The total amount of vaporized seed in these experiments rose to 30%. Thus, it is expected that with an increase in the seed solution superheating, the rate of seed ionization will increase.

This was particularly clearly demonstrated during the injection of a 73% solution at 360°C and 80 bar pressure. The experiments were carried out with the combustion products temperature $T_0 = 2750$ K and a 45% oxygen enrichment. The results are given in Figure 24. Comparison data are also given for injection of a 50% solution (cold and heated to 270°C) at the same spraying pressure.

As can be seen, when a cold 50% K_2CO_3 solution is used, the electrical conductivity in the cross section of the combustion chamber corresponding to a seed residence time the hot gases of 2 ms is very low. When the same solution, but heated to 270°C, was injected, this figure doubled, while when a 73% solution of the same parameters was used, it doubled again. In spite of the significant scattering of the experimental data ($\pm 30\%$) the advantage of using this solution is easily seen: even for $\tau = 10$ ms the conductivity obtained exceeds by almost one-and-one-half times the corresponding value of σ when a 50% solution is used. This advantage is evidently due to two factors. First, there is better dispersion of the solution: when the highly

superheated solution is injected, boiling of the liquid and fragmentation of the droplets occurs. This factor is most clearly felt in the zone of low τ (in our case for $\tau \approx 2$ ms). Second, for the larger seed residence times in the combustion chamber, there is an increased heat reserve due to the substantial reduction in the ballast water amount (2.5-fold). As a result, the value of σ obtained comes quite close to the thermodynamic value ($\sigma_{\max} = 15 \text{ ohm}^{-1} \cdot \text{m}^{-1}$, $\sigma_{\text{equi}} = 20 \text{ ohm}^{-1} \cdot \text{m}^{-1}$).

It is of interest to compare the rate at which the electrical conductivity increases along the combustion chamber axis with the rate of seed vaporization. Figure 25 shows growth curves of the vaporized seed amounts related to the total quantity, g_s . Values of g_s were computed for the following conditions: $d_m = 100$, $n = 1.5$, $T_{cp} = 2700$ K. According to the existing theoretical and experimental data the electrical conductivity is proportional to the square root of the amount of seed in the gaseous state. The curves of $\sqrt{g_s} = f(\tau)$ given in Figure 25 show that for these conditions one could expect at the end of the combustion chamber (if one ignores the time for dissociation and ionization proper) an electrical conductivity equivalent to 40% of its thermodynamic equilibrium value. Approximately these values of $\bar{\sigma} = \sigma_{\text{exp}} / \sigma_{\text{equi}}$ were in fact produced in experiments at the U-02 when dispersing a 50% K_2CO_3 solution with pneumatic nozzles (cf. Figure 22).

This good agreement of experimental and calculated data was somewhat unexpected, since the calculation incorporates data on the dispersal range produced on the basis of experiments involving liquid dispersal with nozzles into normal atmosphere. With a tenfold increase in the temperature the density and viscosity change substantially, and therefore one would expect a substantial change in the range, particularly when centrifugal sprayers are used. Of course, when the liquid is injected through pneumatic nozzles,

the dispersion takes place in cold gas, and evidently the influence of the medium, at least of its temperature will be less pronounced.

Therefore, a calculation of seed vaporization in the combustion chambers of an MHD facility requires careful studies of the influence exerted by the properties of the medium surrounding the liquid on its dispersion.

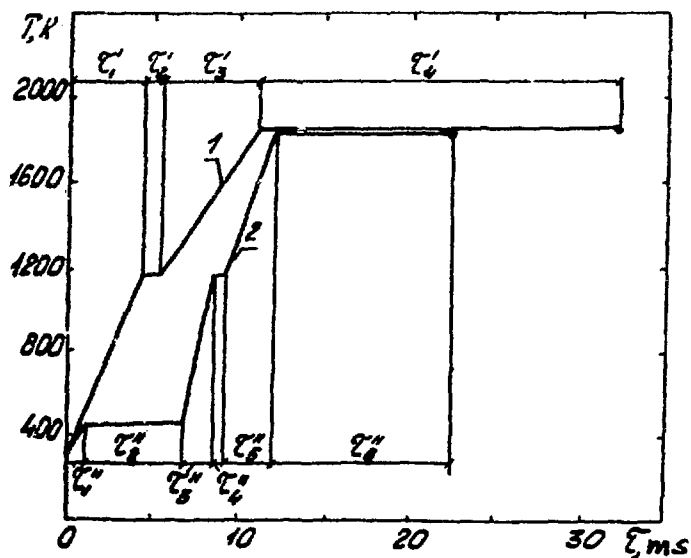


Figure 14. Diagram of seed vaporization process in a combustion chamber.
 $P = 1 \text{ bar}$, $T_{cp} = 3000 \text{ K}$.

(1) dry K_2CO_3 , $d_0 = 100$; (2) 50% aqueous solution of K_2CO_3 , $d_0 = 100$

Figure 15. The change in the diameter (solid lines) and velocity (broken line) of droplet in vaporization process. $T_{cp} = 3000$ K, $P = 10$ bar.

- (1) calculation at constant relative droplet velocity $W = W_0 = \text{m/s}$;
- (2) calculation considering droplet deceleration;
- (3) calculation without relative velocity, $W = 0$

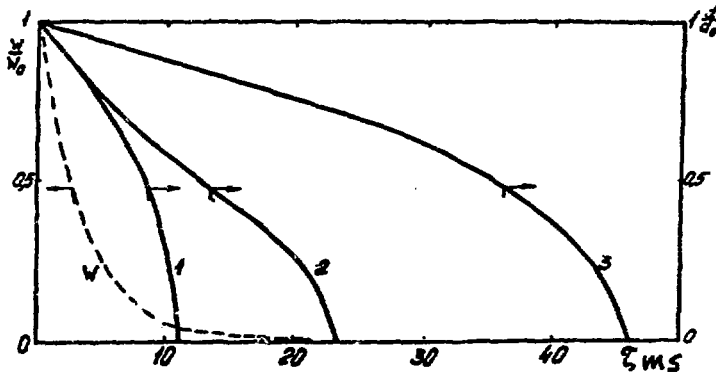


Figure 16. The dependence of the time for total vaporization of a particle (droplet) in the combustion chamber on its initial diameter, $P = 1$ bar.

- (1) dry K_2CO_3 , $T_{cp} = 3000$ K;
- (2) 50% aqueous solution, $T_{cp} = 3000$ K;
- (3) 50% aqueous K_2CO_3 solution, $T_{cp} = 2500$ K

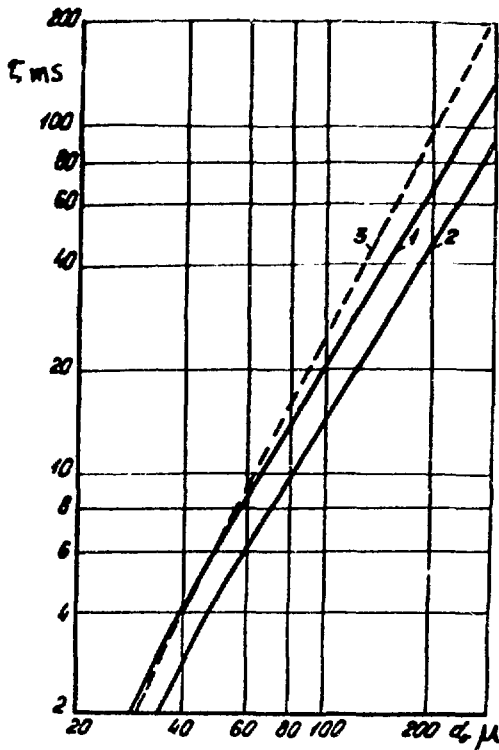


Figure 17. The change in the proportion of seed vaporized as a function of its residence time in the combustion chamber. $P = 1$ bar, $T_{cp} = 3000$ K.

- (1) $d_m = 50$;
- (2) $d_m = 100$;
- (3) $d_m = 150$;

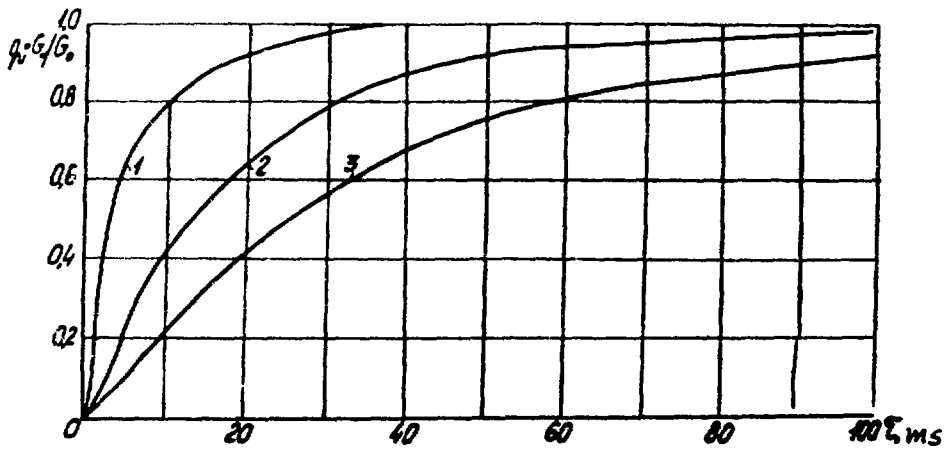


Figure 18. Ionizing seed injection system for U-02 facility, using an aqueous solution of K_2CO_3 .

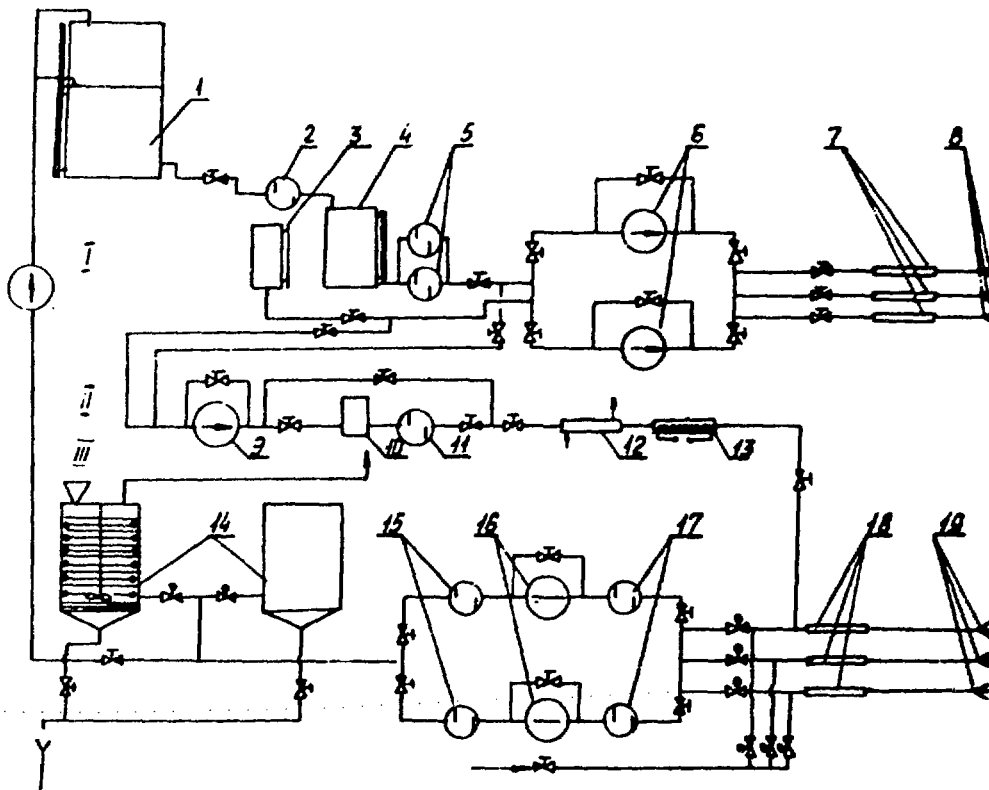


Figure 19. Ionizing seed injection using 75 K_2CO_3 solution at U-02.

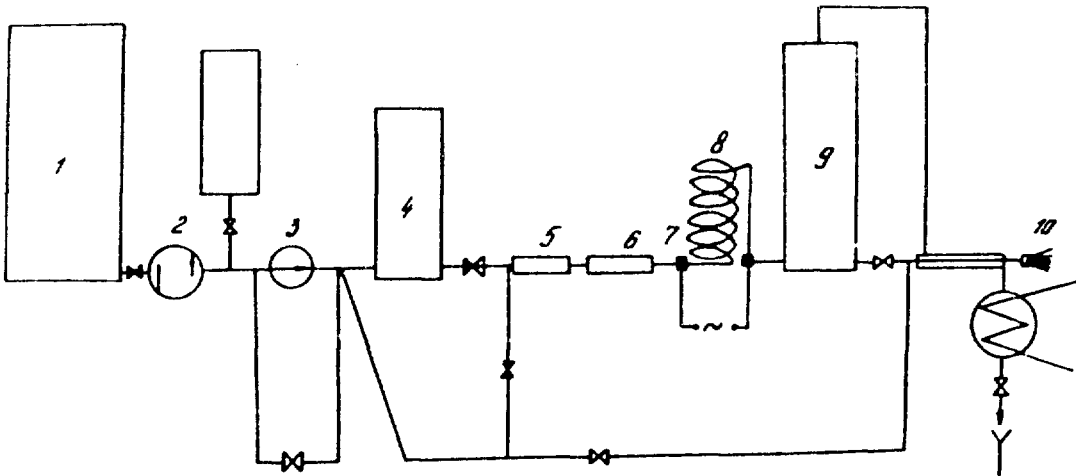


Figure 20. Diagram of experimental once-through combustion chamber.

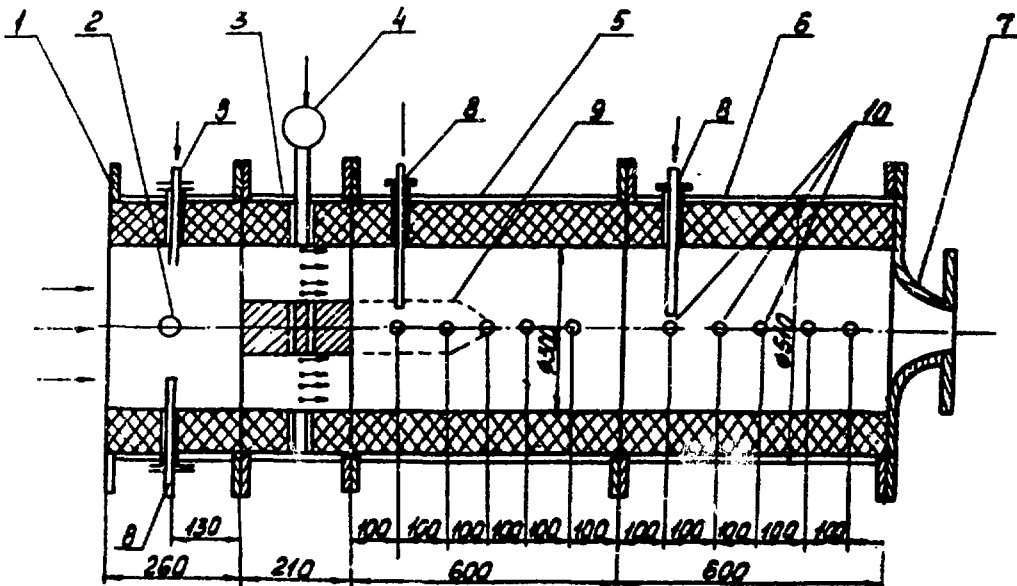


Figure 21. Profiles of electrical conductivity in various cross sections of combustion chamber for injection of seed as cold (a) and heated (211°C) (b) 50% K_2CO_3 solution with centrifugal sprayer having a $d_n = 0.45$ mm.

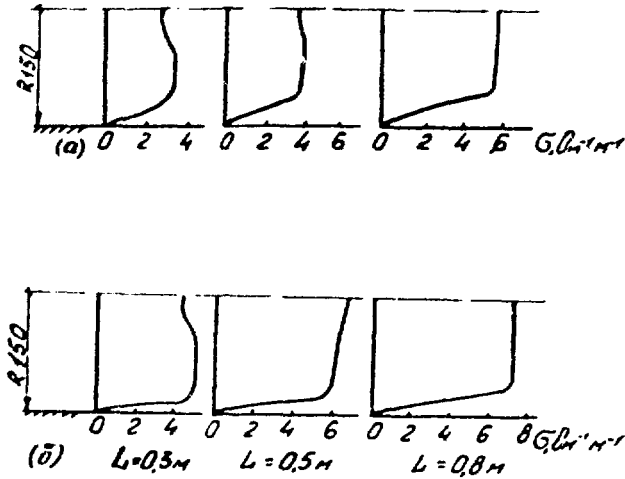


Figure 22. The changes in the electrical conductivity of the gases along the combustion chamber during the injection of a 50% cold solution K_2CO_3 with different sprayers, $T_0 = 2700$ K. (1,2) centrifugal, $d_n = 0.7$ and 1.0 mm, respectively; (3,4) pneumatic, $d_n = 0.7$ and 1.0 mm

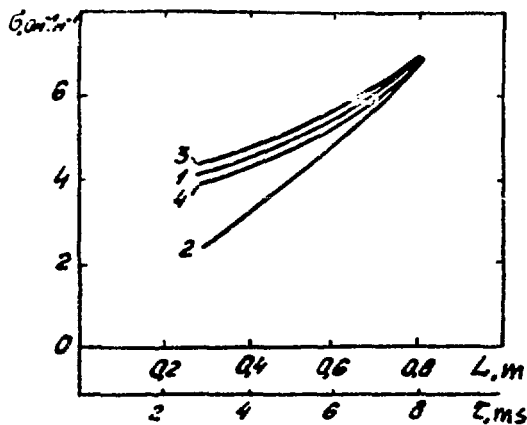


Figure 23. The changes in the electrical conductivity of the gases along the combustion chamber during the injection of K_2CO_3 solutions at different temperatures.

Centrifugal sprayer $d_n = 0.45$ mm. $T_0 = 2760$ K.

(1) $t_s = 20^\circ C$;

(2) $t_s = 150^\circ C$;

(3) $t_s = 211^\circ C$

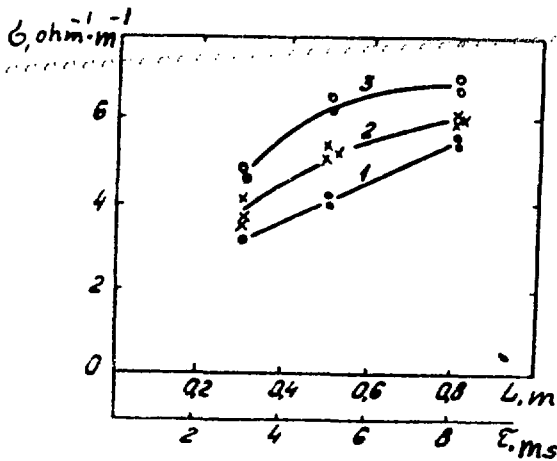


Figure 24. The electrical conductivity of the gases in the combustion chamber when the seed is injected as 50 and 73% K_2CO_3 solutions. Pneumatic sprayer, $d_n = 0.5$ mm. $T_0 = 2700$ K.

(1) 50% K_2CO_3 , $t_p = 20^\circ C$; (2) 50% K_2CO_3 , $t_p = 270^\circ C$; (3) 73% K_2CO_3 , $t_p = 360^\circ C$.

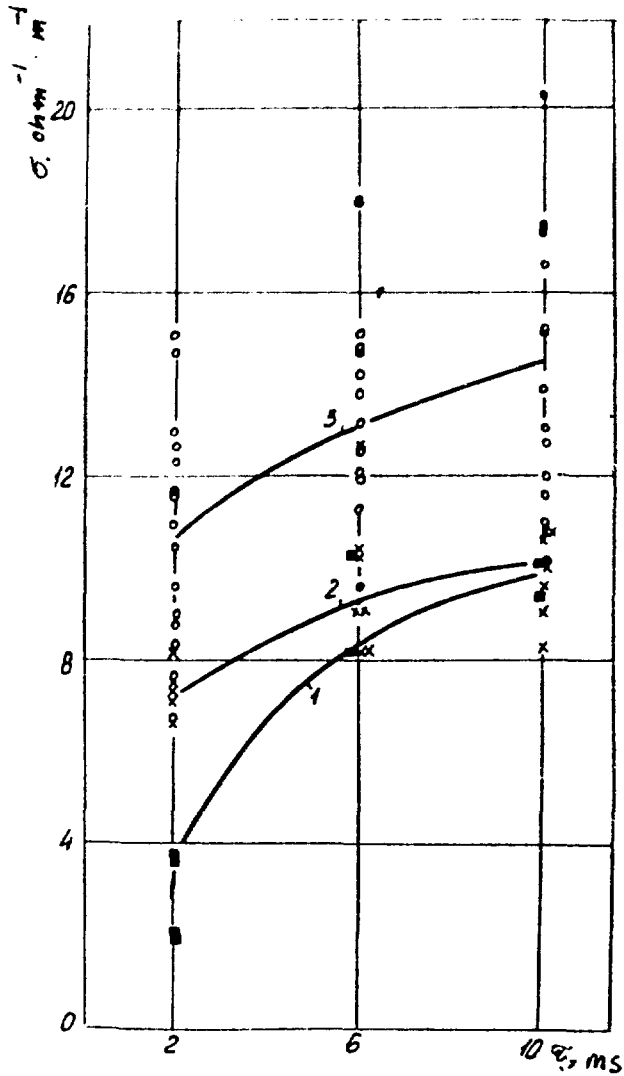


Figure 25. Comparison of the experimental data on the change of electrical conductivity with the results of calculations on seed droplet vaporization. $T_0 = 2700$ K. Pneumatic sprayer $d_n = 0.5$ mm, 50% aqueous K_2CO_3 solution.

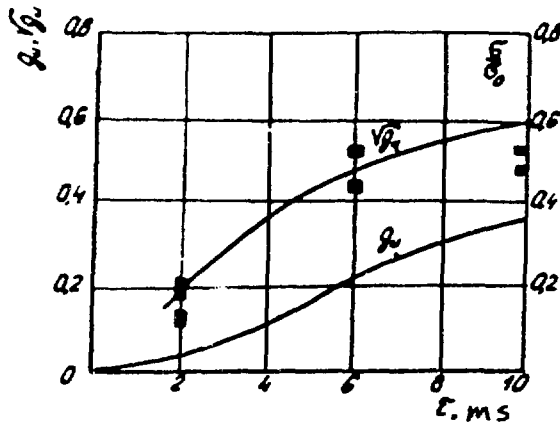


Table VI. Basic system parameters.

Parameter	System			
	I	II	III	IV
Maximum solution flow, kg/hr	120	90	250	90
Maximum spray pressure, bar	50	110	10	110
Maximum temperature, °C	20	250	135	370
Maximum K ₂ CO ₃ concentration in solution, wt %	50	50	67	75

Chapter 3

The Ionizing seed in the Gas Train of the MHD Facility

1. Physical and chemical changes of ionizing seed in the combustion products flow.

The ionizing seed injected into the combustion chamber gradually enters into thermodynamic equilibrium with hot gases and moves together with them through the entire MHD facility loop. During the journey through the MHD channel and the heat exchangers, the combustion products temperature changes from 3000 K to 350-500 K (before entering the exhaust stack). In the process the seed undergoes a number of physical and chemical changes. This process is shown schematically in Figure 26: the temperature of the combustion products is plotted along the abscissa, and the proportion of potassium (to the total potassium in the flow) in various compounds, stable in a given temperature range, is plotted along the ordinate.

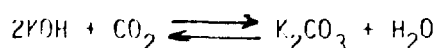
In the high temperature region (above 1500 K) all the seed is in the gaseous phase, i.e., in a state most amenable to thermodynamic calculations. The results of such calculations [8] give a picture of the chemical composition of the potassium compounds (solid lines on Figure 26). At 3000 K the greater portion of the seed ($\sim 80\%$) is found as atomic potassium, and the remainder as KOH. In addition, there are small quantities of potassium oxide KO and ionized potassium K^+ in the gases. At 2500 K the proportions of potassium as K and KOH even out, and at lower temperatures KOH becomes the prevalent compound.

Theoretical data [9] for the products of fuel oil combustion with K_2CO_3 seed are also plotted on Figure 26 (triangles). Over the entire investigated range of temperatures from 2800 to 2000 K the divergence between

the data of [8] and [9] is small and is caused primarily by a slight difference in the $CO_2/H_2O/N_2$ ratio in the combustion products of natural gas (methane) and fuel oil. The presence of ~2.3% sulfur in the fuel oil does not play a significant role in this case, because at these temperatures seed and sulfur do not form stable compounds.

According to data produced in [27], in natural gas combustion products at 1500-1300 K (cf. Figure 26) potassium hydroxide begins to react with CO_2 forming the carbonate:

(41)



At this temperature the water has a relatively low vapor pressure, and therefore the combustion products rapidly begin to be saturated with K_2CO_3 vapor. As a result, at 1470-1430 K bulk condensation of K_2CO_3 occurs, a mist forms, and when the combustion products cool below the fusion point of K_2CO_3 ($T_{fu} = 1174$ K) a condensation aerosol is produced.

The data in [27] and [13] assist in determining the temperature at which condensation begins. Knowing the total quantity of potassium in the combustion products and, in conformity with [27], the proportion of potassium which has become K_2CO_3 , it is necessary to construct for a given pressure the curve reflecting the increase of the partial pressure in potassium carbonate vapors, that occurs during the reduction in temperature. The dependence of saturated K_2CO_3 vapor pressure on temperature is given in [13]. The point at which these two curves intersect will be the temperature at which the K_2CO_3 vapor reaches the saturation state. Given the abundance of very fine dust particles, no substantial supersaturation is necessary for condensation of the K_2CO_3 vapor to occur, and one can reckon

with accuracy sufficient for calculations that the onset of mist formation occurs when the saturation temperature is reached.

Normally, in the process of bulk condensation, droplets (particles) of submicron dimensions are formed, which gradually increase in size because of vapor condensation or because of coagulation [32]. In the case at hand, condensation must be completed very rapidly, in a narrow temperature range, because of the very strong dependence of the K_2CO_3 vapor pressure on temperature. It is unlikely that any increase in the size of the droplets or solid particles would occur due to coagulation, because their volumetric concentration in the flow is very low (10^{-5} through 10^{-6} m^3/m^3). Therefore, even at the end of the gas flow train of an MHD facility, the majority of dust particles should retain their submicron dimensions.

This conclusion was experimentally confirmed by measuring K_2CO_3 particles taken from the U-02 loop. In order to avoid coagulation of the particles or an increase in size because of condensation on them of water vapor from the air, the samples were taken by passing the aerosol through hot ($t = 100^\circ C$) spectrally pure toluene. Then the cuvette containing the toluene and K_2CO_3 particles was placed in an FPS-2M* instrument, where the average particle diameter was determined by light scattering. It was 0.2 μ . Similar results ($d = 0.4 \mu$) were obtained in measuring the diameter of K_2CO_3 particles (also from the U-02 loop) by a sedimentation method using an ultramicroscope.

Experimental determination of the chemical composition of the condensation aerosol particles made at the U-02 MHD facility showed that the

* evidently a type of photoabsorption spectrometer-Tr.

carbonate is practically speaking the only potassium compound in the combustion products of natural gas in the temperature range from 1100 to 500 K. Further on, in the low-temperature section of the gas train, a large quantity of potassium bicarbonate (KHCO_3) was found. Studies at the U-02 MHD facility established the temperature region in which the K_2CO_3 is transformed into KHCO_3 and determined the equilibrium concentration of both potassium compounds in their mixture at various combustion product temperatures. The tests were made for combustion product temperatures from 65 to 250°C at a pressure of 0.55-0.75 bar (abs). The amount of CO_2 in the combustion products was 8-9.5 vol %.

The data obtained are shown in Figure 27, where the temperature of the combustion products is plotted along the abscissa and the ordinate shows the weight percents of potassium in KHCO_3 in relation to the total potassium in the flow. As can be seen, the upper limit of KHCO_3 formation is about 165°C. At higher temperatures all the seed is found as K_2CO_3 . With a reduction in temperature, the proportion of potassium as KHCO_3 rises and is 0.35 at $t = 120^\circ\text{C}$. At a temperature below 100-120°C the moisture content of the captured seed increases and a further conversion to KHCO_3 occurs. The dependence of transformation from K_2CO_3 to KHCO_3 assumed in the coordinates used in Figure 27 is satisfactorily approximated by a straight line originating at $t = 165^\circ$. This line, replotted on Figure 26, completes the diagrammatic picture of the physical and chemical conversions of seed in the gas train of the MHD facility.

2. The character and chemical composition of seed deposited on the heat exchange surfaces.

The picture of the physical and chemical conversions of the seed in the flow of combustion products gives a general idea of the deposit forma-

tion process on the heat exchange surfaces. Clearly, in the temperature range below 1200 K the deposits will form as a result of settling submicron K_2CO_3 particles, but it is difficult to predict the character of these deposits.

Still less certain is the process of the deposit formation in the high-temperature zone where the seed is found in the combustion products as potassium hydroxide vapor. Apparently the basis of this process is the condensation of KOH vapor on a surface having a lower temperature than that of KOH condensation (for $P_{cp} = 1$ bar and a potassium level of 0.7 mol %, $T_{cond} = 1120$ K). This hypothesis has been experimentally confirmed [27]: the processing of data on the rate of deposit formation in conformity with a model of KOH condensation with subsequent absorption of SO_2 and CO_2 (on the wall) showed good agreement of theory and experiment.

In order to study the character and chemical composition of the deposits in the various temperature zones, a special study was conducted at IVIAN. The box diagram of the experimental facility used in this study is shown in Figure 28. Hot air, natural gas and seed were injected via a co-axial nozzle (2) into a tube-type combustion chamber (1) ($d_{in} = 70$ mm, $h = 200$ mm). The seed was in the form of an alcohol solution of potassium acetate (75% C_2H_5OH and 25% $KC_2H_3O_2$). Supplying the seed in an organic solvent ensured its rapid combustion. The rather long seed residence time (50 ms) in the combustion chamber helped to achieve a thermodynamic equilibrium. The resultant combustion products at 1800-2000 K passed into the first cooling section (3), a ceramic tube made from chrome-magnesite with a stainless steel tube inserted in it (in the form of a Field tube). Air at $T_{in} = 450$ K descended through the internal tube to its lower end and rose upward through the ring gap, cooling the external tube.

Stable operating conditions in the experiments ranged from 0.5 to 2.4 hours, while from 0.2 to 1.6 kg of the 25% potassium acetate alcohol solution was supplied, providing a 0.15-0.5 mol % concentration of potassium in the combustion products.

The results of the experiments are summarized in Table VII. It can be seen from the table that the gas cooling train can be divided into four parts: in the first part there is no settling of potassium and its compounds, while the remaining sections constituted the three temperature zones with the characteristic form and composition of seed deposits in each of the zones. We will try to make sense of the physical essence of the ongoing processes and to connect them with the general picture represented in Figure 26.

In the experiments the combustion products emerging from the combustion chamber at 1700-1900 K, collided with the lower part of the vertical cooling section, which was specially maintained at a temperature above the "dew point" of KOH. This eliminated the possibility of KOH vapor condensation and made deposition possible only as a result of K_2CO_3 formation in the boundary layer with subsequent deposition on the surface. The experiments showed that in this zone there were no seed deposits, but there was metal corrosion (of stainless steel): the wall was covered with a layer of scale, which was easily removed from the metal of the tube when cooled. Consequently, even though the potassium hydroxide vapor reached the tube surface (otherwise it would be difficult to explain the severe corrosion), they did not condense, while the partial conversion of KOH to K_2CO_3 occurring in the boundary layer evidently did not play a large role in the formation of deposits.

Further downstream was a section with dark-green, crustlike deposits. Chemical analysis of these deposits showed that they contained a small quantity of KOH in addition to K_2CO_3 . When the deposits were washed with water there

was the crackling and sputtering typical of potassium oxides. Evidently, there was a small amount of these oxides in the deposit under the layer of K_2CO_3 and KOH. This section lies in the zone of surface temperatures from 1020-1120 K, which is below the KOH concentration temperature. The crustlike character of the deposit indicates that K_2CO_3 was formed on the wall when CO_2 was absorbed by the previously condensed liquid hydroxide. As the temperature decreased, the dark-green, crustlike deposits became lighter in color, but remained just as hard.

Gradually the crustlike deposits were replaced with porous deposits of a cream or mustard color, similar in appearance to long needle-shaped hoarfrost. The dense, elongated crystals, which stood normal to the surface, rose above rather smooth greenish deposits, and gradually displaced them. The chemical composition and structure are reasons for supposing that they were formed in the process of condensation (more accurately, sublimation) of K_2CO_3 vapor from the supersaturated stream. With the typical 1500-1200 K temperatures in this zone, the reaction of KOH with CO_2 forming K_2CO_3 progresses rapidly in the combustion products. As was mentioned above, because of the low pressure of saturated vapor of K_2CO_3 at these temperatures the vapor rapidly achieves a saturated state and tends to condense. The best conditions for condensation exist at the wall, where the temperature is lower and crystallization centers are in abundance. However, even under these conditions solid particles were not observed in the boundary layer. These were found only in the lower-temperature zone, where there is at first a fine submicron dust between the elongated crystals and then frostlike deposits are replaced by snow-white deposits of this dust, also consisting wholly of K_2CO_3 , evenly distributed around the perimeter of the tube and projections.

According to an earlier hypothesis, the submicron K_2CO_3 dust is formed in the plasma flow as a result of spontaneous K_2CO_3 vapor condensation from a saturated state and under the effect of diffusion and thermophoresis settles on the surface. Snow-white deposits of this dust were observed on the last third of the vertical section and along almost the entire length of the horizontal section. At the end of the horizontal section, with wall temperature below 420 K, a chemical analysis of the deposits, as was to be expected, showed a substantial amount of $KHCO_3$.

Analysis of these data allow us to draw the conclusion that the character of the deposits is determined, primarily, by the temperature conditions in the flow and on the wall.

3. Mass transfer in the condensation of KOH vapor from the combustion products flow.

Analyzing Figure 26 and taking into account the experimental data described above, it can be stated that if, in the combustion chamber of the MHD facility, the channel of the MHD generator, or the high-temperature zone ($T_{pc} > 1500$ K) of the heat exchanger downstream of the channel, there is a surface with a temperature below the "dew point" of potassium hydroxide, then KOH vapor will condense on this surface. The condensation rate depends on the thermal and hydrodynamic conditions near this surface and the diffusion of the KOH molecules in the combustion products.

In the combustion chamber and the MHD channel having smooth electrode and insulating walls, the gases flow longitudinally along the surfaces. The mass transfer rate under these conditions can be calculated by analogy between the heat and mass transfer. The question of the influence of transverse mass flow on heat and mass transfer in the longitudinal streamline flow along a surface was examined in detail in [33]. However, because of the low concentration

of the condensing component in the stream, this influence can be ignored.

The nonisothermal nature of the boundary layer may play a more important role in the process of KOH vapor condensation on a cold surface. This factor is calculated by the expression

(42)

$$\frac{Sh}{Sh_0} = \psi = \frac{4}{(\sqrt{\psi} + 1)^2},$$

where:

Sh and Sh_0 are Sherwood numbers under these conditions and under isothermal conditions without consideration of the transverse flow of the substance

ψ is a coefficient of nonisothermicity;

$\psi = T_{wa}/T_{fl}$ is the ratio of the wall temperature to the flow temperature.

The temperature of the combustion products with seed flowing along the channel of the MHD generator is nearly 3000 K; while the temperature of the cold surface, already covered with a seed layer, is about 1100 K, i.e., $\psi = 0.37$ and $\psi = 1.56$. Consequently, because of the nonisothermal nature of the boundary layer, the rate of mass transfer in the beginning of the MHD channel may be significantly higher than in the results of calculations using the conventional formulas. As the temperature of the flow decreases, (with $T_{wa} = \text{const}$) the value of ψ decreases also, gradually approaching unity, i.e., the influence of nonisothermicity in the steam generator zone is practically absent.

In order to ensure that the analogy is preserved between heat and mass exchange during the potassium hydroxide vapor condensation from the combustion products flow containing seed in the zone of temperatures below 2000 K, an investigation was made of this process under conditions of longitudinal and

transverse washing of the tubes with a gas flow containing 1-3 g/m³ KOH vapor.

The investigation of the condensation of KOH vapor during longitudinal flow was performed in an experimental test facility (cf. Figure 28), with the vertical cooling section made from a tube 25 mm in diameter.

KOH condensation took place only on the initial section of the tube, where the temperature was above 1450 K, since a further reduction of the flow temperature results in KOH and CO₂, contained in the combustion products, forming K₂CO₃, which then precipitates in the form of submicron particles. In this section for $T_{cp} \approx 1500$ K and $T_{wa} = 1100$ K, $\psi \approx 0.73$ and $\gamma = 1.15$, i.e., near to unity.

The limited capabilities of the facility allowed experiments on the flow rate of the combustion products to be conducted only under conditions of laminar flow ($Re_{d_E} < 10^3$). The following dependence was proposed for treating the experimental data on heat exchange under similar conditions [34].

$$Nu_x = 0,33 \cdot Re_x^{0,5} \cdot Pr_{fl}^{0,43} \cdot (Pr_{fl}/Pr_{wa})^{0,25} (x/d_e)^{0,1}, \quad (43)$$

where the distance x from the beginning of the experimental section is taken as the characteristic dimension, and the physical properties of the flowing substance are taken at the temperature of the flow (except for Pr_{wa}).

This formula, transposed for a generalization of the data on mass transfer, has the form

$$Sh_x = 0,33 Re_x^{0,5} Sc_{fl}^{0,43} (Sc_{fl}/Sc_{wa})^{0,25} (x/d_e)^{0,1}. \quad (44)$$

Analysis of the data obtained showed that over the entire investigated range of parameters ($T_{cp} = 1450-1600$ K, $T_{wa} = 1000-1100$ K) the value of (Sc_{sc}/Sc_{wa}) 0.25 was close to unity, and therefore it was not considered in processing the experimental data. The coefficient of KOH vapor diffusion in the natural gas combustion products under standard conditions D_0 necessary for calculations, was computed using the Bird-Hirschfelder-Curtiss formula [35]: $D_0 = 1.1 \times 10^{-5}$ m²/s. The dependence of the diffusion coefficient on temperature and pressure was adopted in conformity with [36]:

$$D = D_0 \left(\frac{T}{T_0} \right)^{1.8} \cdot \frac{P_0}{P} \quad (45)$$

The results of processing the experimental data on mass exchange in the condensation of KOH vapor in the ring channel is given in Figure 29. The experimental points are grouped around a line corresponding to formula (44) with a scattering of $\pm 25\%$. This degree of agreement between the calculated and the experimental data is considered quite satisfactory, particularly in view of the low level of precision of the physical parameters used in the calculation, especially the value of D .

A study of KOH condensation on a cylindrical surface washed by a transverse flow was made at the U-02 facility in a tube ($d_{in} = 200$ mm) mounted in place of the MHD generator channel. Hot gases with seed entered the tube directly from the combustion chamber. Probes made of 1Kh18N10T steel were inserted into the tube normal to the flow through a packing gland and retainer. ($d_p = 40$ mm). They were based on a Field tube principle with water cooling. Probes with outside diameters of 20 and 30 mm were used in the experiments. Grooves 2 x 2 mm were cut in the working section of the probe at an angle of 90°; these grooves contained Chromel-Alumel thermocouples for measuring the tube wall temperature.

The thickness of the deposits was not uniform around the perimeter of the tube: the deposits were thicker on the upstream than on the downstream side. However, this lack of uniformity was not considered in calculating the mass transfer coefficient β : the average mass flow of the KOH across the surface was used.

The experimental data were processed according to the formula for calculating heat exchange during transverse streamline flow for a single tube:

$$Sh = 0,21 Re_d^{0,62} \cdot Sc^{0,38}, \quad (46)$$

which is also recommended [37] for calculation of mass transfer processes.

The results of processing the mass transfer data are shown in Figure 30. The experimental points are grouped around the center line corresponding to formula (46) with a scattering not over $\pm 30\%$. This agreement of experiment and calculation can be considered quite acceptable, particularly if one considers the lack of accuracy of the physical parameters at high temperatures and the error in determining the actual temperature of the plasma flow.

The experimental data concerning the condensation of KOH vapor from the seed mixture with kerosine combustion products [38] are also plotted on Figure 30. They lie slightly below the middle line and almost entirely within the band of 30% scatter. In our experiments the temperature of the combustion products (of the flow) was on the 2000 K level, while the surface temperature changes from 600 K in the initial moment to 1000 K at $\Delta \tau = 10$ minutes. Under these conditions, but with longitudinal washing of the surface with a turbulent flow, it could be expected that the nonisothermicity would have a greater influence, particularly in experiments with small $\Delta \tau$ ($\Delta \tau_E = 2$ min) when the value of Ψ is about 1.5. However, no influence of nonisothermicity was found when the surface was washed by the transverse flow:

experiments with various Δt values from 2 to 10 minutes produced identical values of β , and only for $\Delta t > 15$ minutes was there a stabilization of the quantity of condensed potassium hydroxide, i.e., G_{KOH} . This stabilization is due to the fact that the melting point of a mixture of KOH and K_2CO_3 on the surface of the deposits has been reached, and the resultant liquid film was being carried off by the gas flow. This explanation can be confirmed by the appearance of the extracted deposit samples: for $\Delta t \geq 15$ minutes, they had a smooth fused surface, while for $\Delta t \leq 10$ minutes the deposits were somewhat rough surfaced.

Overall, the experiments showed that under the typical MHD generator conditions, where the seed concentration in the combustion products is not high, the analogy between heat and mass transfer is satisfactorily preserved both for transverse and longitudinal flow around the tubes. To calculate the seed condensation rate on a cold surface conventional formulas for heat transfer can be used if mass transfer criteria are substituted for the heat transfer criteria, and, if for longitudinal flow of a turbulent stream for $T_{cp} = 2500-3000$ K, the nonisothermicity of the boundary layer is taken into account.

4. Study of ionizing seed submicron particle precipitation on the tube surfaces.

In the long MHD generator channels with "cold" (below 1000 K) insulating and electrode walls a boundary layer forms. The thickness of the low temperature portion of this layer may reach several centimeters. The time required for KOH vapor to pass through this layer from the core of the plasma flow is sufficiently great for at least part of the hydroxide to enter into reaction with CO_2 , form K_2CO_3 and then form a condensation aerosol with submicron sized

particles. These particles will settle down on the channel surface and in conformity with [39] one can expect that the crucial role in the rate of deposit formation will not be played by diffusion, but rather by radiometric forces, primarily thermophoresis forces.

The thermophoretic force acting on a particle depends on the size of the particle, the mean free path of a molecule and the temperature gradient and is directed toward lower temperatures.

In the zone of the boundary layer of interest to us ($T_{cp} = 1200$ K, $P = 1-3$ bar) if there is a large temperature gradient, thermophoresis will apparently lead to effective settling of the seed on the channel surface.

This hypothesis was confirmed experimentally. Experiments were conducted using the previously described test facility (Figure 28) to determine the effect of thermophoresis on the settling of submicron seed particles in the horizontal cooling section. The seed deposits were studied on a tube 40 x 29 mm and 1020 mm long, similar in design to a Field tube with internal air cooling.

The experiments were carried out under both isothermal ($T_{cp} = T_{wa}$) and nonisothermal ($T_{cp} > T_{wa}$) conditions. In the first case, in the absence of a temperature gradient, particle precipitation from the flow was determined by diffusion, while in the second case it was determined by diffusion and thermophoresis. A light coating of seed was observed on the experimental tube under isothermal conditions ($T_{cp} = 900-1100$ K). The deposits were white and loose. Under nonisothermal conditions, where the wall temperature was lower than that of the plasma flow by 30-150 K, the experimental tube was covered with a thick, loose seed layer. The rate of precipitation was calculated on the basis of the experimental data:

$$\beta_i = \frac{G_i}{F_i C_i \Delta T}, \quad (47)$$

where:

G_i is the quantity of K_2CO_3 deposited in the i -th segment, kg;

F_i is the surface area of the i -th segment, m^2 ;

Δt is the length of the experiment, hr;

C_i is the concentration of K_2CO_3 in the flow washing the i -th segment, kg/m^3 .

The dependence of ρ_i on the flow temperature is shown in Figure 31. Two groups of points are clearly differentiated on this figure: the upper group corresponds to the experiments under nonisothermal conditions, i.e., with thermophoresis, while the lower group corresponds to isothermal conditions, without thermophoresis. The difference in the experiments was quite significant -- almost tenfold for $T_{cp} = 820$ K.

Similar experiments were carried out with seed precipitating from the transverse flow on a tube bank of tubes 12 mm in diameter, 105 mm high, with a relative transverse and longitudinal pitch $s/d = 1.5$. The tubes were cooled internally with air or water. In this case as well there was a large difference in the rate of particle precipitation on cooled and uncooled tubes. While during the axial wash around a tube of a condensation aerosol flow approximately 90% of the settled dust was due to thermophoresis in the investigated conditions, in transverse flow around a tube bank this figure is 80-85%. In the conditions of MHD facilities the particle size ($0.2-0.4\mu$) is on the same order as the mean free path of a molecule, i.e., the Knudsen number $Kn \approx 1$. According to [39] in this case one should make a correction in the Einstein formula [40] and in the final analysis the expression for calculating the rate of thermophoresis will have the form

(48) *

$$\beta_T = -\frac{1}{8} \frac{e w_g}{T_g} \text{grad } T \exp(-0,38 \frac{r}{e}),$$

where

e is the mean free path of the molecule, m;

w_g is the average velocity of gas molecules for a gas temperature of T_g , m/s;

r is the particle radius, m.

The value of the temperature gradient $\text{grad } T$ near the surface of the tubes was determined using conventional formulas for calculating the heat transfer coefficient under the corresponding conditions:

$$\text{grad } T = \frac{(T_g - T_{wa}) Nu}{d}, \quad (48) *$$

where

T_g and T_{wa} is the temperature of the gas and the surface of the tubes, respectively, K;

Nu is the Nusselt number for the conditions under analysis;

d is the characteristic dimension, m.

* Original Russian language text contains two formulas (48) Tr.

A comparison of the experimental data with those calculated using the formula (48) are given in Figures 32 and 33. Figure 32 characterizes the case of a tube bank washed by a longitudinal flow. Calculations using formula (48), with consideration of the slight change of parameters from experiment to experiment, produced a band of values of $\beta \tau$. With some scattering the experimental data fall in the calculated zone, showing satisfactory agreement of calculation with experiment.

These data on the condensation of KOH vapor and precipitation of solid K_2CO_3 particles point up the high complexity of the processes accompanying the operation of the heat exchange components with seeded combustion products and require experiments designed for conditions maximally approaching those typical of MHD facilities.

5. Tests of a steam generator model at the U-02 facility.

The combustion products leave the MHD generator at a temperature of ~ 2300 K. One of the ways to recover this heat is to generate steam for subsequent use in a steam power cycle. In this case a steam generator with a low-temperature air preheater is placed directly downstream of the MHD generator. Here the combustion products release their heat to the water and air and are cooled to 420-450 K.

The alkaline metal seed -- potassium -- in the combustion products exerts a significant effect on the process of heat transfer, and consequently on the operating reliability of the downstream components. As has already been demonstrated, condensation of KOH vapor on cold surfaces ($T_{wa} < 1120$ K) with subsequent conversion to K_2CO_3 leads to the formation of solid crust-

like deposits on the tubes. The precipitation of very fine droplets of a K_2CO_3 mist on tube surfaces in the $T_{cp} = 1200 - 1500$ K zone leads to considerable trouble due to the appearance of hard, difficult to remove deposits. The effectiveness of methods for removing off the heat exchange surfaces deposits of submicron dust at $T_{cp} 1170$ K, also requires testing.

In order to investigate these processes, a steam generator model (SGM) was built at the MHD U-02 facility, recreating the operating conditions of the heat exchange surfaces washed with seeded combustion products over the entire relevant temperature range.

The layout of the SGM is shown in Figure 34. The steam generator has a Π -shaped layout, i.e., it consists of two vertical shafts connected by a horizontal gas duct (7). The first vertical shaft consists of a radiation chamber (1) with a diffuser (2) and cold funnel (3) and semi-radiation surfaces (4), (5) and (6). There is a 200 x 200 mm tap hole in the lower end of the shaft for molten seed emptying into a special tank containing water. The second shaft includes two transverse circulation tube banks (8) and (9) and a hopper (10). A device for the metal shot release (11) is mounted above the shaft. The entire wall surface in both shafts is lined with tightly fitted shielding tubes cooled with water (waterwalls).

The SGM is calculated for a combustion product flow velocity rate up to 1 m/s and a maximum gas temperature of 2300 K. The gas temperature at the exit is 450 K, the pressure 0.6 - 1 bar (abs). Special portholes 40-70 mm in diameter with hatch covers were installed in the walls of the SGM for monitoring the surface conditions and for introducing the necessary sensors (temperature, pressure) and probes.

The steam generator model was built at the end of 1967 and operated more than 10,000 hours. Approximately 3/4 of the time the SGM acted as an ordinary heat exchanger, supporting experiments with other components of the U-02, while for more than 2000 hours it was itself the chief subject of investigation. During this period its hydraulic and thermal characteristics were determined, as well as the character and the rate of seed deposition in various temperature zones.

1. Operation of the radiation surfaces. These surfaces, located in the zone of highest temperatures, contact the combustion products containing ionizing seed in the form of KOH vapor. This vapor condenses on the tube surfaces, absorb CO_2 from the combustion products and forms crustlike deposits of K_2CO_3 with a high melting point. The chemical analysis of these deposits indicated the presence of a certain amount of KOH. This means that not all the hydroxide has time to react with CO_2 and a mixture of K_2CO_3 and KOH is formed with a melting point significantly lower than the temperature of KOH vapor condensation from the combustion products flow. As a result, condensed seed flows down the radiation surfaces. To remove it a special system was built in the form of a small circulation loop consisting of a drain tank located under the cold funnel, a collection tank and a circulation pump. Experience showed that the molten seed is instantaneously soluble in water and circulates in the loop as solution. The proportion of seed drained in the melted form was determined on the basis of solution volume in the loop and the increase of seed concentration in the solution. This proportion turned out to be quite significant -- up to 40%. The solution concentration reached 50% (as K_2CO_3) containing up to 10-15% KOH. Condensation of such a large amount of seed in the radiation section of the steam generator facilitates the operation of the convective surfaces and of the seed recovery system at the

end of the train, while the presence of a substantial amount of KOH, as will be shown in Chapter IV, simplifies the system for seed regeneration.

The experience of operating the SGM has shown that because of the condensed seed runoff, the thickness of the deposits is stabilized. Analysis of deposits taken from the tube surfaces after the shutdown of the MHD generator showed that three layers can be distinguished. Directly on the metal wall, slightly corroded, lies a loose, porous, very thin (on the order of 0.5 mm) layer, with poor adhesion to the tube surface. Its thermal resistance is high, and the temperature drop across it is hundreds of degrees. A solid monolithic layer, whose thickness depends on the thermal flow, lies on the porous layer. In the central part of the radiation chamber water walls it is several millimeters thick, while in the corners, where the thermal flow is substantially less, it reaches 2-3 mm. The temperature of the external surface of this layer is equal to the melting point. The condensed seed flows along the surface of deposits, forming (when the facility is shut down) the third, molten layer.

A similar picture is observed also on the semi-radiation surfaces, but because of the lower thermal flow the deposits here are thicker.

2. Operation of the convective surfaces. In the experiments conducted the temperature of the combustion products at the entrance to the convection shaft did not exceed 1100 K, i.e., all the convective surfaces were washed with a condensation aerosol containing solid particles 0.2μ in diameter. For the flow velocity typical of the experiments, 10-14 m/s, inertial effect of the settling of the particles on the surface were small, and the tubes were coated with a rather even seed layer, while the spaces between the tubes of the checkerboard bank ($d_{tu} = 18$ mm with a longitudinal pitch of 30 mm and transverse pitch of 54 mm) could be completely covered with deposits.

In the remaining free gas corridors the velocity increased severalfold, but the process of deposition did not stop. This is clearly illustrated by the graphs of the changes in the total hydraulic resistance of the convection shaft in time (Figure 35).

The submicron particles which settle on the surface coagulate forming rather large agglomerates. Figure 36 shows seed particle size distribution in samples taken from the surface of a isothermal probe when combustion products were at 500 and 480 K. Particle sizes were determined by liquid sedimentation. The median diameter of the particles was 14μ in the first case and 21μ in the second.

Potassium carbonate is very hygroscopic. The upper temperature limit for the absorption of water vapor is determined by its pressure in the combustion products. At atmospheric pressure in the combustion products of natural gas burnt in air containing 40 vol % oxygen, the partial pressure of water vapor is 0.33 bar and the limit of hygroscopicity of K_2CO_3 is $T_{cp} = 374$ K. If atmospheric air is used as the oxidant this temperature falls to 357 K. The corresponding temperature limits of K_2CO_3 at a total pressure of 0.5 bar are 353 and 338 K.

If the surface temperature is below this limit the deposited seed absorbs water vapor from the combustion products, and the deposits become moist. If the moistening is slight, the upper layers of the deposits, at a higher temperature absorb less moisture and appear to be dry. If the surface temperature decreases the deposits become pasty and even run downward, which leads to rapid carbonation of K_2CO_3 to $KHCO_3$. Therefore, under industrial conditions the gas temperature at the exit from the steam generator should be maintained no lower than 420 K and the surface temperature no lower than 360-375 K.

A very effective way to remove the deposits off the tubes is to wash them with water without stopping the SGM. This method was used continuously during the operation of the steam generator: 1-2 minutes after 20-40 litres water were released from above [cf. Figure 34 (11)] the hydraulic resistance would fall to its initial level. Washing the tubes for 10 minutes restored their surfaces to a condition in which the process of deposition could begin anew, as it were (cf. Figure 35). The required frequency of this cleaning was every 5-6 hours.

3. Change in heat transfer. Measuring the temperature of the combustion products in the various zones of the SGM was made difficult, on the one hand, by the presence of settling seed, and on the other, by the proximity of cold surfaces.

Therefore, retractable thermocouples, inserted into the stream for only a brief period (2-3 minutes) were used to measure the temperature of the combustion products. The case in which the thermocouple was placed was made from a stainless steel tube with an external diameter of 2.5 mm. This allowed the inertia of the thermocouple to be reduced significantly and the convection component of heat transfer to be increased. As a result the correction factor for the radiation of the thermocouple case was reduced, and consequently the accuracy in determining the gas temperature increased. The measurement error was estimated as $\pm 30^\circ$ at the 1300 K level and ± 10 at the 800 K level.

Such retractable thermocouples were installed between the semiradiation surfaces, at the entrance to the convection shaft and in the line beyond the SGM and upstream of the entrance to the seed recovery system. The measurement results showed that the temperature beyond the radiation surfaces stabilized after 5-6 hours, this could occur only when the seed deposits were stabilized. Evidently the seed layer on the radiation surfaces reached a state of fusion

and ceased to grow. However, in the convection part the deposits did not stabilize: with the temperature at the entrance remaining constant, the temperature at the exit continued to rise, and only washing the surface with water reduced it to its initial value.

The measurements of the temperature of the combustion products made in successive zones were used to estimate the change of heat transfer in the SGM occurring with seed injection (Figure 37). The effective coefficient of heat transfer K_j was taken as the basis for comparison:

$$K_j = \frac{Q_j}{F_j \Delta t_{\lambda j}}, \quad (50)$$

where

Q_j is the heat removal in the given section of the SGM, kW;

F_j is the heat exchange surface of this section, m^2 ;

$\Delta t_{\lambda j}$ is the logarithmic average temperature drop on this section, $^{\circ}C$

The value of K_j corresponding to a given moment of time was compared to the same heat transfer coefficient K_{0j} , measured before seed injection. As can be seen from Figure 37, the total heat transfer in the radiation chamber and in the first semiradiation tube bank (curve 1) was halved before stabilization of the deposits, while the heat transfer in the second and third semiradiation banks practically did not change. Evidently, all this was compensated by an increase in the radiative component and in the total heat flux as a consequence of the increase in the temperature of the plasma flow.

The heat transfer in the convection shaft (curve 3) decreased monotonically. Washing the heat exchange surfaces with water (broken line) brought about an abrupt increase of K , but then it again began to fall. Periodic washing of the surfaces allowed the gas temperature at the exit from the SGM

to be maintained within 370-500 K. This change had almost no effect on the operation of the systems for "wet" seed removal, but had an adverse effect on the operation of the bag filters, where a reduction of T_{cp} beyond the SGM to 100°C led to the moistening of the seed deposits and the impairment of the fabric regeneration.

4. Chemical composition of the seed deposits and their distribution in the MHD facility loop. The successive washing of section with water used to clean all surfaced made it possible to estimate the quantity of seed deposited on a given tube bank, the chemical composition of the deposits and their content of insoluble impurities (the last is very important for seed regeneration).

During the experiments in the U-02 loop, the seed material balance was frequently determined to establish the relationship between the amount injected into the combustion chamber and that trapped by the surfaces and special removal systems. Since the chemical composition of the seed both in the combustion products and on the tube surfaces changes with wetting, the balance was calculated with respect to pure potassium. As a rule, only 20-25% of the injected seed reaches the recovery system and is captured there. Approximately 40% is removed from the radiation chamber in a molten state, while the remainder remains on the heat exchange surfaces.

The deposits on the surfaces do not contain only potassium compounds (hydroxide, carbonate or bicarbonate), but contain a great variety of other components.

A semiquantitative spectral analysis showed that in addition to seed the deposits contain a significant quantity (about 1%) of zirconium, chromium, aluminum, magnesium, copper and sodium, as well as silicon, calcium, iron and vanadium. Some of these substances (Zr, Cr, Al, Mg) appear from the lining

of the hot surfaces and the pebble bed of the high-temperature air preheater, while others, such as iron and copper, come from the metal elements of the channel and heat exchangers. The overwhelming majority of the compounds of these elements (oxides, carbonates, aluminosilicates) are almost insoluble in water.

Analysis of the deposits showed that the insoluble portion is reduced along the gas train: it reaches several percent on the waterwalls of the radiation chamber (especially on the waterwall opposite the diffuser), while at the exit from the SCM and in the recovery system it is under 1%. In seed regenerating a significant portion of insoluble compounds can be separated by precipitation and filtering.

All this shows that the building of a heat exchanger operating on natural gas combustion products with seed in the temperature range from 2300 to 400 K, encounters numerous difficulties caused by the deposition of seed on the tube surfaces and requires the development of special measures for cleaning these surfaces and removing the seed. The operating experience with this heat exchanger made it possible to identify the most dangerous zones and to outline some ways of coping with the deposits (removal of seed as melt, washing of the surfaces). The results of the chemical analysis of the deposits gives an idea of the state of most of the recovered seed, necessary for the design of a proper regeneration system.

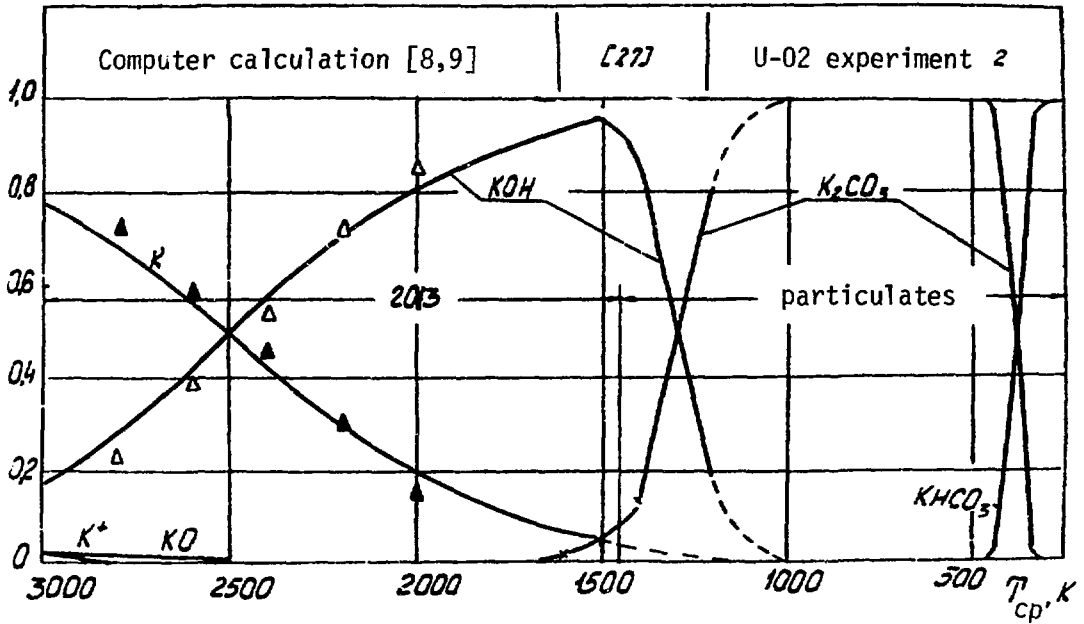


Figure 26, Physical and chemical transformation of the seed in the gas train of the MHD facility.

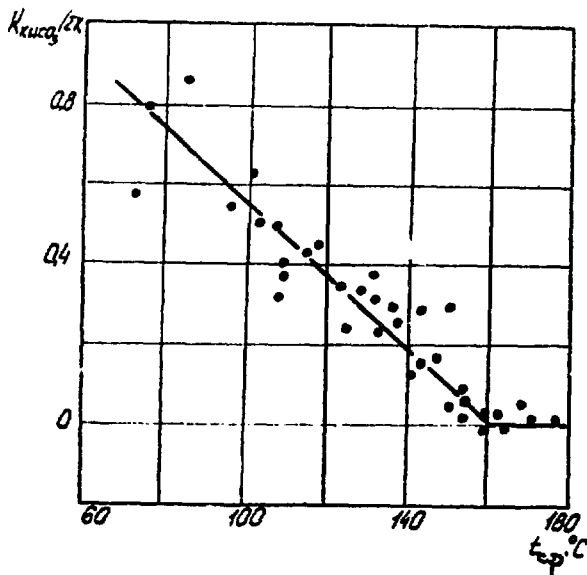


Figure 27. The dependence of the degree of K_2CO_3 transformation into $KHCO_3$ on the temperature of the combustion products flow.

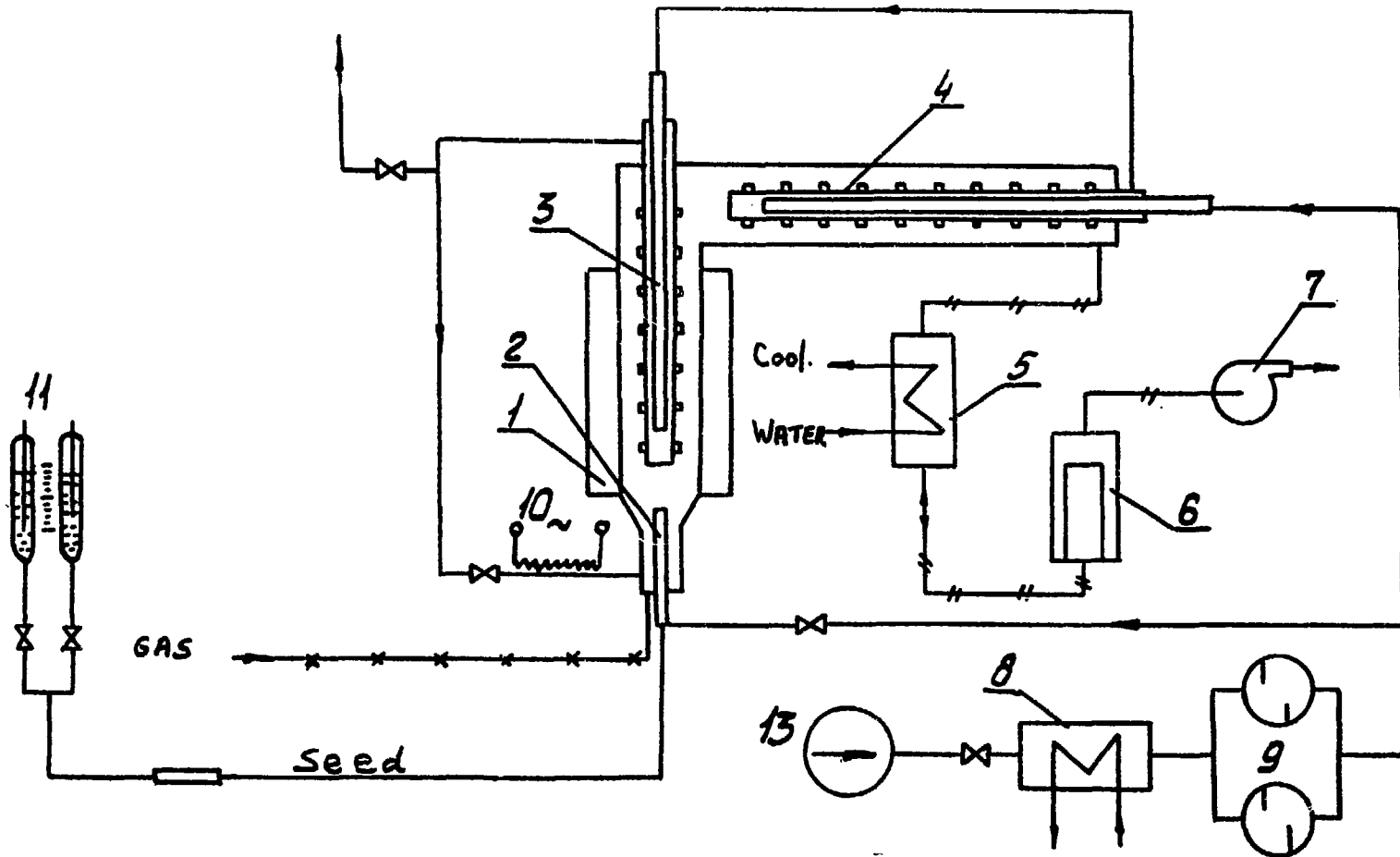


Figure 28. The layout of the experimental facility for the investigation of the physical nature and chemical composition of seed deposited from the flow of natural gas combustion products.

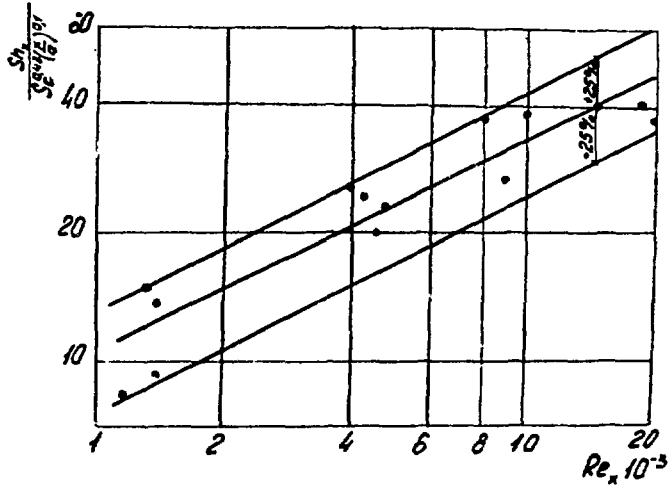


Figure 29. Mass transfer during the condensation of KOH vapor on tube surfaces in axial flow conditions.

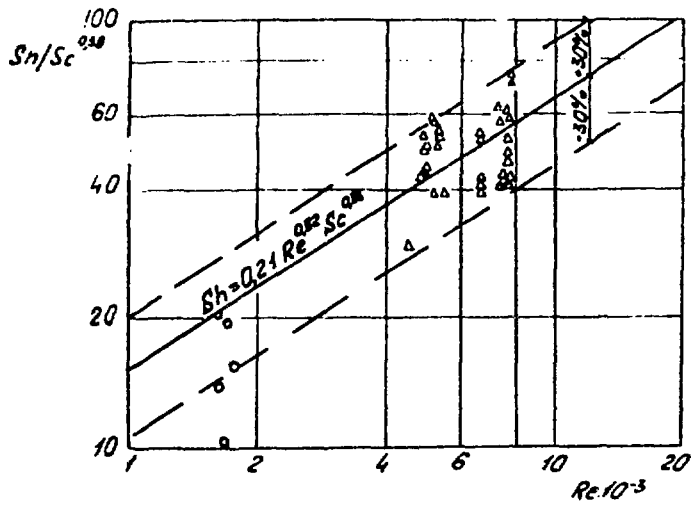


Figure 30. Mass transfer during the condensation of KOH vapor on the tube surface in transverse flow conditions.

Δ - IVTAN data; o - data of [38].

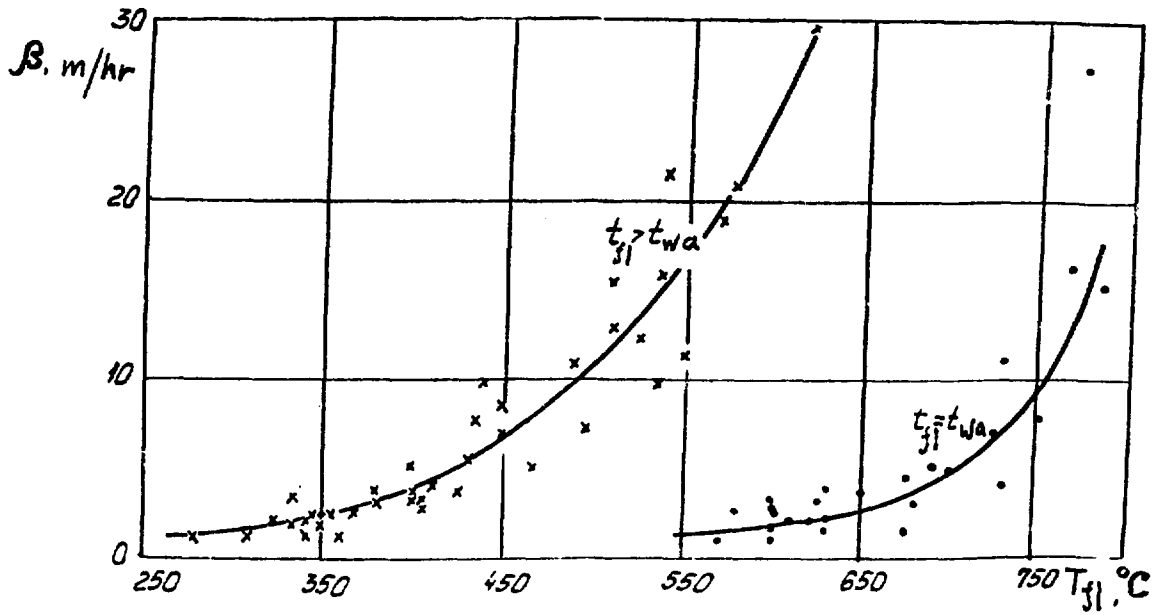


Figure 31. The effect of thermophoresis on the rate of K_2CO_3 particle decomposition from the condensation aerosol flow.

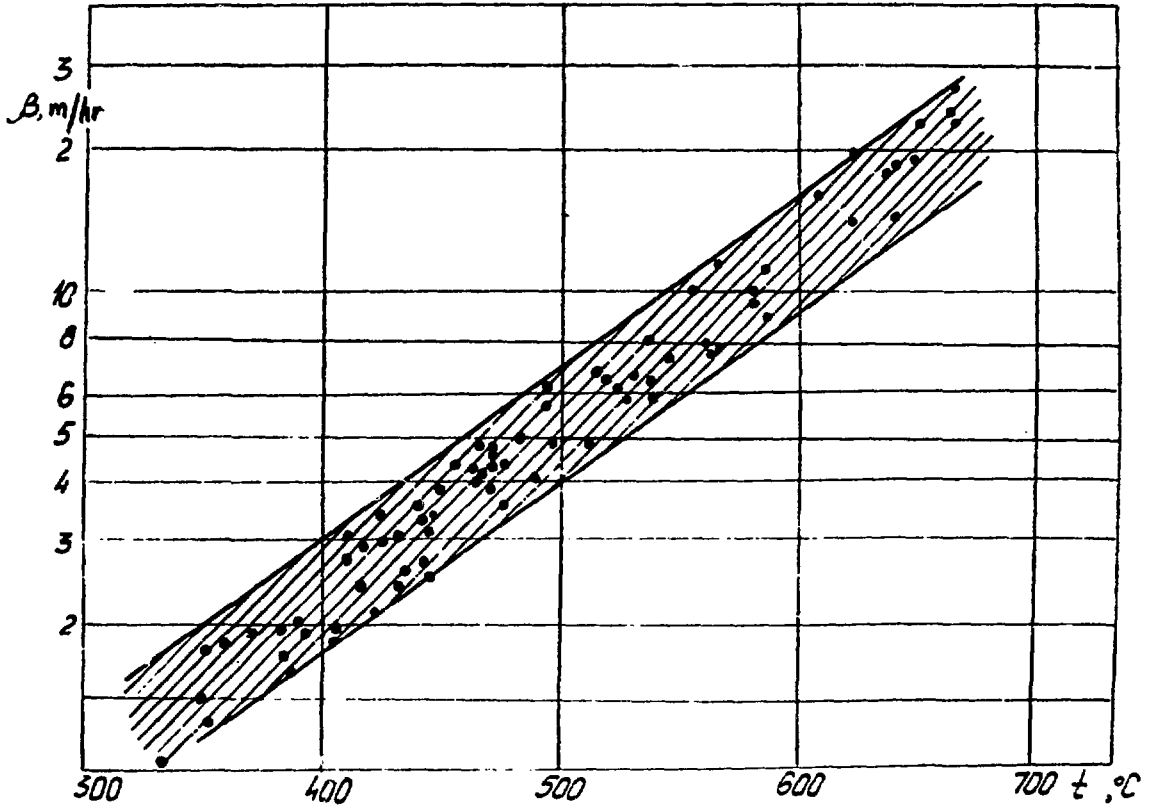



Figure 32. Comparison of experimental and calculated values of thermophoresis velocity in axial flow along tube bank.

● - experimental;  - calculated formula (22)

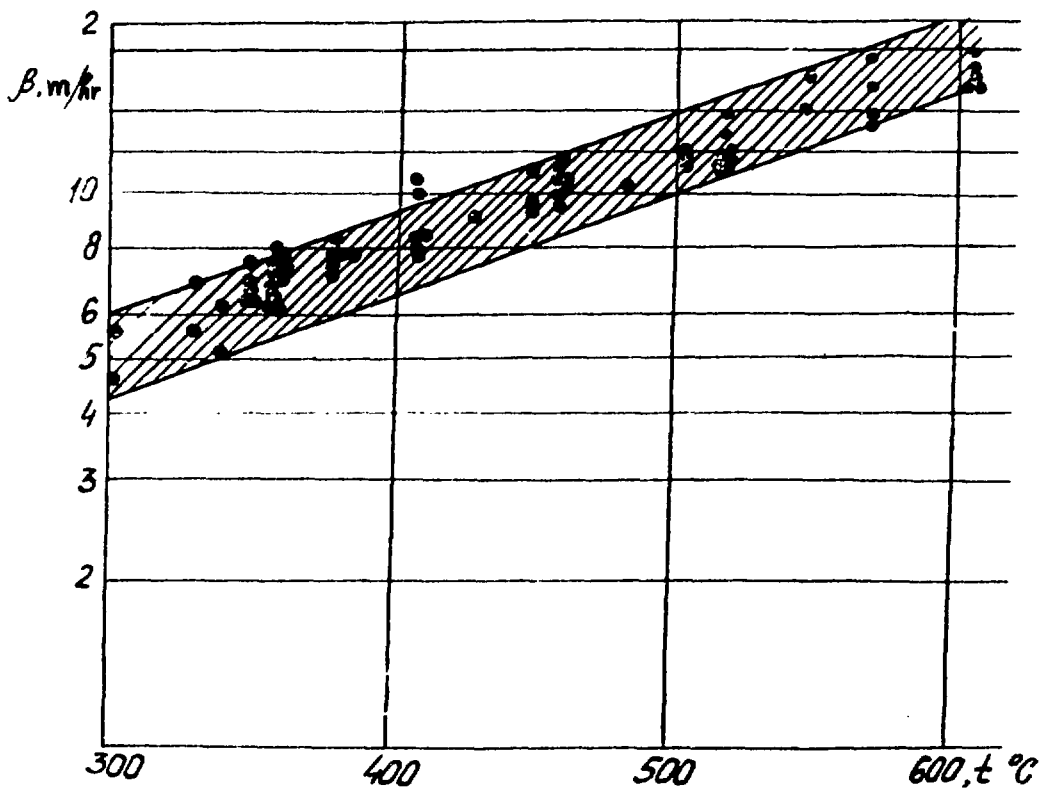



Figure 33. Comparison of experimental and calculated values of thermophoresis velocity in transverse flow around tube bank.

o - experimental;  - calculated formula (22)

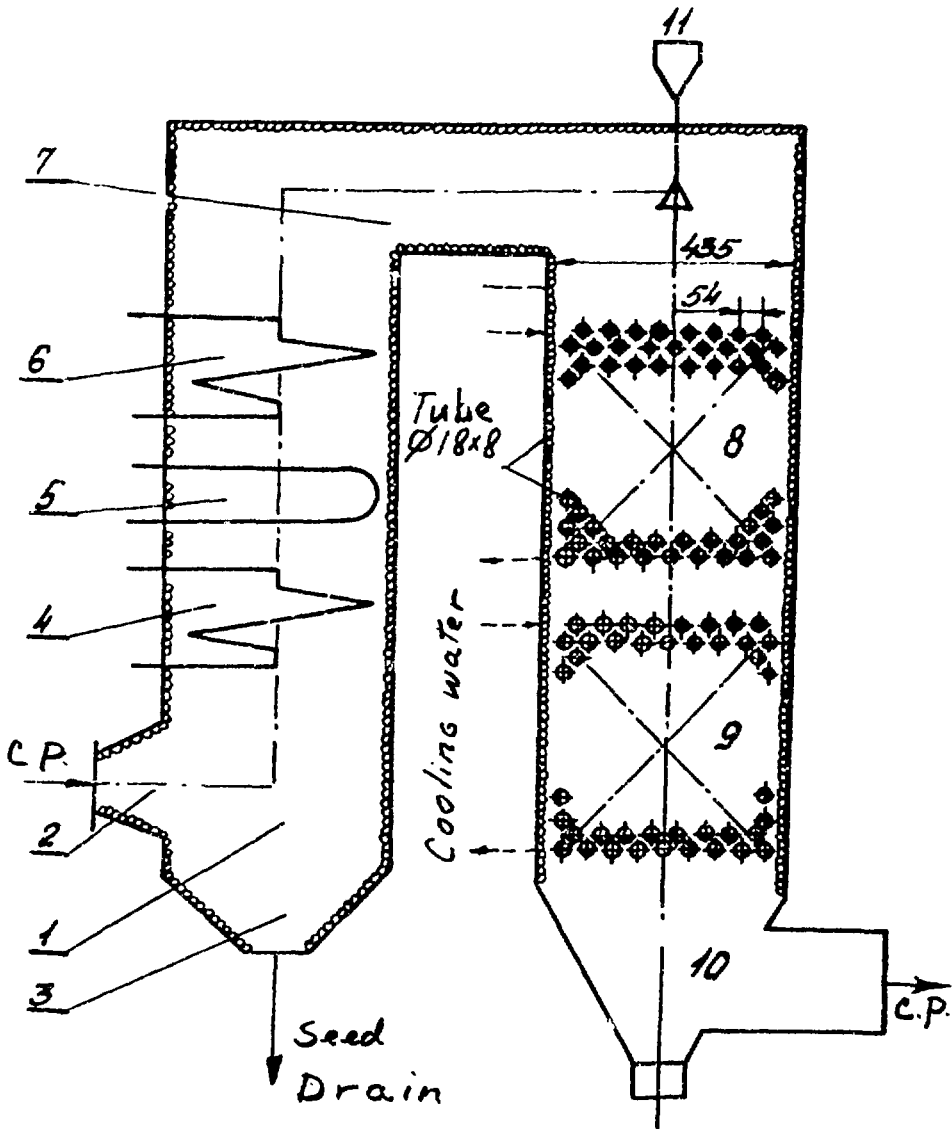


Figure 34. Layout of steam generator model on U-02:

- 1 - radiation chamber; 2 - diffuser; 3 - cold funnel;
- 4, 5, 6 - semiradiation surfaces; 7 - horizontal gas duct;
- 8, 9 - transversely washed tube banks; 10 - hopper;
- 11 - device for feeding metal shot.

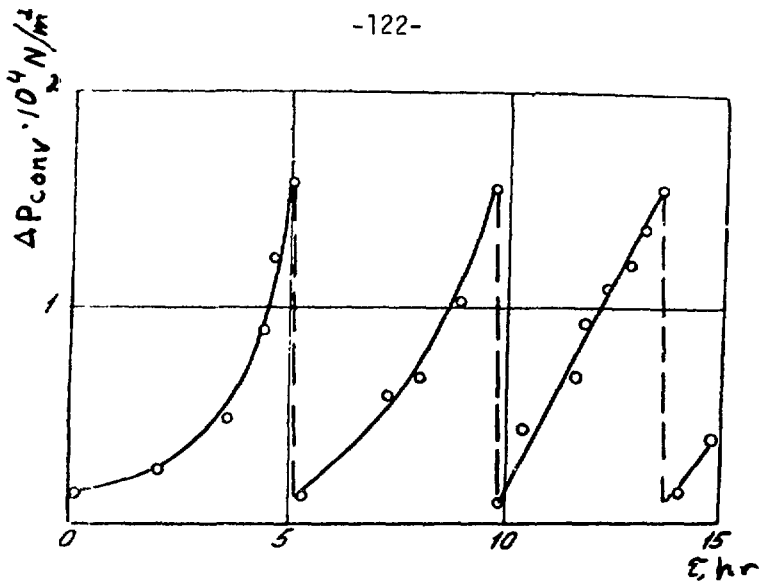


Figure 35. The change in the hydraulic resistance of the convective surfaces during operation with seed (broken line indicates reduction of ΔP when tubes were washed with water).

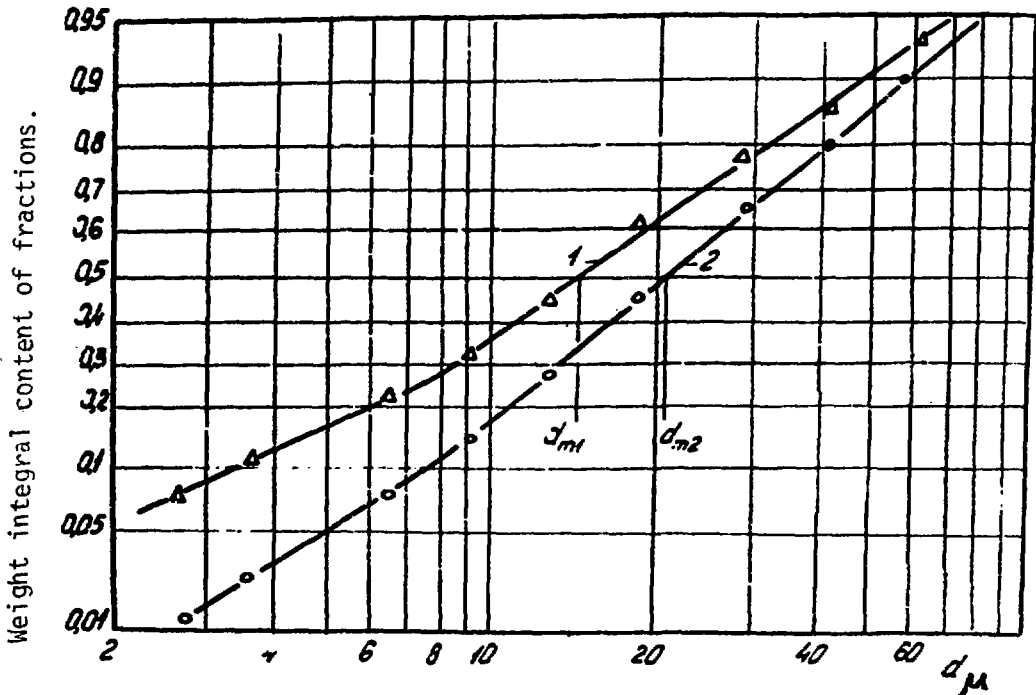


Figure 36. Particle size distribution of K_2CO_3 dust when taken from the isothermal probe surface:

1 - $T_{cp} = 500 \text{ K}$, 2 - $T_{cp} = 480 \text{ K}$

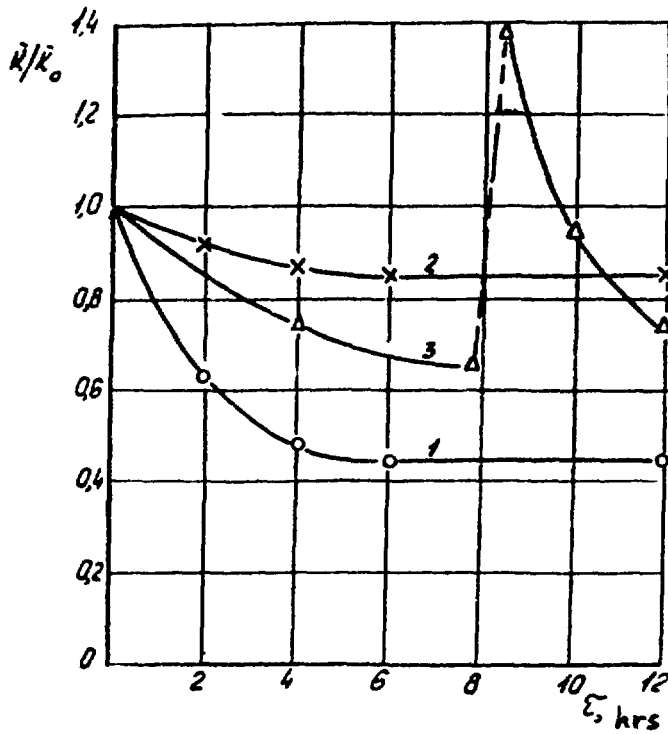


Figure 37. The change of the average heat transfer coefficient:

1 - waterwalls of radiation chamber and first semiradiation surface; 2 - remaining semiradiation surfaces; 3 - convective surfaces (the period of water washing is indicated by broken line).

Table VII. The appearance and chemical composition of seed deposits in various temperature zones.

Section of gas cooling path	T_{st} , K	T_{wa} , K	Appearance of deposits	Composition of deposits
1	1900-1700	>1120	No seed deposits. Wall covered with layer of brittle scale.	-
2	1700-1500	1120-1020	Dense crust-like deposits, dark green then lighter in color	KOH, K_2CO_3 K_2O n
3	1500-1200	1020-900	Loose, cream or mustard colored with long crystals	K_2CO_3
4	1200-600	900-520	Loose, snow-white, made up of submicron particles. Evenly cover perimeter of tubes and projections	K_2CO_3

Note: The external temperature of the metal wall measured in the experiments was taken as the temperature of the cooling surface. The temperature of the surface of the deposits has a value which depends on the nature and quantity of the deposits. Estimation calculations showed that the difference between these temperatures was not over 10, 40 and 25 K for the 2nd, 3rd and 4th zones respectively.

Chapter IV

Seed Capture and Regeneration from Combustion Products Exhaust

1. Requirements for seed capture systems and the selection of promising systems.

One of the most important problems remaining to be resolved by the designers of MHD power generators is the capturing and removal of the ionizing seed and its return into the cycle. This has to be done for reasons of economics and environmental protection.

With the optimum seed (potassium) concentration (0.7 mol %) the natural gas combustion products contain about 1.8 wt % K_2CO_3 . If this quantity is related to a gaseous fuel combusted in air enriched with oxygen to 40%, then it comprises approximately 0.25 of the fuel flow rate. The cost of the technical-grade potassium carbonate used as seed is about 5 times the cost of natural gas. If the ratio of their flow rates is considered, then we find that the total cost of fuel and that of seed are approximately equal. The fuel is combusted, but the seed must be captured and returned to the cycle. A 1% loss of injected seed is equal in cost to a 1% increase in the specific consumption of fuel.

The environmental health regulations also present rigid requirements: the transient maximum allowable concentration of a nontoxic dust, including K_2CO_3 , in the air of populated areas is 0.5 mg/m^3 , and the average daily MAC is 0.15 mg/m^3 . In order to satisfy these requirements at a power station with an MHD generator having a total capacity of 3000 MW and a three-column stack 250 m high and gas exit velocity of 15 m/s, the K_2CO_3 concentration in the stack gases, according to [41], must not exceed 0.5 g/m^3 , which corresponds to K_2CO_3 losses of 2%.

If about 50% of the injected seed leaves the heat exchangers of the MHD power plant as melt and shaken down (or flushed) dust, the efficiency of the seed capturing equipment must be no less than 98%.

Achieving such a thorough cleaning of the gas presents many difficulties, especially, if one considers the submicron particle size, not previously encountered in thermal power stations, since the fly ash particles usually are from 5 to 100μ in size. There is experience in trapping smaller particles in the chemical and metallurgical industries. For example, in the chemical industry sulfuric acid mists with droplets of about 0.1μ in diameter must be trapped, while in metallurgy the gases of blast and open-hearth furnaces of dust containing a substantial portion of particles of the same size.

An analysis of the available data on gas cleaning equipment and its efficiency in capturing dust particles of various sizes allowed the identification of the equipment which is most promising for capturing seed in an MHD power plant. These included cloth and fiber filters, which ensure capturing of 99% of dust particle sizes of 1μ , as well as venturi scrubbers and electrofilters. These findings agree well with the diagram (Figure 38) given in [42], which also shows the seed particle size distribution in the exhaust gases of MHD facilities.

As a result, three methods were selected for the study of seed capturing efficiency from the flow of condensing particulates in MHD facilities: filtration through dry fiberglass cloth, venturi scrubbers and electrostatic precipitators. Systems employing the first two methods were installed at the U-02 facility for seed removal. Each of them was calculated for the total flow rate of gases in the MHD generator loop. They are installed in parallel and were operated alternately. A pilot test facility designed for

10-15% of the total gas flow was set up to investigate the capturing efficiency of the electrostatic precipitator.

All the seed capturing systems (Figure 39) are located downstream of the steam generator in the 0.4-0.6 bar (abs) pressure zone. The gas temperature at the entrance to these systems varies from 340 to 600 K with flow rates from 0.5 to 1 kg/s.

Even though 18 g K_2CO_3 per kg of combustion products was injected in order to produce the optimum potassium concentration, the seed concentration at the entrance to the capturing systems, as a rule, was not over 5 g/m³ (STP). This reduction in the seed level is due to the removal of a significant portion of the K_2CO_3 as melt from the radiation shaft of the SGM and the settling of solid seed particles on the convection surfaces of the SGM and in the heat exchanger (6). Proceeding from the need to trap 99% of the total injected seed, the residual dust level must not exceed 0.2 g/nm³. As experience showed, this task turned out to be within the capability of all three seed capturing methods investigated.

2. Bag filters

The system of "dry" seed removal from the MHD generator loop consists of a 4-section bag filter (7) (cf. Figure 39) with a total filtration surface of 124 m². The cylindrical housing of each section contains 88 filter frames 65 mm in diameter and 2 mm long, supporting bags of fabric being studied. The frame is made of metal angle profiles with a metal screen stretched over them. Here the process of filtration takes place from the external surface of the cloth to the central space. The filters are regenerated by back-washing with purified purge gas.

In order to switch the filters for operation and regeneration, the entrance, exit and purge lines of each section are equipped with electrically operated valves activated by remote control from the U-02 facility control panel. Hatches for manual unloading of the potash are mounted on the outlets from the hoppers. The walls of the equipment, including the hopper sections and gas lines, are thermally insulated.

The degree of ionizing seed removal from the gas was calculated from measurements of the dust levels at the filter entrance and exit. During the tests the temperature and humidity of the gases, the underpressure in the filter and the pressure drop across the sections were monitored. Gases at 150-180°C passed through the filters, practically without heating the hopper sections. The absence of special heating of the hoppers on the U-02 led to the condensation of water vapor. After the tests the hoppers were found to contain much water, with dissolved seed that was captured by and then fell from the filter bags. When the relatively cool combustion products entered the filters and also when the filters were shut off, the layer of seed which had settled on the filter bags became humidified, and a crust was formed as the deposit dried, causing a high initial resistance in the filter. In order to avoid the formation of this crust, the filters had to be heated to 150-160°C by passing hot combustion products through them before supplying seed.

Subsequent experiments showed that at a high gas temperature (T_{cp} 250°C) at the entrance to the filter the hoppers were heated quite well and a powdery seed settled in them.

Continuous tests of the bag filters on the U-02 did not last over 100 hours, which does not allow any conclusion to be made about the service life of the investigated fiberglass cloth under operating conditions with seeded combustion

products. In order to investigate the effect of an alkaline environment on the fiberglass cloth, specimens of clean and dust-treated fabric were tested for breaking strength and flex life (to the point of destruction) under laboratory conditions.

It was established that the breaking strength for dust-laden TSSNF-0 fiberglass cloth was reduced by 26%. In tests for flex life samples of fiberglass cloth clean withstood an average of 1800 cycles before destruction, while the dust-laden samples lasted only 600 cycles, i.e., 1/3 as long.

Of course the results of laboratory tests serve only to some degree as a qualitative evaluation of the behavior of fiberglass cloth in the filtration of gases containing K_2CO_3 and cannot replace long-term service tests of the filters under the varied operating conditions typical of power-producing MHD facilities.

The presently available data on the operation of fabric filters on the U-02 MHD facility allows the following practical conclusions:

1. Fabric filters operate poorly when the temperature of the combustion products is at the 100°C level because of the high hygroscopicity of K_2CO_3 . The working interval for such filters is from 200 to 280°C.

2. Of the three types of filter fabric investigated (baize, Nitron, fiberglass cloth) the best is fiberglass type TSSNF-0, which can operate in this temperature range and at the same time ensure a high efficiency of seed capture (above 99.5%).

3. Fiberglass cloth filters should not be allowed to become moist, since moisture seriously impairs their mechanical properties.

3. System with a venturi scrubber

The venturi scrubber seed capturing system was installed at the U-02 in 1968.

Ease of service and high reliability of operation rapidly made it the principal seed capturing system used when conducting all kinds of experiments with the MHD channel and steam generator model. Long operating experience showed that the equipment made from 1K18N10T stainless steel did not corrode at all, while the corrosion of carbon steel (supplementary tank, heat exchanger) was insignificant, even though contact of the metal with an aqueous solution of K_2CO_3 and $KHCO_3$ was practically continuous during this entire period, i.e., many thousands of hours.

The layout of this system for seed removal is shown in Figure 39. A frothing unit (8) 1400 mm in diameter with three distribution grids was used as the first, preliminary, stage of purification. The grids 5 mm thick were made of stainless steel and had 6 mm openings. The free cross section of the grids was $0.25 \text{ m}^2/\text{m}^2$. A droplet collector was installed in the upper part of the unit to separate entrained droplets. Combustion products at 100-250°C entered from the heat exchanger into the lower part of the frothing unit, whose grids were irrigated with a solution of captured seed. The gas was cooled and partially cleaned in the frothing unit.

The venturi scrubber consisted of a sprayer tube (venturi tube) (9), in which the high velocity of the gas stream caused the particles to agglomerate and to settle on the droplets of irrigating liquid, and a droplet collector (TsN-15U cyclone with a gap in the exhaust pipe) (10), where the droplets were separated from the gas stream under the effect of centrifugal forces.

At first the sprayer tube had an entrance 180 mm in diameter. The combustion products were irrigated through a nozzle mounted on the axis of the tube in front of the entrance with two rows of radial injector holes. However, it became clear during the tests that the hydraulic resistance of the installed tube was not sufficient to ensure the necessary seed capture efficiencies. The tube was redesigned and its entrance was reduced to 130 mm, and then to 110 mm, which significantly increased the gas velocity in the entrance, and consequently the hydraulic resistance of the unit.

Later a venturi tube with an adjustable entrance of rectangular cross section was also tested. The cross section was varied in a single plane by shifting profiling cams. The profile of the cams corresponded to the configuration of the internal surface of the venturi tube entrance and the adjacent sections of the converging tube and diffuser. This design allowed the cross section to be reduced by more than half.

The cyclone droplet collector had the following basic geometric dimensions: diameter 1000 mm, height 6000 mm. The exhaust tube gap of the cyclone was designed to increase the efficiency of droplet collection. Normally, centrifugal forces throw part of the droplets onto the internal surface of the exhaust tube, where they rise in parallel with the stream of exhaust gas. The exhaust tube gap ensures the removal of this liquid from the droplet collector through a special pipe.

An aqueous solution of K_2CO_3 and $KHCO_3$ was used as the spraying liquid for the equipment of this seed removal system. The solution concentration, based on K_2CO_3 , ranged from 0 to 30% during the study. The solution, from delivery tank (11) through a mechanical purification system (12), was delivered by centrifugal pump (13) via two pipelines to the grids of the frothing unit and to the sprayer tube. A water-to-water heat exchanger (14) was installed

between the pump and the frothing unit, allowing the solution temperature to be regulated by changing the flow rate of the cooling water. Spent solution from the frothing unit and the cyclone droplet trap flowed by gravity to the same tank (11). Thus, the seed solution circulated in a closed system.

The character of the thermal process changed as a function of the temperature of the liquid used to spray the grids of the frothing unit. A low liquid temperature (below the dew point of the combustion products) led to water vapor condensation from the combustion products, and a high temperature led to partial evaporation of the solution. The liquid level in the delivery tank served as the indicator of the operating mode. The hydraulic resistance of the frothing unit (including the built-in droplet collector) was 1 kN/m^2 . The seed capturing efficiency of this unit did not exceed 30%.

The fine purification of the gases in this system was provided by the venturi scrubber. The experiments, in complete agreement with theory, showed that the efficiency of seed capturing is basically determined by the hydraulic resistance of the sprayer tube: the higher ΔP_{tu} , the more efficiently the venturi scrubber operates.

Experiments were conducted in order to identify the influence of the venturi tube design on the efficiency of capturing fine seed particles. Several variants of the unit were tested, having different geometric ratios of the individual elements of the venturi tube, different designs and methods of spray injection.

During the tests the flow rate of combustion products at the exit from the system was 0.5-1.2 kg/s, the gas temperature at the entrance varied from 100 to 230°C, the absolute pressure in the system was 0.4-0.6 bar, the dust concentration at the entrance to the unit varied from 1-10 g/m³ (STP), the gas velocity at the entrance of the venturi tube varied from 30 to 200 m/s,

and the specific spray liquid flow rate varied from 0.4-5 litres/m³ (K₂CO₃ solution up to 20% concentration).

The experimental data were processed using this relationship:

(51)

$$N = AK_g^K$$

where $N = \ln \frac{1}{1-n}$; n is the seed capturing efficiency, dimensionless;

K_g is the energy expended in processing the gas, J/m³ gas;

A and K are constants which depend on the properties of the captured particles.

The value of K_g is calculated from the formula

$$K_g = \Delta P_{tu} + \Delta P_{drt} + P_l m,$$

where ΔP_{tu} is the hydraulic resistance of the venturi tube, N/m²;

ΔP_{drt} is the hydraulic resistance of the droplet trap, N/m²;

P_l is the spray liquid pressure, N/m²;

m is the specific flow rate of spray liquid, m³/m³ gas.

As can be seen in Figure 40, the experimental data lie, with some scatter, on a straight line, which can be approximated by the expression

(52)

$$n = 1 - \exp(-0.016 K_g^{0.554}).$$

Thus, the seed capturing efficiency of the venturi scrubbers is determined exclusively by the energy losses and practically speaking does not depend either on the design of the unit or on the spray liquid injection method, while the crucial parameter is the hydraulic resistance of the venturi tube. Rather high energy losses were required to achieve the necessary seed capturing efficiency at the U-02 (98-99%). Thus, the required degree of gas purification,

for which the dust concentration in the exhausted combustion products would be 35 mg/m^3 (STP), was ensured with a venturi tube hydraulic resistance on the order of 20 kN/m^2 .

In order to check the effect of temperature on the efficiency of the venturi scrubber, the frothing unit spray was turned off, i.e., the removal system operated without cooling or humidification of the combustion products. The tests were made using one venturi tube with entrance diameter $d_0 = 100 \text{ mm}$ and relative length $L_0 = 0.15 d_0$ and another tube with $d_0 = 60 \text{ mm}$ and $L_0 = 3 d_0$. Both were sprayed with a 3-4% K_2CO_3 solution.

Interruption of the spraying in the frothing unit allowed the temperature of the combustion products to rise to 300°C . The gas velocity at the tube entrance rose from 62 to 170 m/s during these tests and the specific spray water flow rate rose from 0.6 to 1.15 liters/ m^3 . The test results, processed using the dependence $N = f(K_g)$, shown in Figure 40, indicate that the efficiency of the venturi scrubber, when gas enters at temperatures to 300°C , i.e., without preliminary treatment in the frothing unit, adhering rather strictly to the dependence constructed for similar energy losses, but with the preliminary gas treatment in the frothing unit. This suggests that the cumbersome frothing unit can be eliminated from the system.

However, the tests showed that when operating without a frothing unit a deposit is formed on the spray devices in the particle laden flow. Therefore, either the spray system for the venturi tubes must be removed from the particle containing gas flow, or some water must be introduced into the air line to humidify and dissolve the deposits of K_2CO_3 . Resolution of this purely technical problem will make it possible to eliminate the most cumbersome and metal-intrusive component of the system, the foaming unit.

4. Electrostatic precipitator

The efficiency of an electrical method of capturing the ionizing seed from the exhaust gases of an MHD generator at the U-02 facility was tested using a small experimental electrostatic precipitator (17) (cf. Figure 39), which could receive gas either after preliminary wet treatment or directly from the steam generator. In the first case the temperature of the gas was below the dew point and was 45-55°C, i.e., the electrostatic precipitator was operating in the wet mode. In the second case the gas temperature could be raised to 160°C and the electrostatic precipitator tested in the dry mode.

The study of the ionizing seed capture in a dry electrostatic precipitator is of much interest, since in this case the temperature of the exhaust gases is raised and the stack operating conditions and dispersion of the uncaptured seed are improved. Therefore, the electrostatic precipitator was studied while operating in both wet and dry modes at the U-02 facility.

The height of the flat precipitation electrodes of the experimental vertical electrostatic precipitator was 0.8 m and the active cross section was 0.24 m². Various types of discharge electrodes could be installed in the precipitator. The distance between the precipitation electrodes is 200 mm. A bell-shaped pyroceramic support-conduit insulator was used for the high voltage supply. The insulator box and the gas near the inner surface of the insulator were electrically heated in order to prevent droplets of the conductive seed solution from condensing on the insulator surface. Power supply to the electrostatic precipitator was from a VS-50-50 high voltage unit with double half-wave rectification, a nominal voltage of 50 kV and an average rectified current value of 50 mA. Two spray nozzles were mounted in the upper part of the unit for periodic washing of the electrodes. A special impact

rapping device was installed for shaking the electrodes clean in a dry state.

It was established in testing the electrostatic precipitator than when there are fine seed particles in the gas the corona discharge is significantly dampened, which leads to a sharp reduction in the discharge current. Because of this several high-intensity discharge electrodes of the needle-shaped type and combined type were developed and tested.

A comparative study of the various types of discharge electrodes in a wet electrostatic precipitator with the gas pretreated in the venturi scrubber with an irrigation water flow rate of 1.5 liters/m³ and flow resistance of 2.6 kN/m², showed that for practically identical velocities (0.95-1.0 m/s) and gas temperatures (48-55°C) the average value of gas purification was 97.1% when using the combined electrodes and 93.2% when using the commercially manufactured flat needle electrodes. This increase in the operating efficiency is due to the fact that the combined discharge electrodes create a corona discharge field and an electrostatic field of high voltage in the discharge section of the precipitator.

The results of the investigation of the dry electrostatic precipitator indicate that, in principle, it is possible to obtain efficient purification at elevated temperature (90-160°C), i.e., without wet pretreatment. When the gas velocity in the electrofilter is 0.9-1.0 m/s, the degree of purification decreases somewhat with an increase in the gas temperature (Figure 41). The precipitator was tested in a variety of intervals between vibration cleansing of seed deposits. As was expected, even a thin seed layer reduces the capturing efficiency (Figure 42), i.e., the electrodes require fairly frequent cleaning. The seed deposited on the electrodes is easily shaken off, but because of secondary particle entrainment the capturing efficiency of the dry electrostatic precipitator is lower than that of the

wet one: 90-95% versus 95-98%. It should be kept in mind that this rather high capturing efficiency was achieved with a small active electrical field length and a brief residence time (less than one second) of the dust-containing gas in the field. In industry and in power plants commercially produced multi-pole electrostatic precipitators are used with gas residence times on the order of 20 s.

The experimental electrostatic precipitator built at the U-02 facility and tested in dry and wet modes made it possible to investigate the fundamental problems of capturing submicron seed particles. However, the data needed to design industrial electrostatic precipitators for MHD power plants can be obtained only in a large-scale pilot plant.

5. Carbonation of K_2CO_3 in an aqueous solution

It is well known that when gases containing CO_2 are passed through an aqueous solution of soda or potash [43,44] carbonation of the carbonates occurs with the formation of bicarbonates. The soda (or potash) method for removing carbon dioxide from gases is based on this principle.

This same process must occur when wet methods are used to extract the ionizing seed, though it is quite undesirable, since the seed regeneration will then require additional heat losses to break down the $KHCO_3$. Moreover, $KHCO_3$ is much less soluble in water than K_2CO_3 ; therefore, when K_2CO_3 is converted to $KHCO_3$, there is the danger that a solid phase will precipitate out of the seed solutions circulating in the wet extraction systems (venturi scrubber or wet electrofilter). The solid phase will clog the mechanical filters and, if the purification is not sufficient, the spray nozzles. Thus there is a limit to the solution concentration in the extraction systems, which must be considered both in the operation of the seed capturing systems

and in a system for seed regeneration. Therefore, along with the study of seed capturing efficiency in a venturi scrubber the conversion of potassium carbonate to potassium bicarbonate in aqueous solutions of varying concentrations was investigated. Samples of solution were taken for this purpose every hour or sometimes every half hour, and a chemical analysis of the K_2CO_3 and $KHCO_3$ levels was performed. The investigations showed that the bicarbonate is in fact formed in the circulating solution. Since the temperature of the circulating solution, the gas pressure in the system and the CO_2 level in the gas were practically identical in all the experiments conducted at the U-02 facility, the change in the $KHCO_3$ content was determined on the basis of changes in solution concentration.

The experiments covered a range of potassium concentrations (calculated in potassium cation) C_K from 1 to 13 g of potassium per 100 g water. The solution temperature varied in the 40-50°C range. The data obtained are presented in Figure 43. Here the value of C_K is plotted along the abscissa and the proportion of potassium as $KHCO_3$ related to the total quantity of potassium in the solution $[K_{KHCO_3} / K]$ is plotted along the ordinate.

As can be seen from the graph, at low concentrations practically all the potassium is found as $KHCO_3$. The proportion of $KHCO_3$ decreases with an increase of C_K and is 0.45 at $C_K = 10$ g/100 g H_2O . It is expected that the proportion of $KHCO_3$ will be somewhat lower in the range of concentrations $C_K = 25-40$ g per 100 g H_2O , which corresponds to the 30-40% K_2CO_3 solution planned for power-producing MHD facilities. The Sherwood-Pigford formula [45] was used to extrapolate the data to the zone of higher solution concentrations:

$$P_{CO_2} = \frac{3380 \sqrt{K} N^{1.29}}{S(1-f)(150-t)}, \quad (53)$$

where N is the normality of the solution with respect to the cation (potassium);

f is the proportion of potassium as KHCO_3 , i.e., $f = K_{\text{KHCO}_3} / \Sigma K$;

S is the solubility of pure CO_2 in water at atmospheric pressure, kg-mole/ m^3 ;

P_{CO_2} is the equilibrium partial pressure of CO_2 , N/m^2 .

However, formula (53) is, strictly speaking, valid only for temperatures up to 40°C and the N values from 1 to 2, i.e., from 3.9 to 7.8 g potassium per 100 g water, and its suitability for the range of concentrations pertinent to this discussion required experimental verification.

Experiments conducted at the U-02, using a 25% solution of K_2CO_3 in the system consisting of the frothing unit and venturi scrubber gave values of K_{KHCO_3} close to those calculated by formula (53). For further confirmation tests were conducted at atmospheric pressure under laboratory conditions. Products of methane combustion in air or a synthetic mixture of nitrogen with carbon dioxide (9:1 or 18:1) were bubbled through an aqueous solution of K_2CO_3 at a given temperature. Bicarbonate formed in the solution, and after a certain time K_2CO_3 - KHCO_3 equilibrium was established. The data obtained confirmed the validity of formula (53): the deviation of the points from the theoretical curve was within the limits of experimental accuracy.

6. Composition of the recovered seed and its regeneration

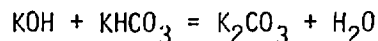
In power-producing MHD facilities ionizing seed is recovered primarily from two sections of the loop: from the radiation section of the steam generator (or the high-temperature part of the regenerative air heater) and from the exhausted combustion products. The recovered seed must be regenerated so that it can be reused in the MHD cycle. The regeneration method is determined by the composition of the recovered seed and by the amount and chemical composition of the acquired impurities.

Some data regarding this were obtained at the experimental U-02 facility.

In investigating the composition of the seed recovered from the radiation shaft of the SGM, a large quantity (up to several percent) of insoluble impurities was found, which rapidly precipitated out in the overflow and receiving tanks. There was an especially large amount in the overflow tank. These impurities consisted of ceramic materials carried from the high-temperature air preheater, the hot-air duct, the combustion chamber and the MHD channel. There was much less ceramic material in the receiving tanks and its particles were much finer -- on the order of 1 mm. The insoluble impurities in the solution circulating downstream of the receiving tank comprised tenths of one percent and consisted of calcium, silicon, magnesium, aluminum and iron. The chemical composition of the seed was K_2CO_3 with some KOH (up to 12%); the greenish color of the solution is evidently due to the presence of potassium chromates (trace levels).

The solution circulating in the system with the venturi scrubber contains additive as K_2CO_3 and $KHCO_2$. Here, the accumulation of insoluble impurities is only one-tenth of the amount in the steam generator and their chemical composition is the same.

The presence of KOH in the seed recovered from the steam generator and $KHCO_3$ in the seed from the main recovery system produces a reaction between these compounds leading to the formation of K_2CO_3 that serves as the first step of seed regeneration:



For this reaction to occur the solutions must be allowed to mix. This was in fact done on the U-02. However, although the quantity of seed recovered from the radiation section of the SGM reaches 40% versus the 25% recovered from

the exhaust gases, the quantity of KOH can be insufficient to convert all the bicarbonate into K_2CO_3 .

One of the ways to break down the $KHCO_3$ is heating and boiling the solution. This method is commonly used in chemical industry for decarbonation of the potash solution circulating in CO_2 capturing facilities [43, 44].

At the U-02 facility these methods produced some results. Seed solutions from both recovery systems were used: this solution from the cold funnel of the steam generator with a concentration of K_2CO_3 near 50%, and from the venturi scrubber system, a 30% solution. The first solution contained a small amount of KOH, while the second contained some $KHCO_3$ ($K_{KHCO_3} / K = 0.5$). After mixing a 40% solution of K_2CO_3 was obtained, containing $K_{KHCO_3} / K = 0.23$. It was placed into one of the evaporating tanks of the seed injection system and concentrated to 52% (based on K_2CO_3). A chemical analysis of samples showed that the amount of potassium as $KHCO_3$ was reduced to 14%. After the solution was cooled a solid consisting mainly (up to 72%) of $KHCO_3$ precipitated on the tank walls. The liquid phase was sufficiently pure and only in the lower (hemispherical) part of the tank did it appear as a greyish gruel. Samples were taken of the solution in the upper and lower parts of the tank and also of the crystals from the tank walls and were analyzed for various chemical elements. The results obtained are given in Table VIII.

The data of this table shows that 10-15 hours settling period of the recovered and concentrated seed solution provides an adequate separation of foreign chemical impurities. This significantly eases the task of removing the impurities from the solution. Thus, the most difficult stage of seed regeneration is the decomposition of the $KHCO_3$ to K_2CO_3 .

Conclusion

The experimental and theoretical investigations of the processes connected with the injection and recovery of the ionizing seed in gas-fired open cycle MHD facilities, as well as the experience of operating the experimental MHD facility U-02, lead to the following conclusions:

1. Potassium carbonate is the most suitable ionizing seed for power generating MHD facilities using sulfur-free fuel.
2. K_2CO_3 powder is hygroscopic and flows poorly, making injection in dry form difficult. It was shown experimentally that it is possible to prepare and inject a high-concentration (to 75%) aqueous solution of K_2CO_3 into the combustion chamber of the MHD facility.
3. A procedure is proposed for calculating the rate of seed vaporization in a flow of hot gases. Calculations showed satisfactory agreement with the experimental data.
4. A significant increase in the rate of seed ionization was demonstrated experimentally when the seed was injected in the form of superheated K_2CO_3 solution.
5. Seed behavior in the various temperature zones of the MHD facility gas train was investigated experimentally.
6. The mass transfer processes during the condensation of KOH vapor and deposition of submicron K_2CO_3 particles under the effects of thermophoresis were experimentally investigated.
7. A method for seed extraction in molten form from the radiation section of the steam generator was proposed and tested. It was shown that up to 40% of the seed can be removed by this method.
8. Three seed capturing systems were tested: dry bag filters, venturi scrubber and electrostatic precipitators. All three systems can provide the required degree of capturing. However, the inadequate reliability of the

bag filters precludes their being recommended for MHD power plants. The two other systems are quite promising.

9. The conversion of K_2CO_3 to $KHCO_3$ in the aqueous solution circulating in the systems for wet seed extraction (venturi scrubber, wet electrofilter) was investigated.

10. Data were obtained on the chemical composition of the extracted seed and the amount of foreign impurities. Proposals regarding the technology of seed regeneration are given.

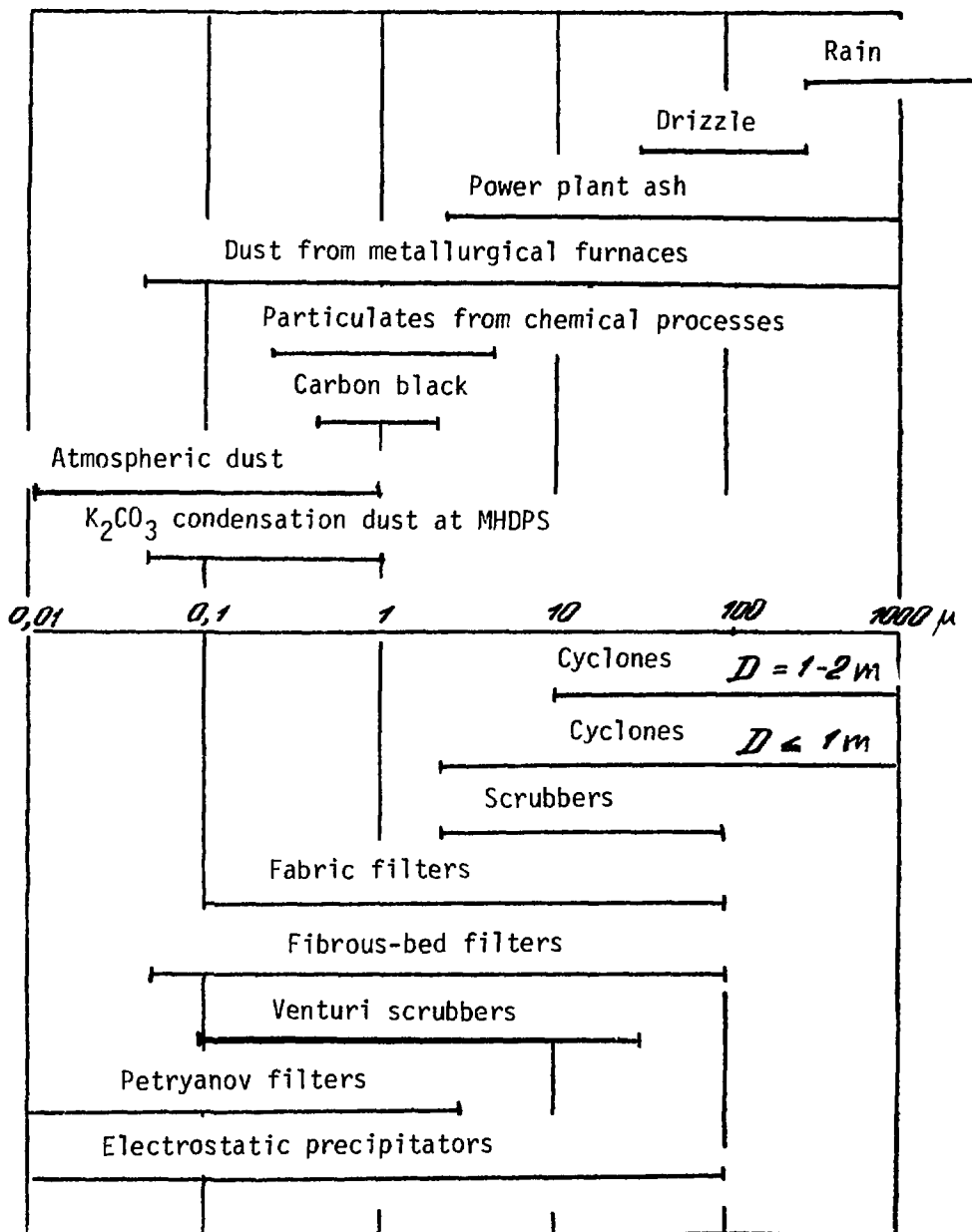


Figure 38. Particulate distribution and capturing devices [42].

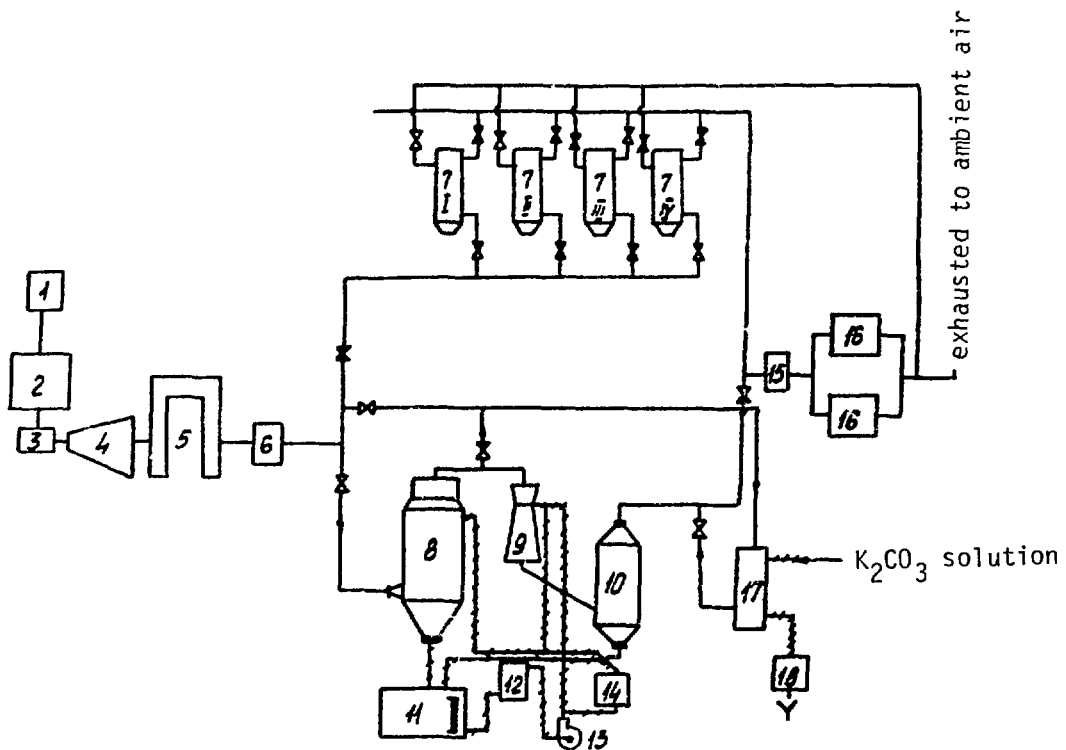


Figure 39. Systems for seed trapping in MHD U-02 facility

- 1 - air blower; 2 - high temperature air preheater;
- 3 - combustion chamber; 4 - MHD channel; 5 - SGM heat exchanger; 6 - heat exchanger; 7 - filters; 8 - frothing unit*;
- 9 - venturi tube sprayer; 10 - cyclone; 11 - delivery tank with K_2CO_3 solution; 12 - grid filter; 13 - circulation pump; 14 - heat exchanger; 15 - gas cooler;
- 16 - vacuum pumps; 17 - pilot electrostatic precipitator; 18 - overflow tank.

*) Bubble tray. Tr.

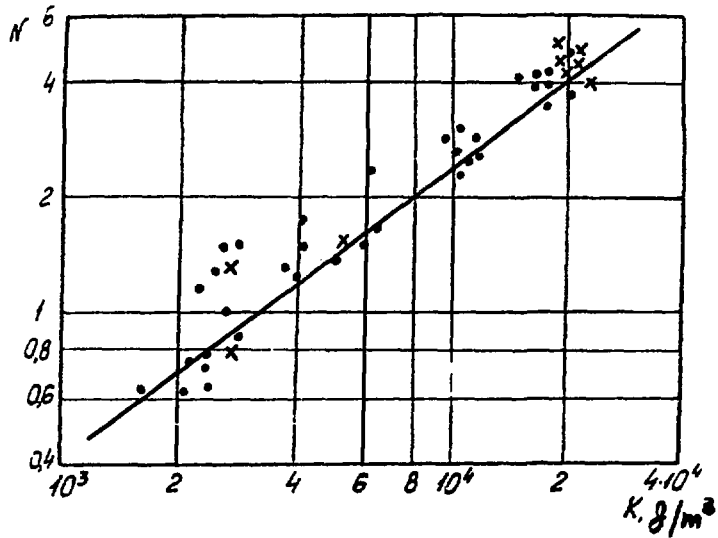


Figure 40. The dependence of seed capturing efficiency in the venturi scrubber system on energy losses:

● - with bubble tray unit; x - without bubble tray unit

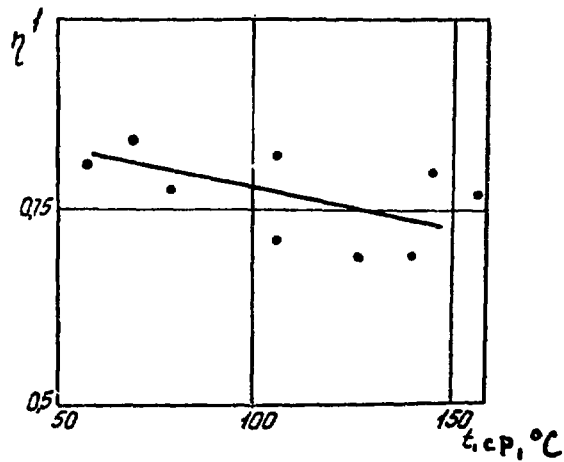


Figure 41. The dependence of seed capturing efficiency of an electrostatic precipitator flat needle electrodes on the combustion products temperature.

= 5-10 min, = 0.86-1.04 m/s
 = 40-50 kV

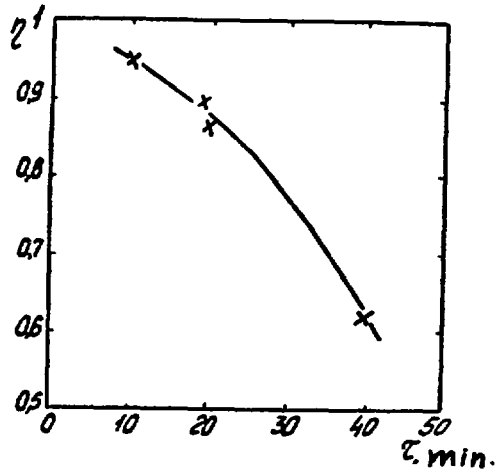


Figure 42. The dependence of seed capturing efficiency of an electrostatic precipitator on the duration of operation between removal of deposits. Cross-shaped combined electrodes,

$t = 65-90^{\circ}\text{C}$,

$w = 1.02-1.23 \text{ m/s}$

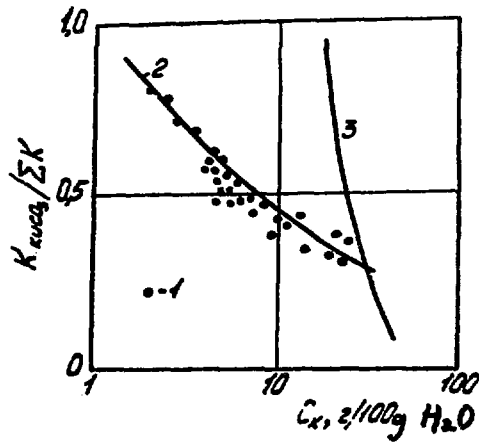


Figure 43. The dependence of the degree of K_2CO_3 to KHCO_3 conversion on the solution concentration C_k (C_k in g potassium per 100 g water):

1 - experimental data; 2 - calculated using (53); 3 - solubility of K_2CO_3 - KHCO_3 mixture at $t = 50^{\circ}\text{C}$.

Table VIII. Quantity of impurities in seed solution extracted from U-02 loop, after concentration to 52% (of K_2CO_3)

Sample number	Description of sample	Quantity of impurity, in % to K						
		Al	Fe	Si	Ca	Mg	Mn	
1	Solution from upper part of evaporative tank	0.002	0.002	0.02	0.06	-	-	0.08
2	Residue from this solution	0.006	0.002	0.02	0.06	0.06	-	0.15
3	Average sample of solution taken for secondary use after standing:							
	clear solution	0.002	0.002	0.002	0.06	-	-	0.07
	residue	0.06	0.2	0.06	2.0	0.06	0.02	2.40
4	Sample from bottom part of tank:							
	settled solution	0.002	0.002	0.002	0.06	-	-	0.07
	residue	1.0	0.2	0.1	2.0	0.06	0.02	3.38

Notes: 1. This figure 0.002% lies close to the limit of instrument accuracy, and therefore it should be viewed as approximate, giving an idea of the quantity of the given impurity.

2. The levels of Cr, Ni and Cu were less than 0.001% with respect to potassium.

References

1. Energetika mira i perspektivy ee razvitiya [World power production and the outlook for its development]. Reports of XII world conference, Moscow, 1968. Collection edited by P. S. Neporozhnii, Moscow, Energiya, 1970.
2. V. A. Kirillin, G. I. Rossievskii, M. A. Styrikovich, A. E. Sheindlin, *Teplofizika vysokikh temperatur*, 1966 (2), 4.
3. V. A. Kirillin, G. I. Rossievskii, A. E. Sheindlin, *ibid.*, 1968 (4), 6.
4. V. I. Vedeneev, L. V. Gurvish, et al., *Energiya razryva khimicheskikh svyasei. Potentially ionizatsii i srodstva k elektronu* [Energy of chemical bonds. Ionization potentials and electron affinity]. Moscow, 1963.
5. M. E. Pozin, *Tekhnologiya mineral'nykh soli* [Technology of mineral salts]. Leningrad, Goskhimizdat, 1961.
6. V. N. Gulyaev, *Metall v teploenergeticheskikh ustanovkakh* [Metal in thermal power installations]. Moscow, Metallurgiya, 1969.
7. I. P. Ipik, Kh. Kh. Arro, E. L. Tomani, *Gorenie tverdogo topliva* [Solid fuel combustion]. Novosibirsk, Nauka, 1969.
8. V. S. Yungman, L. V. Gurvich, N. P. Rtishcheva, *International symposium on MHD power generation*, Salzburg, Austria, 1966.
9. S. Way, W. Young, I. Tuba, R. Chambers, *Power-producing machines and installations*, no. 2. Mir, 1965.
10. M. S. Shkrob, V. F. Vikhrev, *Vodopodgotovka* [Water treatment]. Moscow-Leningrad, Energiya, 1966.
11. *Magnitogidrodinamicheskii metod polucheniya elektroenergii* [MHD method of producing electric power]. Collection edited by V. A. Kirillin and A. E. Sheindlin. Moscow, Energiya, 1968.
12. A. V. Zdanovskii, E. G. Solov'eva, L. D. Ezrokhi, E. I. Lyakhovskaya, *Spravochnik po rastvorimosti solevykh sistem* [Handbook on the solubility of salt systems], vol. 3. Goskhimizdat, 1961.
13. J. Dubois, R. Barde, A. Heuze. "Electricity from MHD, Warshawa, 1968", V, JAEA, Vienna, 1968.
14. JANAF Thermochemical Tables, First Addendum, PB168, 370-1, 1966.
15. E. Gadda. "Electricity from MHD, Warshawa 1968", IV, JAEA, Vienna, 1968.

16. V. A. Kirillin, A. E. Sheindlin, B. Ya. Shumyatskii, V. V. Kirillin, D. K. Burenkov, S. I. Pishchikov, P. G. Poletavkin, I. L. Mostinskii, V. N. Sukhov, L. V. Krauze, *Teplofizika vysokikh temperatur*, 1971 (5) 9.
17. D. G. Zhimerin, V. A. Bashilov, Yu. V. Makarov, V. P. Motulevich, *Fifth International Conference on Magnetohydrodynamic Electric Power Generation*, FRG, 1971, I. 249, 1971.
18. M. I. Ravich, F. E. Borovaya, E. G. Smirnova, *Zhurn. neorg. khimii*, 13 (7), 1922 (1968).
19. I. M. Rodnyanskii, V. I. Korobkov, I. S. Galinker, *Zhurn. fiz. khimii*, 1962 (10), 2216.
20. D. M. Ginzburg, N. S. Pikulina, V. P. Litvin, *Zhurn. prikl. khimii*, 37 (11), 2353 (1964).
21. I. Kh. Khaibullin, N.M. Borison, *Teplofizika vysokikh temperatur*, 1966 (4), 518.
22. B. S. Krumgal'z, V. P. Mashovets, *Zhurn. neorg. khimii*, 1965 (10), 2564.
23. V. P. Mashovets, I. A. Dibrov, B. S. Krumgal'z, *Zhurn. fiz. khimii*, 39, 1723 (1965).
24. Z. L. Miropol'skii, M. E. Shitsman, *Coll. Issledovanie teplootdachi k paru i vode, kipyashchei v trubakh pri vysokikh davleniyakh* [Investigation of heat transfer to steam and water boiling in pipes at high pressure]. Moscow, Atomizdat, 1958.
25. G. V. Alekseev, B. A. Zenkevich, V. I. Subbotin, *Teploenergetika*, 1962, (4), 74.
26. G. V. Vorob'ev, S. V. Karpachev, S. F. Pal'guev, "The density and electrical conductivity of $K_2CO_3-Na_2CO_3$, $Na_2CO_3-Li_2CO_3$, $K_2CO_3-Li_2CO_3$," in *Fizicheskaya khimiya rasplavlennykh solei i shaikov* [The physical chemistry of molten salts and slags]. GNTIL po chernoii i tsvetnoi metallurgii. Moscow, 1962, p. 135.
27. *Open Cycle MHD Power Generation*. Edited by J. B. Heywood and G. Womack. Pergamon Press, London, 1969.
28. D. V. Spalding, *Konvektivnyi massopereenos* [Convective mass transfer]. Moscow-Leningrad, Energiya, 1965.
29. A. E. Hamielec, T. W. Hoffman, L. L. Ross, *AJChE Journal*, March, 1967, 218.
30. W. E. Ranz, W. R. Marshall. *Chemical Eng. Progress*, 48, 141, 173, 1952.

31. V. N. Kondrat'ev, Kinetika khimicheskikh gazovykh protsessov [Kinetics of gaseous chemical processes]. Izd. AN SSSR. Moscow, 1958.
32. Kh. Grin, D. Lein, Aerizoli -- pyli, dymy, tumany [Aerosols -- dusts, smoke, mists]. Leningrad, Khimiya, 1969.
33. S. S. Kutateladze, A. I. Leont'ev, Turbulentnyi pogranychyi sloi szhimaemogo gaze [Turbulent boundary layer of a compressed gas]. Izd. CO AN SSSR. Novosibirsk, 1962.
34. Ma-tun-tsze, in Teploperedacha [Heat transfer]. Izd. AN SSSR, 1962.
35. S. Bretschneider, Sovoistva gazov i zhidkosti [Properties of gases and liquids]. Moscow-Leningrad, Khimiya, 1966.
36. S. Chapman, T. Kauling, Matematicheskaya teoriya neodnorodnykh gazov [Mathematical theory of dissimilar gases]. IIL, Moscow, 1960.
37. E. R. Ekkert, R. M. Dreik, Teoriya teplo- i massoobmena [Theory of heat and mass exchange]. Moscow-Leningrad, Gosenergoizdat, 1960.
38. K. M. Aref'ev, V. M. Borishanskii, T. V. Zablotskaya, N. I. Ivashenko, I. I. Paleev, L. A. Suslova, B. M. Khochenkov, in Teplo-masso-peredacha [Heat and mass transfer], vol. 2. Nauka i tekhnika, Minsk, 1968.
39. N. A. Fuks, Uspekhi mekhaniki aerizolei [Advances in aerosol mechanics]. Izd. AN SSSR, Moscow, 1961.
40. Einstein Z. Phys. 27, 1, 1924.
41. A. A. Rusanov, I. I. Urakh, A. P. Anastasiadi, Ochistka dymovykh gazov v promyshlennoi energetike [Flue gas purification in industrial power production]. Energiya, 1969.
42. V. N. Uzhov, B. I. Myagkov, Ochistka promyshlennykh gazov filtrami [Purification of industrial gases with filters]. Moscow, Khimiya, 1970.
43. V. M. Ramm, Absorbtsiya gazov [Absorption of gases]. Moscow, Khimiya, 1966.
44. A. L. Kouf', F. S. Rizenfel'd, Ochistka gazov [Gas purification]. Moscow, Nedra, 1968.
45. T. K. Sherwood, R. L. Pigford, Absorption and Extraction. N.Y., 1952.

APPENDIX

List of publications relating to material in this report

1. M. A. Styrikovich, I. L. Mostinskii, E. G. Smirnova, "The use of an aqueous solution of potash to input the ionizing additive into the channel of an open-cycle MHD generator," *Teplofizika vysokikh temperatur*, 1967 (5), 5.
2. M. A. Styrikovich, A. E. Sheindlin, I. L. Mostinskii, "The ionizing additive in open-cycle MHD generators operating on gaseous fuel," in coll. MGD metod polucheniya elektroenergii [MHD method of producing electrical power], edited by V. A. Kirillin and A. E. Sheindlin, 1968.
3. I. L. Mostinskii, "Estimation of optimum concentration of ionizing seed in power-producing MHD generators," *Teplofizika vysokikh temperatur*, 1968 (4), 1968.
4. I. L. Mostinskii, E. G. Smirnova, "The reduction of temperature in the combustion chamber of open-cycle MHD installations because of the input seed," *Teplofizika vysokikh temperatur*, 1968 (2), 6.
5. M. A. Styrikovich, I. L. Mostinskii, E. G. Smirnova, "The input of ionizing seed to power-producing open-cycle MHD generators," *Electricity from MHD*, Warszawa, 1968. JAEA, Vienna, 1968.
6. M. A. Styrikovich, I. L. Mostinskii, M. A. Laricheva, "Investigation of deposits of potassium carbonates from a stream of products from the combustion of a sulfur-free fuel," *Teplofizika vysokikh temperatur*, 1969 (6), 7.
7. A. Yu. Val'dberg, I. L. Mostinskii, R. S. Nekhoroshev, "The use of a turbulence washer to input ionizing seed into open-cycle MHD generators," *Teplofizika vysokikh temperatur*, 1970 (1), 8.
8. A. S. Golubkova, N. I. Zakharov, M. A. Laricheva, I. L. Mostinskii, R. S. Nekhoroshev, "Conversion of K_2CO_3 into $KHCO_3$ in the low-temperature zone of the gas path of an MHD generator," *Teplofizika vysokikh temperatur*, 1970 (1), 8.
9. I. L. Mostinskii, E. G. Smirnova, "Investigation of heat transfer in the boiling of aqueous solutions of potassium carbonate," *Teplofizika vysokikh temperatur*, 1970 (5), 8.
10. V. A. Kirillin, A. E. Sheindlin, I. L. Mostinskii et al., "Some results of investigation on the U-02 model MHD unit," Fifth International Conference on MHD Electrical Power Generation, Munich, 1971, vol. V., 1971.
11. V. A. Kirillin, A. E. Sheindlin, I. L. Mostinskii et al., "Investigation of the U-02 MHD installation during operation in extended modes," *Teplofizika vysokikh temperatur*, 1971 (5), 9.

12. M. A. Styrikovich, I. L. Mostinskii, L. S. Popyrin, N. I. Pshenichnikov, L. K. Khokhlov, "Optimizing the consumption of ionizing seed with respect to the electrical conductivity of the plasma and specific power of an MHD generator," in coll. MGD metod polucheniya elektroenergii [MHD method of producing electrical power], edited by V. A. Kirillin and A. E. Sheindlin, 1968.
13. E. G. Apukhtina, V. V. Bordacheva, A. Yu. Val'dberg, E. A. Vikhrov, V. P. Kurkin, I. L. Mostinskii, R. S. Nekhoroshev, G. S. Sorokin, Zh. S. Fedorova, "Investigation of various methods of trapping the ionizing seed on the U-02 experimental MHD unit," *ibid.*
14. I. L. Mostinskii, M. A. Laricheva, D. I. Lamden. Mass transfer in open cycle MHD installations. International seminar "Future Energy Production - Heat and Mass Transfer Problems", Yugoslavia, Dubrovnik, August, 1975.
15. M. A. Styrikovich, A. V. Zagorodnikh, V. E. Kartun, I. L. Mostinskii, R. S. Nekhoroshev, V. P. Pesochin, E. G. Smirnova, V. I. Stepanov, "Input of ionizing seed as an aqueous K_2CO_3 solution high in temperature and concentration," *Teplofizika vysokikh temperatur*, 1975 (6), 13.
16. D. I. Lamden, I. L. Mostinskii, "On the vaporization of a droplet which is decelerating in a hot gas," *ibid.*
17. A. Yu. Val'dberg, F. E. Dubinskaya, V. M. Tkachenko, I. L. Mostinskii, V. V. Bordacheva, A. I. Valuev, P. S. Nekhoroshev, Zh. S. Fainberg, "On simplifying systems for introducing an ionizing seed," *Teploenergetika*, no. 11, 1975.